BECHTEL
SAIC COMPANY LLC

Hydrogen-Induced Cracking of the Drip Shield

Hydrogen-Induced Cracking of the Drip Shield

ANL-EBS-MD-000006 REV 02

August 2004

INTENTIONALLY LEFT BLANK

OCRWM	MODEL SIGNATURE PAGE/CHANGE HISTORY	Page iii
		1. Total Pages: 108

2. Type of Mathematical Model

☒ Process Model   ☐ Abstraction Model   ☐ System Model

Describe Intended Use of Model

To be used as input to License Application.

3. Title   MrØ 10-28-04

Hydrogen-Induced Cracking of the Drip Shield

4. DI (including Rev. No., if applicable):

ANL-EBS-MD-000006 REV 02

5. Total Appendices		6. No. of Pages in Each Appendix		
None		N/A		

	Printed Name	Signature	Date
7. Originator	Fred Hua	SIGNATURE ON FILE	09/07/2004
8. Independent Technical Reviewer	Pasu Pasupathi	SIGNATURE ON FILE	9/7/04
9. Checker	William Downs	SIGNATURE ON FILE	9/7/04
10. QER	Darrell Svalstad	SIGNATURE ON FILE	9/7/04
11. Responsible Manager/Lead	Dennis Thomas	SIGNATURE ON FILE	9/7/04
12. Responsible Manager	Neil Brown	SIGNATURE ON FILE	9/7/04

13. Remarks

Kevin G. Mon was a major contributer for this document.

Change History	
14. Revision No.	**15. Description of Change**
00	Initial Issue.
00/01	Interim Change Notice to include (1) hydrogen induced cracking due to the possible galvanic contact between the Ti Grade 7 drip shield and steel components that may fall onto the drip shield in the case of a no-backfill drip shield design; and (2) approach to issue resolution status report key technical issue: container life and source term. Changes are indicated by vertical lines in the right margin.

3. Title
Hydrogen-Induced Cracking of the Drip Shield

4. DI (including Rev. No., if applicable):
ANL-EBS-MD-000006 REV 02

Change History	
14. Revision No.	15. Description of Change
00/02	Interim Change Notice to remove TBV-4897. Assumption 5.5 added, and Sections 6.3.3 and 8.1 modified. The input statuses of some of the references in the Document Input Reference System (DIRS) report have been revised. Changes made in this Analysis and Model Report are indicated by vertical lines in the right margin.
01	Document revised for Model Validation and NRC comment resolution. This extensive revision generated new sections 5.6, 6.1.6, 6.1.7, 6.2.5, 6.3.4, 6.3.5, 6.3.6, 7, and 10. The modified sections include 1.1, 1.2, 2, 3, 4.1, 4.2, 4.3, 5.3, 5.4, 5.5, 6.1.1, 6.1.5, 6.2.3, 6.2.4, 6.3.2, 6.3.3, 6.3.7, 8, and 9.
02	This revision corrects technical errors identified in BSC(O)-03-D-135 regarding inputs that do not match DTNs LL990610605924.079 and MO0003SPASUP02.003. BSC(O)-03-D-135 (which initiated TER-03-0022) and CR 658C address the same TER. Corrections (from 3.50 x 10^{-4} to 3.20 x 10^{-4}, rate of general passive corrosion) have been made to address DTN LL990610605924.079 (see Tables 4 & 6 and Section 6.2.1, 7.35, and 8.1, DIRS 169845). DTN MO0003SPASUP02.003 is no longer used as input to this AMR. CR 2079D is resolved in Sections 5.2 and 7.3.2. Discussion on Ti Grade 24 has been added. Conservatism in discussing galvanic coupling effect by using carbon steel for stainless steel have been emphasized. More recently acquired 5-year corrosion rate data are used to verify the conservatism of model. This revision also incorporates changes for regulatory integration. The entire document was revised. The changes were too extensive for change bars to be practical.

CONTENTS

Page

CONTENTS (Continued)

Page

CONTENTS (Continued)

INTENTIONALLY LEFT BLANK

FIGURES

TABLES

ACRONYMS AND ABBREVIATIONS

ACM	Alternative Conceptual Model
AECL	Atomic Energy of Canada, Ltd.
ASTM	American Society of Materials and Testing
BSC	Bechtel SAIC Co., LLC
BSW	basic saturated water
DOE	Department of Energy
DTN	Data Tracking Number
FEP	features, event, or processes
LA	License Application
LLNL	Lawrence Livermore National Laboratory
LTCTF	Long Term Corrosion Test Facility
NRC	Nuclear Regulatory Commission
SAW	simulated acidic concentrated water
SCE	saturated calomel electrode
SCW	simulated concentrated water
SDW	simulated dilute water
SSW	simulated saturated water
TSPA	Total System Performance Assessment
TWP	Technical Work Plan
UNS	Unified Numbering System

1. PURPOSE

1.1 PURPOSE AND BACKGROUND

Hydrogen-induced cracking is characterized by the decreased ductility and fracture toughness of a material due to the absorption of atomic hydrogen in the metal crystal lattice. Corrosion is the source of hydrogen generation. For the current design of the engineered barrier without backfill, hydrogen-induced cracking may be a concern because the titanium drip shield can be galvanically coupled to rock bolts (or wire mesh), which may fall onto the drip shield, thereby creating conditions for hydrogen production by electrochemical reaction.

The purpose of this report is to analyze whether the drip shield will fail by hydrogen-induced cracking under repository conditions within 10,000 years after emplacement. Hydrogen-induced cracking is a scenario of premature failure of the drip shield. This report develops a realistic model to assess the form of hydrogen-induced cracking degradation of the drip shield under the hydrogen-induced cracking. The scope of this work covers the evaluation of hydrogen absorbed due to general corrosion and galvanic coupling to less noble metals (e.g., Stainless Steel Type 316 and carbon steels) under the repository conditions during the 10,000-year regulatory period after emplacement and whether the absorbed hydrogen content will exceed the critical hydrogen concentration value, above which the hydrogen-induced cracking is assumed to occur. This report also provides the basis for excluding the features, events, and processes (FEPs) related to hydrogen-induced cracking of the drip shield with particular emphasis on FEP 2.1.03.04.0B, hydride cracking of drip shields (DTN: MO0407SEPFEPLA.000 [DIRS 170760]). This report is prepared according to *Technical Work Plan (TWP) for: Regulatory Integration Modeling and Analysis of the Waste Form and Waste Package* (BSC 2004 [DIRS 169944]).

1.2 BACKGROUND INFORMATION ON TITANIUM ALLOYS

Ti Grade 7 (UNS R52400) is the material for construction of the drip shield for the waste package due to its excellent corrosion resistance (BSC 2004 [DIRS 169845]). This alloy consists of 0.12 to 0.25% palladium, 0.3% iron, 0.25% oxygen, 0.1% carbon, 0.03% nitrogen, 0.015% hydrogen, 0.4% total residuals with the balance being titanium (CRWMS M&O 1999 [DIRS 102933], p. 45; DTN: MO0003RIB00073.000 [DIRS 152926]). Other titanium alloys that are discussed in this report corroboratively include Ti Grades 2, 5, 12, 16, 17, and 24. Ti Grade 2 is commercially pure titanium. The most effective way of reducing hydrogen absorption is to choose a more crevice resistant alloy (Shoesmith et al. 1997 [DIRS 112203], p. 15). The improvement in resistance to crevice corrosion of titanium alloys is attributed to the addition of alloying elements, which reinforce passivity. Therefore, susceptibility to crevice corrosion is reduced through the alloying series Ti Grade 2 $\rightarrow$ Ti Grade 12 $\rightarrow$ Ti Grade 16 (Shoesmith et al. 1997 [DIRS 112203], p. 15). The major additions are nickel (0.6 to 0.9%) for Ti Grade 12 and palladium (0.04 to 0.08%) for Ti Grade 16 (CRWMS M&O 1999 [DIRS 102933], pp. 49 and 51; DTN: MO0003RIB00073.000 [DIRS 152926]).

Shoesmith et al. (1997 [DIRS 112203], p. 21) noted a decrease in the corrosion rate by the addition of a noble metal such as palladium to Ti Grade 16, to yield Ti Grade 7. The composition of Ti Grade 7 is almost identical to that of Ti Grade 16, but the palladium content is

higher in Ti Grade 7 (0.12 to 0.25%) than that in Ti Grade 16 (0.04 to 0.08%) (CRWMS M&O 1999 [DIRS 102933], pp. 45 and 51; DTN: MO0003RIB00073.000 [DIRS 152926]). The similarity between Ti Grades 7 and 16 was also the basis for the general corrosion model of the drip shield (BSC 2004 [DIRS 169845]).

Because hydrogen-induced cracking involves the mechanical properties of the materials, the similarity between the mechanical properties of Ti Grades 7 and 16 is also emphasized. The properties of materials, including mechanical properties and corrosion resistance, largely depend on microstructures that depend on the chemical compositions of the materials. The chemical compositions and mechanical properties of the relevant titanium alloys are shown in Table 1 and Table 2. In Table 1 and Table 2, Ti Grades 2, 12, 16, and 7 are α-alloys while Ti Grades 5 and 24 are α-β alloys. Ti Grade 7 contains slightly higher wt % of palladium (0.12 to 0.25 wt %) than Ti Grade 16 (0.04 to 0.08 wt %). The mechanical properties specified in ASTM B 265-02 [DIRS 162726] are identical for Ti Grades 2, 16, and 7. They are also identical for Ti Grades 5 and 24 and for Ti Grades 9 and 18 (Table 2) (ASTM B 265-02 [DIRS 162726]).
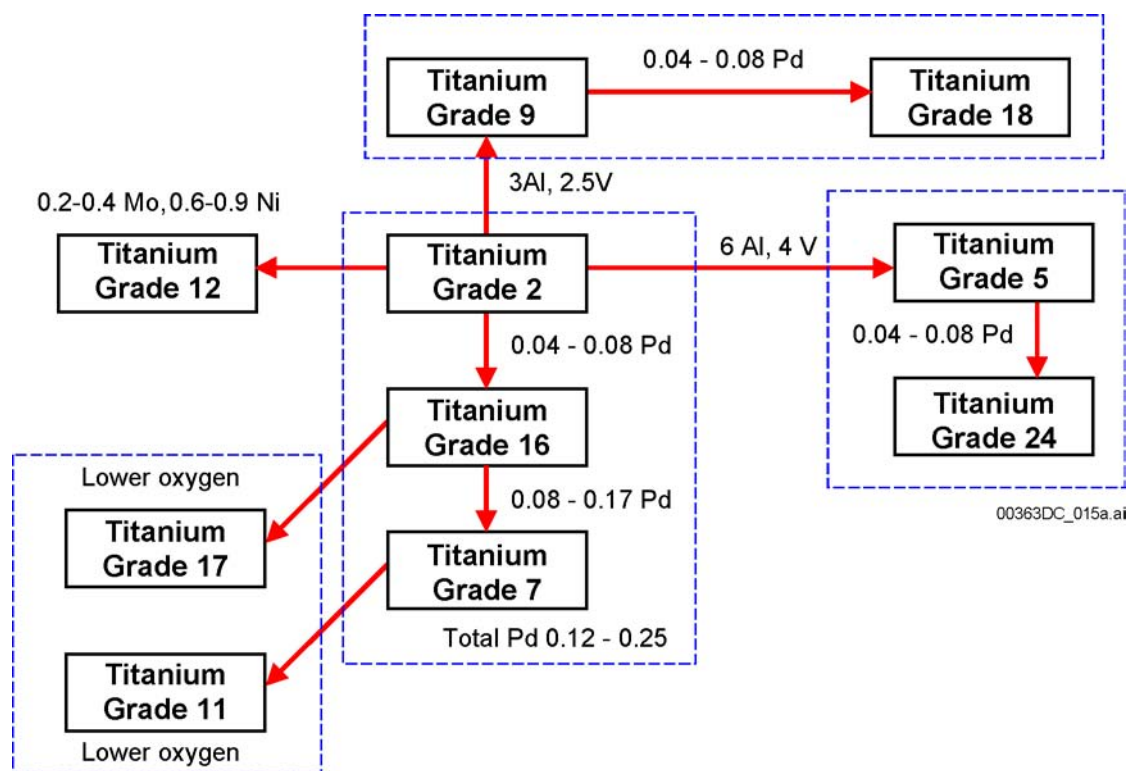
NOTE: Alloys grouped by the dotted lines have same mechanical properties, regardless of the chemical compositions (amount of Pd).

Figure 1. Schematic of the Relationship Between the Relevant Titanium Alloys

Table 1. ASTM B 265-02 Specifications for Chemical Composition Requirements (wt %) of Relevant Titanium Alloys

Material	UNS Designation	N Max**	C max	H max	O max	Fe max	Al	V	Pd	Residual (each)	Residual (total)	Ti
Ti Grade 12	R53400	0.03	0.08	0.015	0.25	0.30	-	-	-	0.2-0.4 Mo	0.6-0.9 Ni	balance
Ti Grade 2	R50400	0.03	0.08	0.015	0.25	0.30	-	-	-	0.1	0.4	balance
Ti Grade 16	R52402	0.03	0.08	0.015	0.25	0.30	-	-	0.04 to 0.08	0.1	0.4	balance
Ti Grade 17	R52252	0.03	0.08	0.015	0.18	0.320	-	-	0.04 to 0.08	0.1	0.4	balance
Ti Grade 7	R52400	0.03	0.10	0.015	0.25	0.30	-	-	0.12-0.25	0.1	0.4	balance
Ti Grade 11	R52250	0.03	0.10	0.015	0.18	0.20	-	-	0.12-0.25	0.1	0.4	balance
Ti Grade 5	R56406	0.05	0.08	0.015	0.20	0.40	5.5 to 6.75	3.5 to 4.5	-	0.1	0.4	balance
Ti Grade 24	R56405	0.05	0.08	0.015	0.20	0.40	5.5 to 6.75	3.5 to 4.5	0.04 to 0.08	0.1	0.4	balance
Ti Grade 9	R56320*	0.03	0.08	0.015	0.12	0.25	2.5 to 3.5	2.0 to 3.0	-	0.1	0.4	balance
Ti Grade 18	R56322	0.03	0.08	0.015	0.15	0.25	2.5 to 3.5	2.0 to 3.0	0.04 to 0.08	0.1	0.4	Balance

Source: ASTM B 265-02 [DIRS 162726], Table 2.

NOTE: * UNS R56320 requires lower N, C, O and H. ** max - maximum concentration level

Table 2. ASTM B 265-02 Specifications for Mechanical Properties of Relevant Titanium Alloys

Material	UNS Designation	Minimum Tensile Strength, ksi		Yield Strength, 0.2 % Offset				Minimum Elongation in 2 in., %
				Mi		Max		
		ksi	MPa	ksi	MPa	ksi	MPa	
Ti Grade 12	R53400	70	483	50	345	-	-	19
Ti Grade 2	R50400	50	345	40	275	65	450	20
Ti Grade 16	R52402	50	345	40	275	65	450	20
Ti Grade 17	R52252	35	240	25	170	45	310	24
Ti Grade 7	R52400	50	345	40	275	65	450	20
Ti Grade 11	R52250	35	240	25	170	45	310	24
Ti Grade 5	R56406	130	895	120	828	-		10
Ti Grade 24	R56405	130	895	120	828	-	-	10
Ti Grade 9	R56320	90	620	70	483	-	-	15
Ti Grade 18	R56322	90	620	70	483	-	-	15

Source: ASTM B 265-02 [DIRS 162726], Table 1.

The fact that addition of a small amount of palladium does not alter the mechanical properties of titanium alloys is shown in Figure 1 and Table 2. The alloys grouped by dotted lines in Figure 1 have identical mechanical properties regardless of their chemical compositions, implying that these alloys have very similar, if not exactly the same, microstructures. While further addition of palladium to Ti Grade 16 to yield Ti Grade 7 does not deteriorate the mechanical properties of the titanium alloy, the resistance to general and localized corrosion is improved (Schutz 2003 [DIRS 168772]). These two materials have almost identical chemical compositions, except that Ti Grade 7 contains 0.12 to 0.25 wt.% palladium while Ti Grade 16 contains 0.04 to 0.08 wt % palladium (Table 1). Ti Grade 16 was used as an analog of Ti Grade 7 at the Long Term Corrosion Test Facility (LTCTF) for the 1- and 5-year weight-loss tests due to its compositional similarity to Ti Grade 7. The corrosion performance of Ti Grade 7, because of its higher palladium content, is superior or at least equivalent to that of Ti Grade 16 (Schutz 2003 [DIRS 168772]). As this modeling activity uses corrosion rate data obtained at the LTCTF for Ti Grade 16, justification of the similarity between Ti Grades 7 and 16 is important. Their analogous relationship is further discussed in Section 5.1.

1.3   BACKGROUND ON IN-DRIFT ENVIRONMENTAL CONDITIONS

This report uses the corrosion rate data obtained at the LTCTF in test media listed in Table 3 as direct inputs, to calculate the hydrogen contents in the metal and evaluate whether hydrogen-induced cracking will occur within the 10,000 years after emplacement. It is, therefore, important to briefly describe the relevance of the in-drift chemical conditions and test media before discussing the model development and model validation. The description of the in-drift environmental conditions in Section 1.3 supports the use of the LTCTF corrosion test data for modeling hydrogen-induced cracking of the drip shield.

The drip shield will experience a wide range of conditions during its service life (BSC 2004 [DIRS 161237]). Figure 2 shows a summary of the range of waste package temperature and humidity histories for all waste packages (a and b), all CSNF waste packages (c and d) and all DHLW waste packages (e and f) (BSC 2004 [DIRS 169565], Figure 6.3-53). The ranges include the lower-bound, mean and upper-bound infiltration flux cases and use of the mean thermal-conductivity values for unsaturated zone model layer unit, including the host-rock units. The repository design enables the repository to operate in three temperature regimes: dryout, transition, and low-temperature. The relevant attributes of each regime are summarized below (BSC 2004 [DIRS 169565]):

(a) All waste packages

(b) All waste packages

(c) All CSNF waste packages

(d) All CSNF waste packages

(e) All DHLW waste packages

(f) All DHLW waste packages

00446DC_001.ai
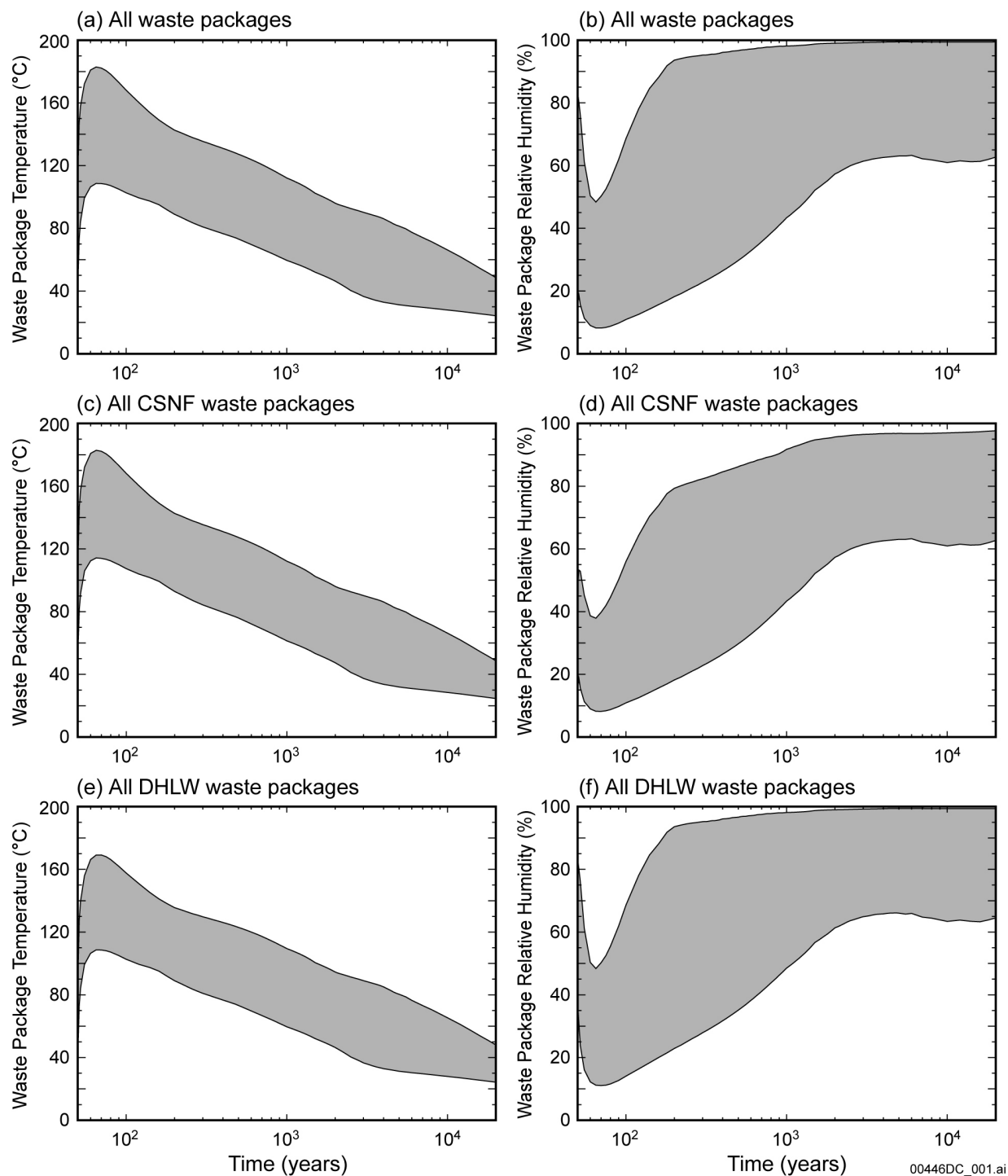
Source: BSC 2004 [DIRS 169565], Figure 6.3-53.

NOTES: The summary of the range of waste package temperature and humidity histories for all waste packages (a and b), all CSNF waste packages (c and d) and all DHLW waste packages (e and f). The ranges include the lower-bound, mean and upper-bound infiltration flux cases and use of the mean thermal-conductivity values for all Unsaturated Zone Model layer unit, including the host-rock units.

Figure 2. Waste Package Temperature and Humidity Histories

Dryout–Drift walls will first be dried by ventilation air during the preclosure period. During postclosure, heat generated by radioactive decay increases the temperature of waste packages and drift walls to above the boiling point of water. Because no significant seepage is expected for drift wall temperatures above the boiling point of water, no aqueous phase corrosion due to seepage is expected (calcium chloride type brines are possible and predicted to occur in this regime, but they occur in the host rock when temperatures are above boiling and seepage into the drift is prevented by the vaporization barrier effect as described in the technical basis document on the in-drift chemical environment). However, depending on the surface temperature and relative humidity conditions, the existence of liquid-phase water on the waste package or drip shield is possible due to the presence of a dust or salt deposit. In the presence of such a deposit, a thin-film liquid phase can be established at a higher temperature and lower relative humidity than otherwise possible. Thus, formation of deliquescent brines in the absence of seepage may occur, and corrosion of the waste package and drip shield is considered in the context of these solutions.

Transition–Seepage into the drifts is possible as the waste package cools, as the temperature of the drift wall drops below the boiling point of water, and while the waste package surface temperature is at or above the boiling point of the water. Seepage waters will undergo evaporative concentration on the drip shield surface or the waste package surface at the time when the drip shield seepage diversion function is lost, thereby evolving into either carbonate- or sulfate-type brines. The drip shield will mitigate seepage effects on the waste package. However, as in the dryout regime, formation of deliquescent brines could occur in this regime.

Low Temperature–As the waste package cools to a temperature below the boiling point of water, the in-drift relative humidity increases, so evaporated solutions are not as concentrated. With further cooling, the temperature drops to below the threshold for localized corrosion for the repository-relevant environments. This threshold temperature is a function of the presence of beneficial ions, such as nitrates and sulfates.

The project has developed an understanding of the in-drift chemical environment for the three temperature regimes. The understanding is based on geochemical models and supporting data and analysis appropriate for the repository conditions. A detailed description of the evolution of the chemical environment is provided in *Engineered Barrier System: Physical and Chemical Environment Model* (BSC 2004 [DIRS 169860], Section 6), which includes detailed discussions of the relationship between the geochemical process model results, the range of expected in drift environments, and the chemical environments used in corrosion related testing. The model output is in the form of lookup tables, listing ion concentrations and pH as a function of relative humidity, temperature, and carbon-dioxide partial pressure. A brief summary of the chemical environment applicable to corrosion related testing has been excerpted from the technical basis document on in-drift chemical environment follows.

Brines that develop on the waste packages and drip shields are the result of either evaporative concentration of seepage water or deliquescence of deposited salts. Deposited salts can be due to entrained matter in the ventilation air, dust and debris deposited within the drifts, or seepage waters that have evaporated to dryness. Seepage waters will not enter the drifts until host rock temperatures fall below 100°C. Dust salts will deliquesce water from the atmosphere to form

thin films on waste packages and drip shields above the normal boiling point of water (up to about 140°C) (BSC 2004 [DIRS 169860], Section 6).

Corrosion testing to determine the response of waste package, drip shield, and other in-drift materials is carried out in environmental conditions consistent with those predicted by in-drift chemical modeling. Corrosion testing environments were chosen based on the three types of natural brines: (1) calcium chloride, (2) carbonate, and (3) sulfate. Initial studies focused on the carbonate-type brine, based on reasoning that carbonate-type waters, typified by J-13 well water from the saturated zone near Yucca Mountain, are the expected types of waters at the repository (Harrar et al. 1990 [DIRS 100814]). Aqueous corrosion test solutions include several multi-ionic solutions based on a carbonate-base J-13 well water and test solutions containing the major species expected to effect corrosion. The standardized solutions developed as relevant test environments are presented in Table 3. These solutions include simulated dilute waste (SDW), simulated concentrated water (SCW), and simulated acidic water (SAW) at 30°C, 60°C, and 90°C, as well as SSW at 100°C and 120°C. The SSW formulation is based upon the assumption that evaporation of J-13 well water eventually leads to a sodium–potassium–chloride–nitrate solution. The following discussion on the relevance of the test media to the in-drift chemical environmental conditions is an abstraction from Section 6 of *Engineered Barrier System: Physical and Chemical Environment Model* (BSC 2004 [DIRS 169860]) and is used as the corroborative information only.

Table 3. Composition of Standard Test Media Based upon J-13 Well Water

Ion	SDW (mg/L)	SCW (mg/L)	SAW (mg/L)	SSW (mg/L)	BSW-12 (mg/L)
K^{+1}	3.400E+01	3.400E+03	3.400E+03	1.420E+05	6.762E+04
Na^{+1}	4.090E+02	4.090E+4	3.769E+04	4.870E+04	1.0586E+05
Mg^{+2}	1.000E+00	<1.000E+00	1.000E+03	0.000E+00	0.000E+00
Ca^{+2}	5.000E-01	<1.000E+00	1.000E+03	0.000E+00	0.000E+00
F^{-1}	1.400E+01	1.400E+03	0.000E+00	0.000E+00	1.331E+03
Cl^{-1}	6.700E+01	6.700E+03	2.425E+4	1.280E+05	1.313E+05
NO_3^{-1}	6.400E+01	6.400E+03	2.30E+4	1.313E+06	1.395E+06
SO_4^{-2}	1.670E+02	1.670E+04	3.86E+4	0.000E+00	1.392E+04
HCO_3^{-1}	9.470E+02	7.000E+04	0.000E+00	0.000E+00	0.000E+00
Si	27 (60°C), 49 (90°C)	27 (60°C), 49 (90°C)	27 (60°C), 49 (90°C)	0.000E+00	0.000E+00
pH	9.8 to 10.2	9.8 to 10.2	2.7	5.5 to 7	12

Source: LL040803112251.117 [DIRS 171362]

NOTE: pH measured for actual solutions at room temperature.

The brine name reflects a characteristic that distinguishes it from the other brines. Characterization of earth surface brines has, in part, guided the expected range of brine water chemistry in the repository. However, some differences exist between brines formed at the earth's surface and brines formed in the repository. These differences are mainly due to differences in the chemistry of seepage waters and surface waters giving rise to brines, and

differences between the salt chemistry of dust and the dissolved salt content of such surface waters. Two important general factors specific to the repository brines are the presence of nitrate and more effective mechanisms for the removal of magnesium. Nitrate will be present in the deliquescent brines owing to multiple potential sources (BSC 2004 [DIRS 161237], Section 6.7.2.8) and the high solubility of nitrate minerals (BSC 2004 [DIRS 161237], Section 4.1.1.7). Magnesium will not be significant due to a combination of low source (for the dust, as well as for at least some groundwaters) and multiple removal mechanisms, most of which are enhanced by elevated temperature (BSC 2004 [DIRS 161237], Sections 6.7.2.10 and 6.7.2.11).

1.3.1   Calcium-Chloride Brines

The calcium-chloride brines have near-neutral pH and no significant bicarbonate/carbonate, fluoride, or sulfate content. These brines contain other cations such as sodium, potassium, and magnesium and other anions such as nitrate. The endpoint of the evaporative concentration of this type of brine contains $Ca-Cl/NO_3$ or a mixture of $Ca/Mg-Cl/NO_3$. The quantity of magnesium and calcium is limited due to the precipitation of calcium carbonates, sulfates, and magnesium silicates. This is consistent with information on saline lakes where sodium is the dominant cation with the percentage of calcium varying from insignificant to about 20 percent (Drever 1997 [DIRS 147480]). Nitrate will be present, and an endpoint brine of this type is to be dominated by calcium chloride and calcium nitrate. A calcium chloride brine will also be very limited in the repository. Brine generated by dust deliquescence is more of a potassium nitrate–sodium chloride brine with only a small probability of calcium due to the compositional nature of the dust leachate. Relative humidity dependence of the calcium-chloride brine composition is as follows. At low relative humidity, the aqueous solution is dominated by calcium cations (very low sodium and potassium) and chloride and nitrate anions, because both calcium nitrate and calcium chloride are very soluble. At higher relative humidity, chloride and nitrate salts of sodium and potassium become soluble and dominate the aqueous solution compositions. This occurs at or above the deliquescence relative humidity for salts composed of these ions.

Corrosion test solutions corresponding to the calcium chloride type of brine include calcium chloride, calcium chloride plus calcium nitrate, the simulated saturated water (SSW), and sodium chloride aqueous solutions. The SSW and sodium chloride test solutions simulate the moderate relative humidity scenario where calcium is a minor component in the aqueous solution.

1.3.2   Carbonate Brines

The carbonate brines are alkaline and do not contain significant calcium or magnesium content. In the early stages of the evaporative concentration, calcium precipitates predominately as carbonate mineral (calcite or aragonite) under equilibrium conditions. Magnesium precipitates as a minor component in the calcium carbonate species and as magnesium silicate. Potassium is significant in some of these brines. Nitrate is also expected to be an important component, and a brine of this type may evolve through a high extent of evaporation into one in which nitrate is actually the dominant anion. The carbonate brine is represented as an alkali-metal (sodium, potassium) carbonate brine. Relative humidity dependence of carbonate brine composition is as follows. At low relative humidity, the aqueous solutions are dominated by nitrate and chloride anions with nitrate ions dominating at the lowest relative humidity. At moderate relative

humidity (greater than 70 percent relative humidity), chloride ions dominate the solution composition. The nitrate-chloride solutions will have slightly elevated pH due to residual carbonate in solution and dissolved CO_2 from the atmosphere. Significant amounts of carbonate and sulfate ion are not expected until the relative humidity is greater than 85 percent.

Corrosion test solutions corresponding to the carbonate type of brine include the simulated dilute water (SDW), simulated concentrated water (SCW), basic saturated water (BSW), and under certain circumstances, SSW and simulated acidic water (SAW) aqueous test solutions (Table 3). The BSW test solution is a highly concentrated alkaline solution under repository conditions where temperatures measure its boiling point of nominally 112°C to 113°C or where the relative humidity is nominally 70 to 75 percent. The SCW test solution is a moderately concentrated alkaline solution and solutions in this concentration range form at relative humidity in the range of 90 to 95 percent. The SDW test solution is a dilute alkaline solution and solutions in this concentration range form at high relative humidity (greater than 99 percent). These may have characteristics of solutions at the drift wall that are typical of in-drift seepage waters.

Under conditions of extreme evaporative concentration (i.e., low relative humidity), this type of brine containing high nitrate and chloride content evolves into a nitrate-chloride brine with low carbonate content. The SSW test solution has characteristics of this type of brine. Likewise, the SAW test solution has characteristics of low carbonate brine and of solutions in equilibrium with relative humidity of nominally 90 percent. The calcium and magnesium addition to this test solution increases the ability to sustain lower pH values due to the hydrolysis properties of these cations.

1.3.3 Sulfate Brines

The sulfate brines have near-neutral pH and no significant bicarbonate/carbonate and calcium content. Calcium precipitates as carbonates and possibly sulfates. In addition, they typically have only a small amount of magnesium, though some surface brines have been observed to have high magnesium (Drever 1997 [DIRS 147480], Table 15-1, p. 333, brines 1-3). The dominant cation is typically sodium. In the repository brines, potassium may be comparable to sodium, and magnesium is expected to be insignificant. A brine of this type may also evolve, through a high extent of evaporation, into one in which nitrate is the dominant anion.

Relative humidity dependence of the sulfate brine composition is as follows. At low relative humidity, the aqueous solutions are dominated by nitrate and chloride anions with nitrate ions dominating at the lowest relative humidity. At moderate relative humidity (greater than 70 percent relative humidity), chloride ions will dominate the solution composition. However, unlike the carbonate brines, these brines will have near-neutral to slightly acidic pH because of the lack of a carbonate component. Significant amounts of carbonate and sulfate ion are not expected until the relative humidity is greater than 85 percent because of the increase in solubility of sulfate minerals (sodium and potassium sulfates). Magnesium sulfate is expected to be present in insignificant quantities in these brines.

The corrosion test solutions corresponding to sulfate brines include SAW and SSW. This type of brine has near-neutral to slightly acidic pH and, as noted, magnesium will not be present in seepage waters to any significant extent. The SAW test solution has characteristics of solutions

in equilibrium with nominally 90-percent relative humidity. The SSW has characteristics of water that have undergone evaporative concentration to the extent that sulfate precipitates out of solution (magnesium-free situation).

Two important general factors specific to the repository brines are the presence of nitrate and more effective mechanisms for the removal of magnesium. Nitrate will be present in the deliquescent brines because of multiple potential sources (BSC 2004 [DIRS 161237], Section 6.7.2.8) and the high solubility of nitrate minerals (BSC 2004 [DIRS 161237], Section 4.1.1.7).

Magnesium ions will not be significant because of a combination of low concentration (for the dust, as well as for at least some groundwaters) and multiple removal mechanisms, most of which are enhanced by elevated temperature (BSC 2004 [DIRS 161237], Sections 6.7.2.10 and 6.7.2.11).

Carbonate will help buffer pH in any occluded geometry such as a crevice, and sulfate can act as a corrosion inhibitor. The compositions of these environments, as well as the solution known as BSW, are provided in Table 3. Small amounts of carbonate will form in the SSW, SAW, and BSW solutions by interaction with gas-phase carbon dioxide. The amount of carbonate formed was not determined experimentally because the small amounts are not expected to affect the corrosion processes significantly.

BSW can have a pH between 11 and 13, and has a boiling point near 110°C (BSW-12 with a pH of 12 shown in Table 3). This test medium was established based on results from a distillation experiment. The total concentration of dissolved salts in the starting liquid was more concentrated than that in the standard SCW solution. After evaporation of approximately 90 percent of the water from the starting solution, the residual solution reaches a maximum chloride concentration and has a boiling point of approximately 110°C, with a pH of about 11. The synthetic BSW solution composition can be slightly modified (mainly by adding sodium hydroxide) to cover a range of pH values, yielding BSW-11, BSW-12, and BSW-13.

Deliquescence of dust deposited on the waste packages and drip shield is another means by which brines can form on these engineered barrier system components. In the absence of salts, condensed water can be present on smooth surfaces only if the relative humidity is 100 percent. At lower relative humidity values, most of the water evaporates, with residual water existing on the surface as a very thin adsorbate layer. Dissolved salts lower the relative humidity at which such dryout occurs. Salt minerals in a dry system lower the relative humidity required for an aqueous solution to form. If the dissolved salt composition of a solution is known, the relative humidity at which dryout occurs at a given temperature can be determined. Conversely, the relative humidity for a given salt or set of salt minerals at which deliquescence occurs at a specified temperature can also be estimated.

In all cases, the nitrate component is the most soluble species and will dominate the solution composition at the deliquescent relative humidity or eutectic point of a mineral assemblage at elevated temperatures. At higher relative humidity, chloride minerals become soluble and could become a dominant ion. It is not until the relative humidity is much higher that the sulfate and carbonate compositions become appreciable. In essence, solutions are by dominated chloride and

nitrate at low to moderate (less than 70 percent) relative humidity and at higher relative humidity, sulfate and carbonate enter solution. This is discussed in more detail in *Environment on the Surfaces of the Drip Shield and Waste Package Outer Barrier* (BSC 2004 [DIRS 161237]).

1.4 BARRIER CAPABILITY

10 CFR 63 [DIRS 156605] defines a barrier as "any material, structure, or feature that, for a period to be determined by NRC, prevents or substantially reduces the rate of movement of water or radionuclides from the Yucca Mountain repository to the accessible environment, or prevents the release or substantially reduces the release rate of radionuclides from the waste." 10 CFR 63.102 (h) and 10 CFR 63.113 (a) [DIRS 156605] requires that the repository system must include multiple barriers, both natural and engineered.

The capability of a barrier is defined by its ability to achieve one or more of the functions described above (i.e., the extent to which it can prevent or delay the movement of water or radionuclides, or prevent or reduce the radionuclide release rate from the waste). In this report, the drip shield is considered as the barrier to prevent or reduce water flow that could contact the waste package and, in the event of a waste package breach, prevents or reduces water flow from contacting the waste form. This ability is the property that makes the drip shield a part of the engineered barrier system. The probability of failure of the drip shield concurrently with breach of the waste package is such that it is highly likely the combined mechanisms will continue to divert water.

1.5 APPLICABILITY OF MODEL

Hydrogen-induced cracking is a scenario of premature failure of the drip shield. This report develops a realistic model for the hydrogen-induced cracking degradation of the drip shield under a variety of corrosion conditions (general, crevice, and galvanic corrosion). The assessment is based upon the data generated by the project and from the literature. The model will follow the approach of Shoesmith et al. (1997 [DIRS 112203]). Also, qualitative and quantitative assessments are made to evaluate the effect due to the galvanic coupling of titanium alloy to less-noble metals.

The model developed in this report applies to the drip shield made of Ti Grade 7 exposed to repository environments for up to 10,000 years after the emplacement. Corrosion is considered as the only source of hydrogen generation.

Although models in this report are developed on the basis of information from a wide variety of titanium alloys, they are primarily intended to apply to the corrosion behavior of palladium-containing titanium alloys, especially Ti Grade 7. The critical hydrogen concentration of Ti Grade 24 is also estimated based on that of Ti Grade 5 and the role of palladium addition to titanium alloys.

INTENTIONALLY LEFT BLANK

2. QUALITY ASSURANCE

The Quality Assurance (QA) program applies to the development of this document (BSC 2004 [DIRS 169944], Section 8). The technical work plan associated with this activity (BSC 2004 [DIRS 169944]), was prepared per AP-2.27Q, *Planning for Science Activities*. The drip shields have been determined to be important to waste isolation in accordance with AP-2.22Q, *Classification Analyses and Maintenance of the Q-List* and, therefore, are classified as Safety Category (SC) on *Q-List* (BSC 2004 [DIRS 168361]) and by *Safety Classification of SSCs and Barriers* (BSC 2003 [DIRS 164554]). The methods used to control the electronic management of data as required by AP-SV.1Q, *Control of the Electronic Management of Information*, were accomplished in accordance with *Technical Work Plan For: Regulatory Integration Modeling and Analysis of the Waste Form and Waste Package* (BSC 2004 [DIRS 169944]).

This document is prepared in accordance with AP-SIII.10Q, *Models,* and reviewed in accordance with AP-2.14Q, *Document Review.*

INTENTIONALLY LEFT BLANK

3.   USE OF SOFTWARE

No computer software or models have been used to support the development of the analysis and modeling activities described in this report.

INTENTIONALLY LEFT BLANK

4. INPUTS

4.1 DIRECT INPUT

The following direct input data or parameters are obtained from *CRC Handbook of Chemistry and Physics* (Weast 1978 [DIRS 128733], p. B-177):

ρ_{Ti} = Density of titanium (g/cm^3)

M_{Ti} = Atomic weight of titanium (g/mol)

These parameters are established facts. No qualification is required.

The following direct input data and/or parameters for Ti Grade 7 are obtained from *General Corrosion and Localized Corrosion of the Drip Shield* (BSC 2004 [DIRS 169845], Section 6.5), which uses DTN: LL990610605924.079 [DIRS 104994] as one of the direct inputs:

R_{uc} = Passive general corrosion rates (mm/yr)

The source DTN: (LL990610605924.079 [DIRS 104994]) and the report (BSC 2004 [DIRS 169845]) that uses the DTN are qualified documents. No further qualification activities are needed.

The following design parameters are obtained from *Interlocking Drip Shield* (BSC 2003 [DIRS 171024]) and 10 CFR 63.114(d) [DIRS 156605], respectively:

d_0 = Half of drip shield thickness (mm)

t = Duration of emplacement (years)

The thickness of the drip shield is from the project design document and does not need further qualification. The time of emplacement is based on 10 CFR 63.114(d), which can be considered as the established fact.

The following data are from literature (Okada 1983 [DIRS 115556]):

f_h = Fractional efficiency of hydrogen absorption

The fractional efficiency range of hydrogen absorption used in this report is discussed in more detail throughout this report. The data are published in peer-reviewed literature (*Electrochimica Acta, 28,* (8), 1113-1120) and referenced by other investigators. The following further qualify the data as a direct input to the model developed in this report.

Electrochimica Acta is published by Elsevier, a world leading, multiple-media publisher of scientific, technical, and health information products and services. *Electrochimica Acta* is peer-reviewed by internationally respected scientists, researchers and practitioners in the field of electrochemistry. The quality of the data and publication have been ensured by independent review of respected scientists familiar with other sources of thermodynamic data and would

recognize flaws in either the approach, data collection methods, or interpretation. Dr. Okada is an internationally recognized scientist with a life long career with the Research Institute of the Ministry of Economy, Technology, and Industry in Japan. He has authored dozens of publications in the field of electrochemistry.

The data obtained by Okada (1983, [DIRS 115556]) were measured for commercially pure titanium (equivalent to Ti Grade 2) at pH values from 3.5 to 4.5. The author indicated that only a marginally higher value was obtained under the same conditions for titanium plated with the noble metal platinum (Okada 1983 [DIRS 115556]). This clearly indicates that the primary controlling factor is the presence of oxide films, not the noble metal content of the electrode surface. In fact, according to Schutz (2003 [DIRS 168772] and references therein), alloy hydrogen absorption measured after corrosion in hot reducing acid media supports the slightly beneficial influence of platinum group metals in titanium. Therefore, the palladium-containing Ti Grade 7 alloy would be expected to exhibit similar absorption efficiency. This similarity between the absorption behavior of commercially pure titanium (Ti Grade 2) and Ti Grade 7 is supported by the measurements of Fukuzuka et al. (1980 [DIRS 151105]), who showed that, even under nonpassive conditions (boiling HCl), the rate of hydrogen absorption by Ti 0.15%Pd (equivalent to Ti Grade 7) was only a factor of two greater than for commercially pure titanium (Ti Grade 2). Since surface analytical evidence exists to show that the oxide film formed on Ti 0.15%Pd (1.25% HCl at 125°C) becomes more passive (i.e., thickens more slowly) with time than that on titanium (Shimogori et al. 1982 [DIRS 159778]), its ability to prevent hydrogen formation and absorption will improve more with time than that of pure titanium. This fact makes the adoption of a hydrogen absorption efficiency measured on titanium for use in the model with Ti Grade 7 conservative.

The majority of hydrogen absorption measurements have been performed under aggressive conditions not relevant to Yucca Mountain; i.e., under acidic conditions or with a large cathodic potential applied to simulate cathodic protection conditions. For more relevant conditions (concentrated brines at 150°C), Westerman (1990 [DIRS 151188]) measured only marginal hydrogen absorption (10 to < 30 μg/g) by Ti Grade 12 (an alloy more susceptible to hydrogen absorption than Ti Grades 16 and 7) over 12 to 18 months of exposure. The majority of the absorption appeared to occur in the first 6 months and then stopped. These measurements were made in the presence of a radiation field (3×10^4 Rad/h) and it is possible that the hydrogen permeability of the oxide films was reduced. An improvement in resistance of the passive film on Ti Grade 12, to hydrogen absorption in the presence of a radiation field, was also observed by Kim and Oriani (1987 [DIRS 110237]). Under cathodic polarization conditions in NaCl (pH = 1) negligible amounts of hydrogen were absorbed into Ti Grade 16 for applied potentials ≤ -600 mV$_{(SCE)}$ (Ikeda et al. 2000 [DIRS 159760]; Ikeda and Quinn 1998b [DIRS 152481]). In the absence of galvanic coupling, such negative potentials are unattainable under Yucca Mountain conditions.

Of particular relevance are the results of Shimogori et al. (1985 [DIRS 159784]) who measured the amount of hydrogen absorbed in dilute HCl as a function of pH (2 to 4), temperature (50°C to 250°C) and degree of aeration (deaerated and aerated). Over an exposure period of 10 days the amount of hydrogen absorbed increased with a decrease in pH and an increase in temperature for deaerated conditions. For the most relevant condition (pH = 4), absorption was immeasurable at

50°C and only 1-2 µg/g at 250°C. For aerated conditions, essentially no measurable hydrogen was absorbed irrespective of the pH or temperature over a similar exposure period. There is also experimental evidence that aeration suppresses hydrogen absorption by Ti-0.15Pd (equivalent to Ti Grade 7) more than it does to titanium (1% HCl, 70°C) (Fukuzuka et al. 1980 [DIRS 151105]). Because conditions within Yucca Mountain are expected to be oxidizing these results are consistent with the expectation that hydrogen absorption by the drip shield will be minor.

In light of this, it can be concluded that the input parameter values used in the hydrogen-induced cracking model are reliable and conservative. Therefore, the data provided by Okada (1983 [DIRS 115556] are qualified for its intended use in this model.

These parameters have been tabulated as shown in Table 4 as direct inputs. All of these direct input data and parameters are used to develop the model for evaluation of hydrogen-induced cracking effects on the drip shield.

In general, for the input parameters of the hydrogen-induced cracking model, a conservative approach is used in that input values at (or near) lower or upper bounds (as appropriate) are used to ascertain that the estimated output value is conservative. However, the primary sources of uncertainty in the hydrogen-induced cracking model are associated with the selection of values for the rate of general passive corrosion, R_{uc}, discussed in Section 5.5, and the fractional hydrogen absorption efficiency, f_h, discussed in Section 5.6. In evaluating the model, the maximum values for these parameters are used for a conservative estimate of hydrogen concentration in the drip shield.

Table 4. Direct Input

Parameter Name	Parameter Source	Parameter Value(s)	Units	Distribution (or single value if fixed)
ρ_{Ti} = Density of titanium	Weast 1978 [DIRS 128733], p. B-177	4.5	g/cm^3	Fixed value
M_{Ti} = Atomic weight of titanium	Weast 1978 [DIRS 128733], p. B-177	47.9	g/mol	Fixed value
R_{uc} = Rate of general passive corrosion (maximum)	LL990610605924.079 [DIRS 104994] BSC 2004 [DIRS 169845], Tables 13 and 14	3.20×10^{-4}, 1.13×10^{-4}	mm/yr	Maximum values from crevice specimens and from weight-loss specimens.
f_h = Fractional efficiency of hydrogen absorption	Okada 1983 [DIRS 115556]	0.015	N/A	Established upper bound value (see rationale for Assumption 5.6)
d_0 = Half of drip shield thickness	BSC 2003 [DIRS 171024]	7.5	mm	Fixed value
t = Duration of emplacement	10 CFR 63.114(d) [DIRS 156605]	10,000	years	Fixed value

4.2 CRITERIA

The technical work plan for *Regulatory Integration Modeling and Analysis of the Waste Form and Waste Package* (BSC 2004 [DIRS 169944], Table 3-1) has identified the following acceptance criteria (AC) from *Project Requirements Document* (Canori and Leitner 2003 [DIRS 166275]) and *Yucca Mountain Review Plan, Final Report* (NRC 2003 [DIRS 163274]). According to Table 3-1 of the TWP, this report is to address the following applicable acceptance criteria:

1. System Description and Demonstration of Multiple Barriers (Canori and Leitner 2003 [DIRS 166275], PRD-002/T-014, PRD-002/T-016; NRC 2003 [DIRS 163274], Section 2.2.1.1)

   - AC1: Identification of Barriers is Adequate
   - AC2: Description of the capability of Identified Barriers is Acceptable
   - AC3: Technical Basis for Barrier Capability is Adequately Presented.

2. Degradation of Engineered Barriers (Canori and Leitner 2003 [DIRS 166275], PRD-002/T-015; NRC 2003 [DIRS 163274], Section 2.2.1.3.1)

   - AC1: System Description and Model Integration are Adequate
   - AC2: Data are Sufficient for Model Justification
   - AC3: Data Uncertainty is Characterized and Propagated Through the Model Abstraction
   - AC4: Model Uncertainty is Characterized and Propagated Through the Model Abstraction
   - AC5: Model Abstraction Output is Supported by Objective Comparisons.

These criteria will be addressed in Section 8.4.

4.3 CODES, STANDARDS, AND REGULATIONS

The acceptance criteria listed in Section 4.2 are consistent with the methodology described in the ASTM Standard Practice C 1174 for prediction of the long-term behavior of engineered barrier system components in a geologic repository (ASTM C 1174-97 1998 [DIRS 105725]).

5. ASSUMPTIONS

The following assumptions are used for the hydrogen-induced cracking model in this report. The technical basis for each assumption is also provided so that each requires no further verification.

5.1 TI GRADE 7 IS SIMILAR OR SUPERIOR TO TI GRADE 16

Assumption: Due to the virtually identical chemical compositions and mechanical properties between Ti Grades 7 and 16 except the palladium content (and slightly lower carbon content for Ti Grade 16), available materials property data for Ti Grade 16 are assumed to be applicable to Ti Grade 7 if the said material property data are not available for Ti Grade 7.

Rationale: The background information on the various titanium alloys on this subject has been described in Section 1.2. This assumption is justified as follows:

The properties of materials, including mechanical properties and corrosion resistance, largely depend on microstructures that depend on the chemical compositions of the materials. The chemical compositions and mechanical properties, per ASTM B 265-02 [DIRS 162726], of the relevant titanium alloys, are shown in Table 1 and Table 2. In Table 1 and Table 2, Ti Grades 2, 12, 16, and 7 are α-alloys while Ti Grades 5 and 24 are α-β alloys. Ti Grade 7 contains slightly higher weight percent (wt %) of palladium (0.12 to 0.25 wt %) as compared to Ti Grade 16 (0.04 to 0.08 wt %). ASTM B 265-02 [DIRS 162726] specified mechanical properties are identical for Ti Grades 2, 16, and 7. They are also identical for Ti Grades 5 and 24 and for Ti Grades 9 and 18 regardless of the palladium contents of these materials (Table 2) (ASTM B 265-02 [DIRS 162726]).

The fact that addition of a small amount of palladium does not alter the mechanical properties of titanium alloys is schematically shown in Table 1 and Table 2. The alloys grouped by dotted lines in Figure 1 have identical mechanical properties regardless of their chemical compositions (particularly, palladium), implying that these alloys have very similar, if not the same, microstructures. While further addition of palladium to Ti Grade 16 to yield Ti Grade 7 does not affect the mechanical properties of the titanium alloys, the resistance to general and localized corrosion is improved in Ti Grade 7 (Schutz 2003 [DIRS 168772]). These two materials have almost identical chemical compositions, except that Ti Grade 7 contains 0.12-0.25 wt.% palladium while Ti Grade 16 contains 0.04 to 0.08 wt % palladium (Table 1). Ti Grade 16 was used as an analog of Ti Grade 7 at the LTCTF for the 1-year and 5-year weight-loss tests due to its compositional similarity to Ti Grade 7. The corrosion performance of Ti Grade 7, because of its higher palladium content, is superior or at least equivalent to that of Ti Grade 16 (Schutz 2003 [DIRS 168772]).

Confirmation Status: This is a reasonable assumption based on the above rationale. No further confirmation is required.

Use in the Report: This assumption is used throughout this report.

5.2 THE CRITICAL HYDROGEN CONCENTRATION (H_C) OF TITANIUM GRADES 7 AND 16

Assumption: The H_C value for Ti Grade 7 is assumed to be at least 1,000 µg/g. This assumption is based on the results reported by Ikeda and Quinn (1998 [DIRS 144540], p. 7), indicating that the H_C value for Ti Grade 16 is between 1,000 and 2,000 µg/g and the similarity between Ti Grades 7 and 16 is rationalized in Section 5.1. This assumption is necessary because H_C data are not available for Ti Grade 7.

Rationale: The rationalization of this assumption is as follows:

- The only possibility that addition of palladium might deteriorate the resistance of titanium alloys to hydrogen-induced cracking is microstructural change. Ti Grade 16 was developed based on the corrosion performance of Ti Grade 7 with a more cost effective palladium content (0.04 to 0.08 wt %). Ti Grades 7 and 16 are virtually identical alloys except for palladium content (Figure 1, Table 1 and Table 2). Further increases of the palladium content from 0.04 to 0.08 wt % to 0.12 to 0.25 wt % does not influence the mechanical properties of the material as addition of palladium does not alter the microstructure of titanium alloys (Schutz and Xiao 1993 [DIRS 151167]).

- It is agreed that the titanium-palladium alloys should exhibit a higher H_C than titanium alloys without palladium (Greene et al. 2001 [DIRS 165241]). This is due predominantly to the prevention of hydrides formation in the matrix as a result of the higher solubility of hydrogen in the palladium-containing intermetallic particles (Shoesmith et al. 1997 [DIRS 112203]; Ikeda et al. 2000 [DIRS 159760]). Among the titanium alloys, the higher the H_C, the more resistant the alloy is to hydrogen-induced cracking.

- H_C is a function of the stress intensity factor (Shoesmith et al. 1995 [DIRS 117892]) and, therefore, is determined by both the hydrogen solubility and response to material stress. Ti Grades 7 and 16 are α-alloys containing minimal amounts of β-phase. It is reasonable to expect that both alloys (Ti Grades 7 and 16) will exhibit very similar responses to applied stresses in an acidic environment. Thus, the controlling factor in determining the H_C will be the solubility of the hydrogen in the alloy, which increases with palladium-content. Ti Grade 7 contains more intermetallic particles that can absorb more hydrogen.

The above evidence clearly suggests that the hydrogen-induced cracking behavior of Ti Grade 7 should be at least as good as, if not superior to, that of Ti Grade 16 (i.e., approximately 1,000 to 2,000 µg/g). Choosing the H_C as 1,000 µg/g that was at the lower end of those obtained for Ti Grade 16 for Ti Grade 7, is not only appropriate but also conservative.

The value of H_C for Ti Grade 7 in this assumption is conservative on a number of counts: (1) the value of 400 µg/g is the lower limit of the measured range of 400 to 1,000 µg/g measured at room temperature (~25°C) for Ti Grade 2 (Shoesmith et al. 1997 [DIRS 112203], pp. 7 to 11); (2) the temperature of the drip shield will be well above room temperature for the majority of its anticipated lifetime and Clarke et al. (1995 [DIRS 151093]) have shown H_C for Ti Grade 2 rises

to ~1,000 µg/g at a temperature of 92°C to 100°C; and (3) the value of 400 µg/g was measured for Ti Grade 2, whereas the value for Ti Grade 16, a palladium-containing α-alloy with identical chemical composition to Ti Grade 7, appears to be >1,000 µg/g (Ikeda and Quinn 1998 [DIRS 144540], p.7).

Confirmation Status: This assumption will be further validated in Section 7.3.2.

Use in the Report: This assumption is used in Sections 6.1.3 and 6.2.2.

5.3 OCCURANCE OF FAST FRACTURE WHEN CRITICAL HYDROGEN CONCENTRATION IS REACHED

Assumption: Failure of Ti Grade 7 drip shield by fast fracture is assumed to occur only when critical hydrogen concentration (i.e., H_C) has been achieved.

Rationale: For hydrogen concentrations below this value, the material can only fail by ductile overload, and requires a very high stress intensity factor that measurements have shown to be effectively independent of hydrogen concentration (Clarke et al. 1994 [DIRS 151092]; 1995 [DIRS 151093]; 1997 [DIRS 159758]). Under these conditions, plastic deformation and crack blunting occurs. For hydrogen concentrations above this critical value, a stress intensity factor sufficient to cause fast (brittle) fracture can be achieved before plastic deformation can blunt the crack. Once this condition is achieved, it is assumed that the stress intensity factor will be large enough for instantaneous brittle fracture to occur. This is a conservative assumption as the stress may not always be high enough when the critical hydrogen concentration is reached. Therefore, this assumption is conservative.

Confirmation Status: This is a conservative assumption and no further confirmation is required.

Use in the Report: This assumption is used throughout the report.

5.4 SOURCES OF HYDROGEN

Assumption: Only generation and absorption of hydrogen produced by general passive corrosion, localized corrosion and galvanic corrosion are considered in this report. Hydrogen generation by radiolysis of water is not a significant contributor to the sources of hydrogen.

Rationale: Mechanisms for hydrogen generation and absorption on a titanium surface may include a galvanic couple, hydrogen in atomic form from the corrosion process, and the direct absorption of hydrogen produced by water radiolysis. However, as indicated by Shoesmith et al. (1997 [DIRS 112203], p. 17), the direct absorption of radiolytically produced hydrogen is insignificant except at a combination of high dose rate ($>10^2$ Gy/h, where Gy is a unit of radiation exposure equal to 100 rad) and high temperature (>150°C), clearly unattainable under Yucca Mountain drip shield conditions. Therefore, hydrogen generated by radiolysis of water is not considered in this report.

Confirmation Status: This is a reasonable assumption and no further confirmation is required.

Use in the Report: This assumption is used in Sections 6.2.3 and 6.3.3.

5.5   CONSTANT CORROSION RATE

Assumption: The passive oxide film growth rate and, hence, the corrosion rate are assumed to be constant in time for the formula used to calculate the concentration of hydrogen in the metal (Shoesmith et al. 1997 [DIRS 112203], p. 22).

Rationale: This assumption is conservative. A less conservative assumption is that the rate decays with time as predicted by *General Corrosion and Localized Corrosion of the Drip Shield* (BSC 2004 [DIRS 169845], Section 7.2). It is also implicit in this assumption and this formula that any hydrogen absorbed into the titanium remains within the remaining wall thickness and is not subsequently removed as the general corrosion progresses with time.   This is another conservative assumption, as any titanium hydride formed within the alloy will be unstable with respect to titanium oxide (Beck 1973 [DIRS 151089]) and should, therefore, be removed by the general corrosion process.

Confirmation Status: This is a conservative assumption and no further confirmation is required.

Use in the Report: This assumption is used in Sections 6.1.5, 6.1.6, and 6.2.3.

5.6   FRACTIONAL EFFICIENCY OF HYDROGEN ABSORPTION

Assumption: The upper boundary of the fractional efficiency of hydrogen absorption, f_h, for titanium alloys, in the range of 0.005 to 0.015, as reported by Okada (1983 [DIRS 115556]) (which is used as the direct input in this report) can be used as the value for modeling hydrogen-induced cracking in this section.

Rationale: These values were taken from the results of experimental measurements by Okada (1983 [DIRS 115556]) performed under extremely aggressive environmental and test conditions. These aggressive electrochemically polarized conditions are considered unachievable in the repository. For example, in the work by Okada (1983 [DIRS 115556]), the fractional efficiency of hydrogen absorption was measured on Ti Grade 2 under constant applied current conditions with an applied current of 0.5 mA/cm^2 in acidic sodium sulfate solutions of pH = 4 (25°C). Under these conditions, the electrode potential achieved is < -1.0V$_{(SCE)}$, or 250 to 400 mV more negative than would be anticipated under even galvanic coupling conditions to carbon steel (Hodgkiess et al. 1987 [DIRS 159787]). At these potentials, redox transformations in the oxide render it permeable to hydrogen (Shoesmith et al. 1997 [DIRS 112203], Figure 2, p. 2). However, this permeability is not present under nongalvanic conditions.

Furthermore, although f_h decreases with time as noted by Noel et al. (1996 [DIRS 111940], Figure 18) and Tomari et al. (1999 [DIRS 159786], Table 1), a value of 0.015 has been conservatively assumed constant throughout 10,000 years.   This value is exceedingly conservative in comparison with the f_h value of 0.00014 reported by Tomari et al. (1999 [DIRS 159786], Table 1) on the basis of experiments conducted for 1,440 hours under electrochemically polarized conditions.

Confirmation Status: This is a conservative assumption and no further confirmation is required.

Use in the Report: This assumption has been used in Sections 6.1.5, 6.1.6, 6.2.3, 6.3.3, and 6.3.6.

5.7   GALVANIC COUPLING EFFECT

Assumption: The extent of galvanic corrosion due to coupling between carbon steel and Ti Grade 7 will be limited by the small area of wet contact between these two metals and the low cathode-to-anode ratio (Ti/Fe), which is likely to approach unity.

Rationale: This is a rational assumption because the point of galvanic contact also simultaneously experiencing seepage drips will be an incident of very low probability. The resulting inability of the site to remain wet due to runoff and the accumulation of iron oxide corrosion products will significantly impede galvanic corrosion. The passivating effects of iron oxides on the titanium surface and the presence of ferric ions in the corrosive solutions are well known in the scientific literature (Covington and Schutz 1981 [DIRS 151098]; Schutz and Thomas 1987 [DIRS 144302]). In view of these limitations, the mass of steel that could be consumed by galvanic corrosion and the initial contact area are assumed to be limited to 22.73 kg (50 lbs) and 75 cm^2, respectively.

Confirmation Status: This is a reasonable assumption and no further confirmation is required.

Use in the Report: This assumption is used in Section 6.3.4 and Section 6.3.6.

INTENTIONALLY LEFT BLANK

6. MODEL DISCUSSION

6.1 DESCRIPTION OF MODEL FOR HYDROGEN-INDUCED CRACKING

6.1.1 Introduction

The purpose of this report is to evaluate whether the drip shield will fail by hydrogen-induced cracking under repository conditions within 10,000 years of permanent closure. This report provides the basis for excluding FEP 2.1.03.04.0B, Hydride Cracking of Drip Shields, in the LA FEP List (DTN: MO0407SEPFEPLA.000 [DIRS 170760]).

The drip shield will experience a wide range of conditions during its expected service life, as briefly reviewed in Section 1.3 and detailed in *Engineered Barrier System: Physical and Chemical Environment* (BSC 2004 [DIRS 169860]) and *Environment on the Surfaces of the Drip Shield and Waste Package Outer Barrier* (BSC 2004 [DIRS 161237]). Initially, the underlying waste packages will be relatively hot, and drip shield surfaces will be dry due to the heat generated from radioactive decay. The temperature will eventually drop to levels where both humid air and aqueous phase corrosion will be possible. Crevice corrosion and slow general passive corrosion may be initiated and propagate in the metal. Both types of corrosion will produce hydrogen, which can be absorbed into the metal (Shoesmith et al. 1997 [DIRS 112203], p. 2). In a drip shield design without backfill, hydrogen generation may be caused by the galvanic couple between the titanium drip shield surface and the ground support (such as rock bolts, wire mesh, and steel liners used in the drift), which can fall onto the drip shield surface.

Breach occurs if (1) the wall penetration by corrosion exceeds the corrosion allowance or if (2) the amount of hydrogen absorbed exceeds the critical hydrogen concentration, H_C, for breach due to hydrogen-induced cracking (Clarke et al. 1994 [DIRS 151092], Figure 8). The first type of breach mechanism (i.e., wall penetration by crevice and general corrosion) is treated in another report (BSC 2004 [DIRS 169845]). This report deals with the breach mechanism associated with hydrogen-induced cracking.

Hydrogen-induced cracking is characterized by decreased fracture toughness and loss of ductility of the metal due to absorbed atomic hydrogen. The usual mechanical breach mode for a ductile material is the ductile tearing observed during slow crack growth. Decreased fracture toughness causes fast crack growth (brittle fracture) of a normally ductile material under sustained load. During slow crack growth, the material will fail as the stress intensity factor, K, reaches a value K_S, defined as the threshold stress intensity factor for slow crack growth. During fast crack growth sustained by slow straining, the same material will fail as the stress intensity factor K reaches a value K_H, the threshold stress intensity factor for hydrogen-induced cracking, which is lower than K_S (Shoesmith et al. 1997 [DIRS 112203]).

Figure 3 schematically represents the combinations of stress intensity factor and hydrogen concentration leading to (1) fast crack growth (brittle fracture) controlled by K_H, (2) slow crack growth controlled by K_S due to either sustained load cracking or ductile rupture, or (3) no breach (Shoesmith et al. 1997 [DIRS 112203], p. 9, Figure 7). Provided that the hydrogen concentration is lower than the critical value (i.e., H_C), then $K_S < K_H$ and crack growth will occur by either ductile tearing or slow crack growth. For this process, the required K_S varies almost

insignificantly with hydrogen content (Clarke et al. 1994 [DIRS 151092]; 1995 [DIRS 151093]; 1997 [DIRS 159758]). In the case where the hydrogen content in metal exceeds H_C, $K_S > K_H$, the slow crack growth or ductile rupture can no longer prevent the achievement of a high enough stress intensity factor for brittle (fast) failure. For this process, the threshold stress intensity factor (K_H) decreases with hydrogen content, as shown schematically in Figure 3.
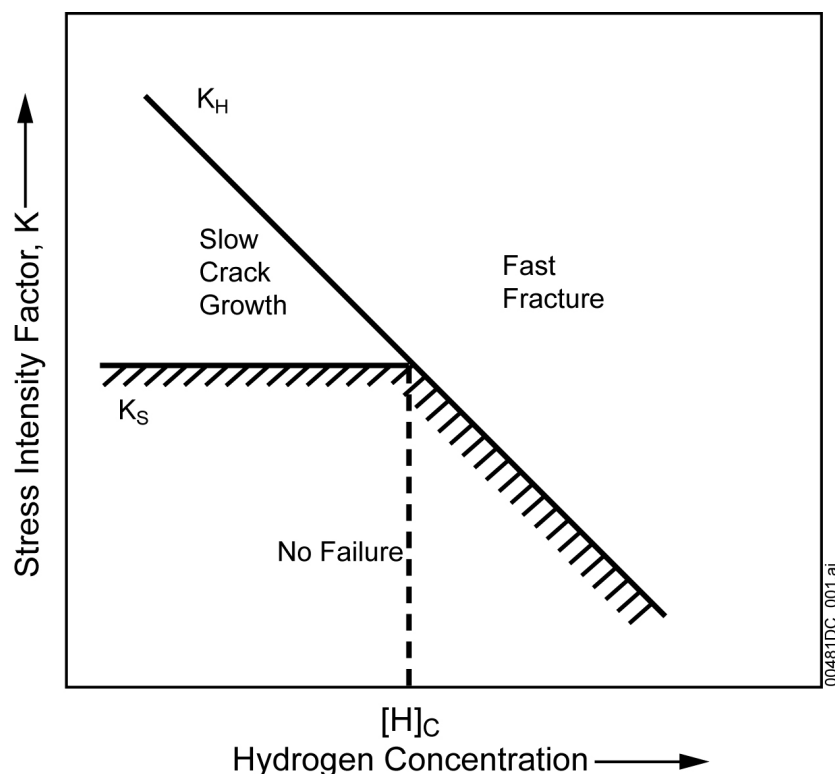
Source: Shoesmith et al. 1997 [DIRS 112203]

NOTE: This schematic shows the combinations of stress intensity factor and hydrogen concentration leading either to fast crack growth (brittle failures) or to slow crack growth due to either sustained load cracking or ductile rupture or to no failure.

Figure 3. Combinations of Stress Intensity Factor and Hydrogen Concentration

It should be pointed out that fast crack growth does not always occur even when the hydrogen content in metal exceeds H_C if the stress intensity is not high enough in the area. However, as a conservatism, the stress intensity is always sufficiently high such that fast fracture occurs once H_C is achieved (Section 5.3).

For hydrogen-induced cracking due to corrosion processes, an approach has been adopted to predict when hydrogen-induced cracking might become a potential failure process for the drip shield, following a Canadian precedent (Shoesmith et al. 1997 [DIRS 112203]). The basic premise of the model is that failure will occur once the hydrogen content exceeds a certain limit or critical value, where $K_S > K_H$.

The major corroborating or supporting information and how it is used in this section is listed in Table 5. Other references cited in this section are also used as the corroborating or supporting

information for model development. The input status of these references is detailed in the DIRS report (Column 5) and throughout the discussion in this section.

Table 5. Source of Major Corroborating and Supporting Information and its Usage in Model Development

Source	Description	Used In
Schutz and Thomas 1987 [DIRS 144302]	Three conditions for hydrogen-induced cracking to occur.	Section 6.1
Shoesmith et al. 1997 [DIRS 112203]	Combinations of Stress Intensity Factor and Hydrogen Concentration. Hydrogen concentration in metal as calculated from corrosion rate.	Section 6.1
Ikeda and Quinn 1998 [DIRS 144540]	H_C for Ti Grade 16	Assumption 5.2
ASM International 1987 [DIRS 103753], p. 235.	Galvanic series of metals in seawater.	Section 6.3
BSC 2004 [DIRS 169845]	*General Corrosion and Localized Corrosion of the Drip Shield*	Entire

6.1.2   Processes by Which Hydrogen is Absorbed

Schutz and Thomas (1987 [DIRS 144302], p. 673) identified factors that can lead to hydrogen-induced cracking in aqueous media. The three general conditions that must exist simultaneously for the hydrogen embrittlement of α alloys are:

1. A mechanism for generating nascent hydrogen on a titanium surface. The mechanisms may include a galvanic couple, hydrogen produced in the atomic form by a corrosion process, and the direct absorption of hydrogen produced by water radiolysis. As indicated in Section 5.4, the direct absorption of radiolytically produced hydrogen is insignificant except at a combination of high dose rate ($>10^2$ Gy/h (10^4 rad/h)) and high temperature ($>150°C$), clearly unattainable under Yucca Mountain drip shield conditions. Therefore, only hydrogen produced by possible corrosion processes are considered in this report.

2. A metal temperature above approximately 80°C (175°F) when the diffusion rate of hydrogen into α titanium becomes significant.

3. A solution pH less than 3 or greater than 12 or impressed potentials more negative than 0.7 $V_{(SCE)}$. Both crevice corrosion and general passive corrosion will be accompanied by hydrogen production and, hence, possibly by the absorption of hydrogen into the metal.

For crevice corrosion, the hydrolysis of dissolved metal cations leads to acidification within the occluded area and the development of active conditions in which the metal is unprotected by an oxide film. Once initiated, crevice corrosion is supported by reduction of oxygen on passive surfaces external to the crevice and reduction of protons (Ti + 4H$^+$ $\rightarrow$ Ti^{4+} + 2H$_2$) on metal surfaces inside the crevice. The latter process can lead to the absorption of atomic hydrogen into the metal in sufficient quantities to produce extensive hydride formation (Shoesmith et al. 1997 [DIRS 112203], Figure 3, p. 4).

For the passive noncreviced or inert crevice conditions expected to prevail, the corrosion of the titanium alloy will be sustained by reaction with water under neutral conditions ($Ti + 2H_2O \rightarrow TiO_2 + 2H_2$) and will proceed at an extremely slow rate. This process will generate hydrogen, which must pass through the TiO_2 film before absorption into the underlying titanium alloy. Redox transformations (Ti(IV) $\rightarrow$ Ti(III)) in the film are required before the oxide becomes significantly transparent to hydrogen (Hua et al. 2004 [DIRS 167022]). Significant cathodic polarization of the metal (only achievable by galvanic coupling to carbon steel or the application of a cathodic protection potential) is required for these transformations to occur. Measurements of absorbed hydrogen suggest a threshold potential of -0.6 $V_{(SCE)}$, above which no absorption occurs (Shoesmith et al. 1997 [DIRS 112203], p. 4; Murai et al. 1977 [DIRS 111926]). Only impressed current cathodic protection or galvanic coupling to active alloys such as iron, Zn, or Mg could produce such cathodic potentials. The general corrosion rates of titanium alloys (e.g., Ti Grade 7) under the repository conditions are very low (BSC 2004 [DIRS 169845]). Thus, hydrogen generation rates, and, hence hydrogen absorption rates, are expected to be very low on titanium alloy surfaces under the repository conditions.

6.1.3 Critical Hydrogen Concentration, H_C

Provided that wall penetration by corrosion does not exceed the corrosion allowance, cracking failure is assumed (Section 5.3) to occur when the material has absorbed sufficient hydrogen so that the hydrogen content in metal exceeds the critical hydrogen content (H_C). This is a conservative assumption as it assumes that the slightest hydrogen-induced degradation in fracture toughness will lead to instant brittle fracture (i.e., there is always a sufficiently high stress intensity factor that brittle (fast) fracture is inevitable). In view of the uncertainties involved in stress intensity features such as that introduced by rock impact, this conservatism is judicious.

H_C can be experimentally measured. Some of the observations regarding the critical hydrogen content, H_C, for Ti Grades 2 and 12 are summarized below:

- Using the slow strain rate technique on precracked compact tension specimens precharged with known amounts of hydrogen, it has been shown that the fracture toughness of Ti Grades 2 and 12 is not significantly affected until the hydrogen content exceeds H_C. Once above H_C, there is no slow crack growth, and only fast crack growth is observed.

- H_C is sensitive to the microstructure and texture of the material with respect to the orientation of the crack and the applied stress. Preferential pathways for cracking are formed along β-phase stringers introduced through the manufacturing process. An H_C of 500 µg/g has been measured in Ti Grade 12 containing cracks propagating in the directions defined by these stringers. Crack propagation perpendicular to these features is not observed up to H_C = 2,000 µg/g. Heat treatment to remove this laminar structure by randomly reorienting the residual β-phase can lead to a decrease in H_C to ~400 µg/g.

- Even for manufactured plate materials that do not have high β-phase content (e.g., Ti Grade 2) the laminar structure introduced by rolling appears to dominate the

cracking behavior. As a consequence, depending on crack orientation, H_C varies between ~400 and 1,000 µg/g. Since Ti Grade 2 does not contain as much β-phase as Ti Grade 12, heat treatment does not exert a significant influence on H_C. Welding produces a larger change in the microstructure than does heat treatment. The high weld temperature results in significant microstructural changes in the weldment. This results in a small decrease in strength. The heat affected zone does not appear to be sufficiently large to influence the cracking behavior because, for both Ti Grades 2 and 12, H_C is slightly decreased near the weld metal compared to the base metal. It did not decrease below 500 µg/g.

- Hydrogen solubility would be higher at elevated temperature. It has been shown experimentally that H_C increases markedly with temperature (Clarke et al. 1995 [DIRS 151093]). While the maximum critical stress intensity factor for Ti Grade 2 decreases slightly from ~50 MPa·m$^{1/2}$ to ~40 MPa·m$^{1/2}$ at 95°C, only slow crack growth was observed up to hydrogen concentrations of ~2,000 µg/g, clearly indicating an enhanced resistance to growth of brittle-like cracks as the temperature is increased. Therefore, the failure is less likely at elevated temperature. A similar increase in resistance to brittle fracture was observed for Ti Grade 12 at 95°C, the maximum stress intensity factor decreasing from ~60MPa·m$^{1/2}$ to ~45 MPa·m$^{1/2}$, while H_C increased to ~1,000 µg/g (Clarke et al. 1995 [DIRS 151093]). Preliminary creep measurements clearly indicate that increased creep deformation at higher temperatures was a major factor in preventing the development of a sufficiently high stress concentration to initiate fast fracture (Clarke et al. 1995 [DIRS 151093]).

- H_C data are not available for Ti Grade 7, but more recent data reported by Ikeda and Quinn (1998 [DIRS 144540], p. 7) indicates that the H_C value for Ti Grade 16 is between 1,000 and 2,000 µg/g. As noted in Section 1, Ti Grades 7 and 16 are similar alloys because of their similar chemical compositions.

- The H_C value for Ti Grade 7 is assumed to be at least 1,000 µg/g (Section 5.2). This assumption is based on the discussion in Section 1.2 and Section 5.1 and the data reported by Ikeda and Quinn (1998 [DIRS 144540], p. 7), which, as indicated earlier, concluded that the H_C value for Ti Grade 16 is between 1,000 and 2,000 µg/g. This assumption is necessary because H_C data are not available for Ti Grade 7. This assumption has been justified in Section 5.2 as it is agreed that the titanium-palladium alloys should exhibit a higher H_C than titanium alloys without palladium (Greene et al. 2001 [DIRS 165241]) and this is due predominantly to the prevention of hydrides formation in the matrix as a result of the higher solubility of hydrogen in the palladium-containing intermetallic particles (Shoesmith et al. 1997 [DIRS 112203]; Ikeda et al. 2000 [DIRS 159760]).

6.1.4 Hydrogen Absorption During Crevice Corrosion

Crevice corrosion, if it initiates, will propagate at a rate much higher than that of general corrosion and, therefore, generate more hydrogen on the metal surface. Crevice propagation can lead to failure by wall penetration as well as failure due to hydrogen-induced cracking because of the hydrogen absorbed into the metal.

The most effective way to reduce hydrogen absorption is to choose a more crevice corrosion resistant alloy (Shoesmith et al. 1997 [DIRS 112203], p. 15). Improvement in resistance to crevice corrosion, in case of titanium alloys (e.g. Ti Grades 16 and 7) has been attributed to alloying elements, which reinforce passivity (Schutz 2003 [DIRS 168772]; Hua et al. 2004 [DIRS 167022]). Susceptibility to crevice corrosion is eliminated through the alloying series Ti Grade 2→Ti Grade 12→Ti Grade 16 (Shoesmith et al. 1997 [DIRS 112203], p. 15). In accordance with *Waste Package Materials Properties* (CRWMS M&O 1999 [DIRS 102933], pp. 49 and 51), the major additions (to Ti Grade 2) are molybdenum (0.2 to 0.4%) and nickel (0.6 to 0.9%) for Ti Grade 12 and palladium (0.04 to 0.08%) for Ti Grade 16. Decreased crevice corrosion rates are achieved by adding alloying elements such as molybdenum and nickel to produce Ti Grade 12 and palladium to produce Ti Grade 16 are noted in Shoesmith et al. (1997 [DIRS 112203], p.16), and discussed in recent reviews of titanium crevice corrosion behavior (Schutz 1988 [DIRS 151163]; Schutz 2003 [DIRS 168772]; Hua et al. 2004 [DIRS 167022]). The nickel and molybdenum in Ti Grade 12 segregate at grain boundaries and form intermetallics that improve the resistance to crevice corrosion of the alloy. Thus, while some crevice corrosion occurs in Ti Grade 2, only minor crevice corrosion damage prior to repassivation occurs in Ti Grade 12. The effect of adding palladium to ennoble titanium while avoiding segregation in Ti Grade 16 further improves the resistance to crevice corrosion, and no crevice corrosion damage is observed in Ti Grade 16 experiments.

Crevice corrosion is one form of localized corrosion of a metal surface (ASM International 1987 [DIRS 103753], p. 4). The model developed by *General Corrosion and Localized Corrosion of the Drip Shield* (BSC 2004 [DIRS 169845], Section 6.6) for the Ti Grade 7 drip shield assumes that localized attack occurs only if the corrosion potential, E_{corr}, equals or exceeds the threshold potential for breakdown of the passive film, $E_{critical}$. Experimental measurements reported by *General Corrosion and Localized Corrosion of the Drip Shield* (BSC 2004 [DIRS 169845], Section 6.6) for E_{corr} and $E_{critical}$ were obtained from experiments under various test environments expected in the repository. These test environments include simulated dilute water (SDW), simulated concentrated water (SCW), and simulated acidic concentrated water (SAW) at 30°C, 60°C, and 90°C, as well as simulated saturated water (SSW) at 100°C and 120°C. SCW is about one thousand times more concentrated than J-13 well water and is slightly alkaline (pH~8). SAW is about one thousand times more concentrated than J-13 well water and is acidic (pH~2.7). J-13 well water (Harrar et al. 1990 [DIRS 100814]) representative of that expected at Yucca Mountain. The experimental measurements show that the threshold $E_{critical}$ is consistently greater than E_{corr}. The relevance of these test media to the in-drift chemical environments in the repository is briefly reviewed in Section 1.3 of this report.

It is, therefore, concluded that although enhanced hydrogen absorption due to crevice corrosion or any other form of localized corrosion such as pitting will not occur, it is treated the same as the general corrosion in the hydrogen-induced cracking model.

6.1.5 Hydrogen Absorption During General Passive Corrosion

According to Shoesmith et al. (1997 [DIRS 112203], p. 15), there are two processes by which hydrogen could be produced, and possibly absorbed, under passive conditions: (1) direct absorption of hydrogen produced by water radiolysis and (2) absorption of atomic hydrogen

produced by the corrosion process to produce oxide. The direct absorption of radiolytically produced hydrogen is insignificant except at high dose rate ($>10^2$ Gy/h (10^4 rad/h)) and high temperature ($>150°C$) (Shoesmith et al. 1997 [DIRS 112203], p. 17). Therefore, the direct absorption of radiolytically produced hydrogen is not considered in this report, as the condition will be unattainable under Yucca Mountain drip shield conditions. This leaves the corrosion process as the only feasible source of hydrogen for absorption.

Under anoxic conditions, when passive corrosion should prevail, the corrosion potential for passive titanium must reside at a value, at which water reduction can couple to titanium oxidation:

$$Ti + 2H_2O \rightarrow TiO_2 + 2H_2$$
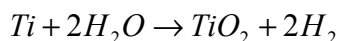
and, hence, must be at or more negative than the thermodynamic stability line for water. At such potentials, titanium hydrides are thermodynamically stable with respect to the metal. Consequently the passive film can be considered only as a transport barrier and not as an absolute barrier. The rate of hydrogen absorption at the corrosion potential will be controlled by the rate of the corrosion reaction, which dictates the rate of production of absorbable hydrogen. Since titanium oxide, TiO_2, is extremely stable and protective in the drip shield environment, the corrosion reaction will be effectively limited to an oxide film growth reaction.

While the rate of hydrogen production and, hence, absorption may be assumed directly proportional to the rate of film growth, the fraction of hydrogen absorption must be determined. Based on experimental measurements by Okada (1983 [DIRS 115556]), a value in the range of 0.005 to 0.015 may be adopted for f_h. These values represent the minimum and maximum pH values measured between 4 and 5.

Using this range of fractional efficiency of hydrogen absorption for Ti Grade 7 under repository conditions is conservative because (1) they were measured on Ti Grade 2, which is an unalloyed titanium; and (2) they were obtained under constant applied current conditions with an applied current of 0.5 mA/cm^2 at 25°C in sodium sulfate solutions at pH = 4, a condition not achievable under the repository condition. Indeed the electrode potential achieved during these experiments (-1.14 V$_{(SCE)}$) was about 500 mV more negative than the threshold value (-0.6 V$_{(SCE)}$) for hydrogen absorption. Moreover, the applied current density used was 5×10^5 nA/cm^2 (0.5 mA/cm^2), about five orders of magnitudes higher than a value of 2.85 nA/cm^2 (2.85×10^{-3} mA/cm^2), a current density value converted from the general corrosion rate of 50 nm/yr (the 70th percentile value of general corrosion rates measured on weight loss and crevice specimens of Ti Grade 16 at the LTCTF) (BSC 2004 [DIRS 169845], Section 6.5). Similar measurements on platinum- and nickel-coated Ti Grade 2 specimens gave a value of f_h only marginally higher under these conditions. Therefore, using a fractional efficiency of hydrogen absorption of 0.005 to 0.015 for Ti Grade 7 under repository conditions is sufficiently conservative.

Based on a constant film growth rate and, hence, corrosion rate, Shoesmith et al. (1997 [DIRS 112203], p. 22) indicated that the concentration of hydrogen in the metal, H_A, (in g/mm^3) can be calculated as a function of time of emplacement (t in years) from the expression:

$$H_A = 4(\rho_{Ti}/10^3)f_h R_{uc}t[M_{Ti}(d_o - R_{uc}t)]^{-1} \qquad \text{(Eq. 1)}$$

where

H_A = hydrogen content in metal (g/mm^3)

ρ_{Ti} = density of Ti (g/cm^3) = 4.5 (Weast 1978 [DIRS 128733], p. B-177)

f_h = fractional efficiency for hydrogen absorption

R_{uc} = rate of general passive corrosion (mm/year)

t = duration of emplacement (years)

M_{Ti} = atomic mass of Ti = 47.9 (g/mol) (Weast 1978 [DIRS 128733], p. B-177)

d_0 = half of drip shield thickness (mm)

Considering a Ti Grade 7 plate with 1 mm^2 surface area, it is noted in Equation 1 that (1) the amount of hydrogen in grams produced by the general corrosion after t years of emplacement is $4(\rho_{Ti}/10^3)R_{uc}t/M_{Ti}$ from the reaction $Ti + 2H_2O \rightarrow TiO_2 + 2H_2$, (2) multiplication by the factor f_h converts the produced hydrogen into absorbed hydrogen, and (3) the remaining volume of Ti Grade 7 alloy in mm^3 is represented by $(d_o - R_{uc}t)$. The derivation of Equation 1 is based on a constant general corrosion rate. It was noted in *General Corrosion and Localized Corrosion of the Drip Shield* (BSC 2004 [DIRS 169845], Section 7.2) that the assumption of constant corrosion rate is conservative, and less conservative corrosion cases consider the corrosion rate decreases with time. It was also noted above that it is conservative to assume that all the hydrogen absorbed during general corrosion is retained within the remaining drip shield wall thickness as the general corrosion process proceeds. It is most likely that the majority of it will be removed by conversion to the more thermodynamically stable titanium oxide as corrosion progresses or diffuse out.

Using the relationship H (μg of H/g of titanium) = H (g of H/mm^3 of titanium)(1,000)/($10^{-6}\rho_{Ti}$), Equation 1 can be rewritten for H_A in μg/g as follows:

$$H_A = 4 \times 10^6 f_h R_{uc}t[M_{Ti}(d_o - R_{uc}t)]^{-1} \qquad \text{(Eq. 2)}$$

where

H_A = hydrogen content (μg/g)

The rate of general passive corrosion, R_{uc}, can be calculated from the rate of oxide film thickness, R_{ox} by the following formula:

$$R_{uc} = R_{ox}(\rho_{ox}/M_{ox})(\rho_{Ti}/M_{Ti})^{-1} \qquad \text{(Eq. 3)}$$

where

ρ_{ox} = density of the oxide (g/cm^3)

M_{ox} = *molecular* mass of the oxide (g)

Since the value of $(\rho_{ox}/M_{ox})(\rho_{Ti}/M_{Ti})^{-1}$ is always greater than unity, it is conservative to assume that $R_{uc} = R_{ox}$.

The average general corrosion rate (R_{uc}) of the values reported in Section 4.1 (Table 4) will be used for the estimation of hydrogen concentration of the drip shield (Section 6.2.3).

6.1.6 Alternative Conceptual Model for Hydrogen-Induced Cracking Under General Passive Corrosion Conditions

The model developed herein, as described in Section 6.1.5, is based on the use of a constant general passive corrosion rate of titanium, which is constant over the lifetime of the drip shield. It is assumed that this process will be driven by the reaction of titanium with water to produce hydrogen and that a constant fraction of the corrosion-generated hydrogen will be absorbed into the alloy (Assumptions 5.4 and 5.6).

Since the measured corrosion rates (taken from LTCTF measurements) are low, absorbed hydrogen will diffuse deeply into the alloy rather than accumulate at the corroding surface to be released as the corrosion front progresses into the metal. As a consequence, hydride formation would occur uniformly throughout the wall thickness. Furthermore, it is assumed (Assumption 5.6) that, once absorbed, hydrogen would not be released, leading to a predicted long term acceleration in the rate of hydrogen accumulation as the volume of available metal is reduced by conversion to oxide. As failure by hydrogen-induced cracking could occur once a critical hydrogen concentration (H_C) is achieved, this acceleration leads to a very rapid achievement of this critical value and, hence, a very conservative prediction of failure times by hydrogen-induced cracking.

Key conservatisms adopted in the primary model are the following:

1. Corrosion of titanium will be driven by interaction with water to produce absorbable hydrogen (Assumption 5.4). Since conditions will be oxidizing, reaction will be predominantly with dissolved oxygen, a process that does not produce hydrogen.

2. Corrosion rates will be maintained constant over the lifetime of the drip shield (Assumption 5.5).

3. Hydrogen release by conversion of the metal containing hydrogen to oxide as the corrosion progresses is negligible (Assumption 5.5).

4. The value of the fractional efficiency of hydrogen absorption (f_h) obtained under extremely aggressive test conditions is used and assumed to be constant (Assumption 5.6).

An alternative, more realistic, and hence, less conservative, conceptual model can be defined by relaxing conservatisms (2) and (3). The retention of the first conservatism is judicious, because

titanium corrosion could be, at least partially, supported by water reduction in the concentrated saline environments possible as a consequence of evaporative concentration of seepage waters contacting the alloy surface. In these environments, the dissolved oxygen concentration would be low until temperatures cooled and salinity levels declined. This assumption is conservative as, with time, support of the general passive corrosion of titanium would be expected to shift from water reduction to oxygen reduction as the concentration of dissolved oxygen in the water increased with decreasing temperatures. As a consequence, the total amount of hydrogen produced and, hence, the fraction absorbed would decrease.

In this alternative model, the corrosion rate is given by the passive oxide film growth rate as before but is taken to decrease with time as the oxide thickens and becomes more impermeable to hydrogen. The rate of hydrogen absorption is directly proportional to the corrosion rate and the amount of hydrogen absorbed, calculated in the identical manner to that used in the performance assessment model. This means that this alternative model incorporates the same efficiency factor for hydrogen absorption. Consequently, the new model will predict a decrease in hydrogen absorption rate with a time-dependency equal to that for the decrease in corrosion rate.

As in the primary model, the rate of diffusion of hydrogen in the titanium is taken to be rapid compared to the corrosion rate. Consequently, absorbed hydrogen will be dispersed throughout the full wall thickness (i.e., the concentration of hydrogen in the metal will be the same throughout). However, some hydrogen will be released as corrosion of the hydrogen-containing alloy continues. The rate of release will be proportional to the corrosion rate and to the concentration of hydrogen that exists in the metal at that time.

The criterion for failure remains the same as in the primary model (i.e., failure could occur instantly once the amount of hydrogen in the material (H_A) exceeds the critical value (H_C)). The value of H_C remains unchanged.

A schematic comparison of the original and the alternative conceptual models is given in Figure 4 and Figure 5. The terms are defined as follows:

R_{Corr} = corrosion rate of titanium
R_{HA} = rate of hydrogen absorption into titanium
f_h = fractional efficiency of hydrogen absorption
R_{HR} = rate of absorbed hydrogen release due to continuing corrosion
n_1 = time exponent for the decrease in corrosion rate with time, t
k = oxide film growth constant
J_H = flux of hydrogen in the metal at time t
$(H_{Ti})_t$ = concentration of hydrogen in the metal at time t
H_C = critical hydrogen concentration in the metal for failure by hydrogen-induced cracking.

Repository Environment | **Titanium Drip Shield**

R_{Corr} = Constant

$J_H \gg R_{Corr}$

$R_{HA} = f_h R_{Corr}$

$R_{HR} = 0$

H_C

R_{Corr}

H_A

R_{HA}

Predicted time to failure by HIC   Time

00142DR_Figure 2.ai
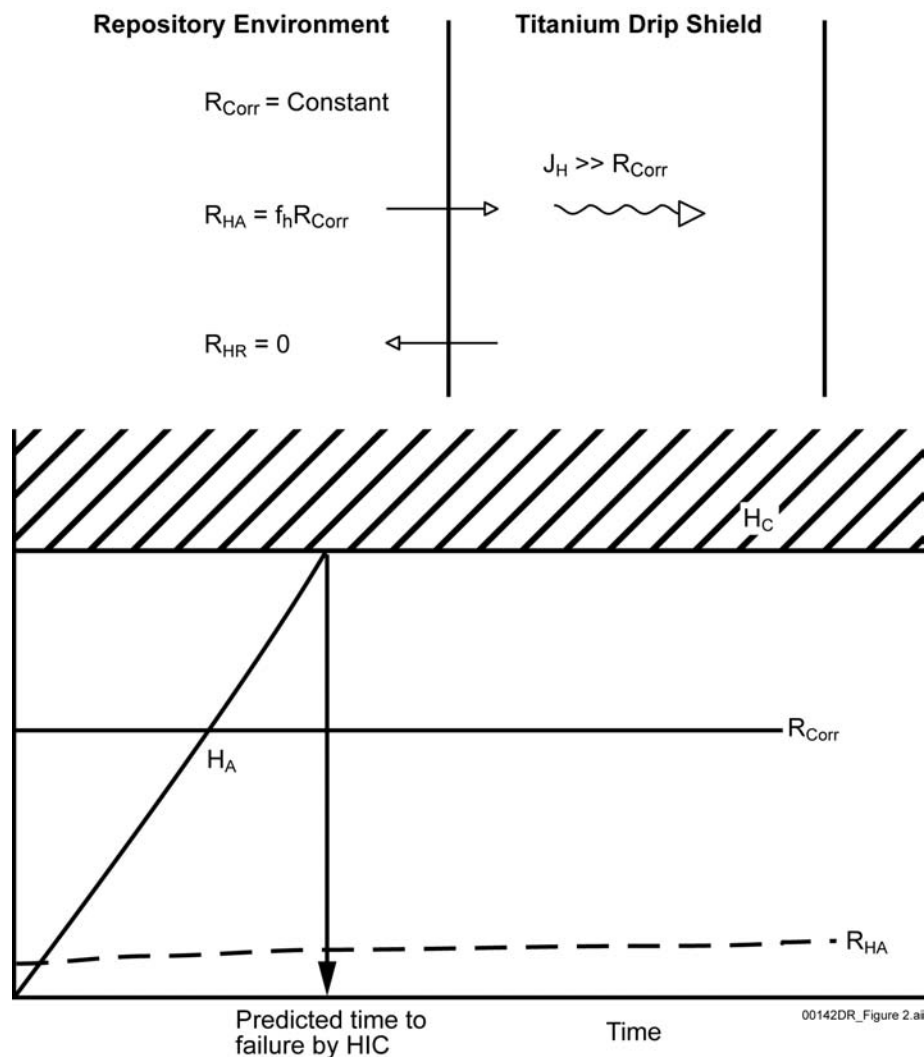
NOTE: This schematic shows hydrogen absorption during passive general corrosion of titanium (refers to the mathematical model described in Section 6.1.5)

Figure 4. A Schematic Representation of the Hydrogen Absorption Conceptual Model

The expected decrease in corrosion rate with time is the accepted mechanism for passive film growth in exposure environments in which the metal cation has a very low solubility as is the case for titanium in neutral to alkaline solutions (Baes and Mesmer 1986 [DIRS 100702]). Such a decrease in corrosion rate has been observed for titanium alloys in tests conducted in the LTCTF at LLNL (BSC 2004 [DIRS 169845], Section 7.2).

Considerable electrochemical evidence exists to demonstrate that the rate of film growth decreases with time (Leitner et al. 1986 [DIRS 159791]; McAleer and Peter 1982 [DIRS 159793]; Nishimura and Kudo 1982 [DIRS 159794]; Beck 1982 [DIRS 159792]) according to the field-assisted ion-transport mechanism when subjected to a constant applied potential.   While in these studies the potential driving oxide growth was applied electrochemically, a similar decrease in film growth rate with time would be expected to occur due to the open-circuit polarization of titanium by a soluble redox reagent in an aqueous solution (e.g., O_2).

Repository Environment | **Titanium Drip Shield**

$$R_{Corr} = kt^{-n_1}$$

$$J_H \gg R_{Corr}$$

$$R_{HA} = f_h R_{Corr}$$

$$R_{HR} = kR_{Corr}(H_{Ti})_t$$

H_C

H_A

R_{Corr}

R_{HA}
R_{HR}

Time

Predicted time to
failure by HIC

00142DR_Figure 3.ai
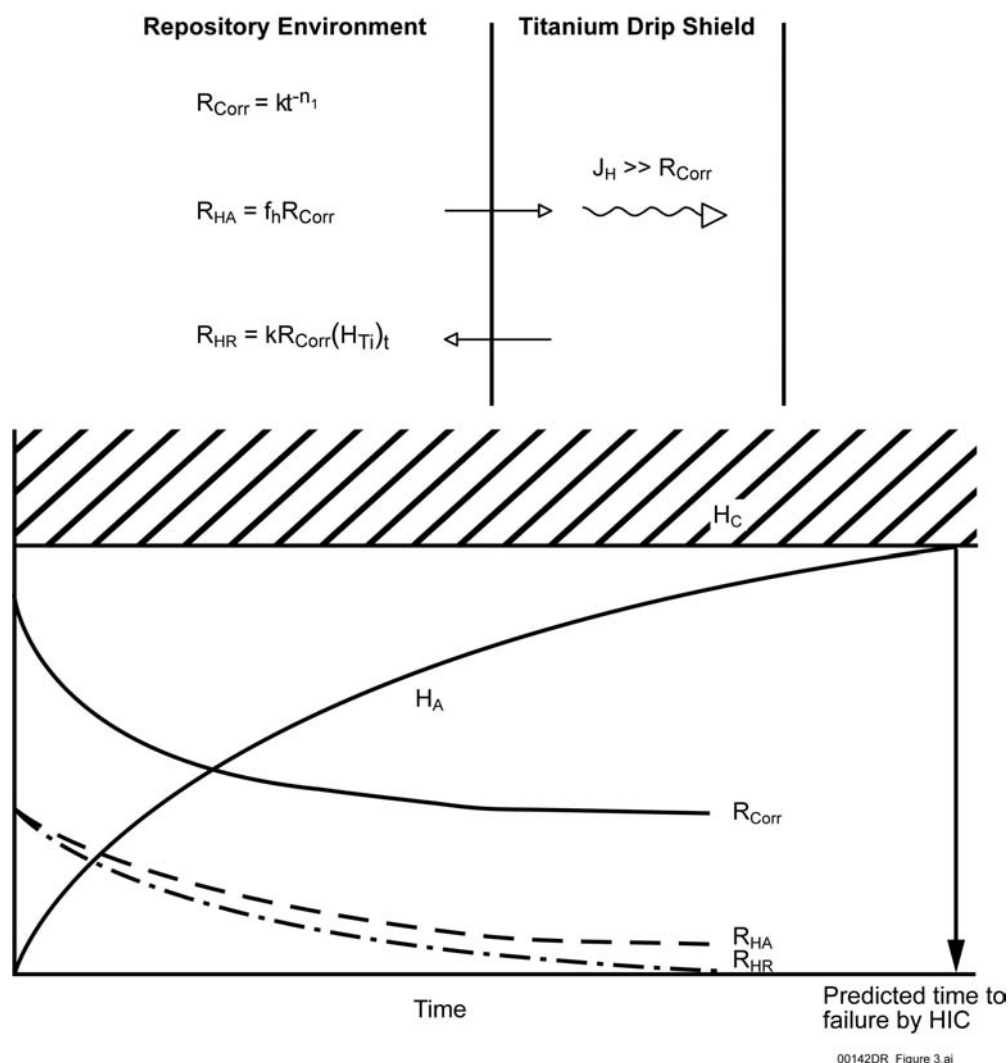
Figure 5.   A Schematic Representation of the Alternate Performance Assessment Conceptual Model for
Hydrogen Absorption During Passive General Corrosion of Titanium

The universally accepted structure for passive films, an inner protective barrier layer covered by
an outer more-porous and, hence, less-protective hydrated layer, has been demonstrated for
passive films on titanium (Pan et al. 1994 [DIRS 159795]), and a number of features of passive
oxide film growth, besides an increase in thickness, have been shown to lead to a decrease in
corrosion rate with time. Since defect transport, or ion transport via defects, is the primary
mechanism for film growth (Macdonald 1999 [DIRS 154721]) and film dissolution
(Blackwood et al. 1988 [DIRS 151090]), a defect annealing process (Leitner et al. 1986 [DIRS
159791]) will lead to a decrease in corrosion rate. Such a decrease has been observed in neutral
(pH ~5 to 6) hydrogen peroxide solutions (Fonseca and Barbosa 2001 [DIRS 159797]).

Studies in phosphate-buffered saline solutions (Pan et al. 1994 [DIRS 159795]) have shown that
the incorporation of ionic species into the outer porous hydrated layer leads to a sealing, at least
partially, of the porosity and an increase in film impedance, equivalent to a decrease in corrosion
rate. Even under the aggressive conditions experienced in pulp and paper bleaching plants, the
incorporation of Ca^{2+}, Mg^{2+}, and particularly SiO_4^{2-}, into the oxide film have been shown to

inhibit corrosion (Schutz and Xiao 1994 [DIRS 159798]; Wyllie et al. 1994 [DIRS 159799]). Based on these observations, it is reasonable to expect that the accumulation of silica on the surface will lead to a suppression of corrosion rate with time.

The use of a hydrogen absorption rate that is directly proportional to the corrosion rate, and, hence, can be determined by multiplying the corrosion rate by a time-independent absorption efficiency, is very conservative. When a coherent oxide is present on titanium, hydrogen absorption would not be expected until the passive film became a degenerate semiconductor, a condition requiring the application of a potential $\leq$ -0.6V$_{(SCE)}$ (Shoesmith and Ikeda 1997 [DIRS 151179]). Conditions that would allow hydrogen absorption, therefore, require that one of the following conditions apply:

1. There is a source of polarization to a potential $\leq$ -0.6V$_{(SCE)}$

2. Destruction of the oxide occurs such that active conditions are achieved

3. The presence in the alloy of intermetallics can act as hydrogen absorption windows in the otherwise impermeable oxide (CRWMS M&O 2000 [DIRS 154666], Appendix A).

Since passive corrosion conditions prevail, condition (2) will not occur, and the cathodic polarization of titanium achieved by galvanic coupling to carbon steel sections within the repository is modeled separately. Corrosion potential measurements on Ti Grade 7 conducted in simulated Yucca Mountain groundwaters at General Electric Corporate Research and Development yielded a value of approximately -120 mV$_{(SCE)}$ for immersion times greater than two days (BSC 2001 [DIRS 157151], Section 3.3.3). Providing the potential remains within the band gap region of the TiO$_2$ passive film (-0.6V to ~2.4V$_{(SCE)}$, then there is considerable published evidence to show that the oxide is an excellent barrier to hydrogen absorption (Been and Grauman 2000 [DIRS 159767]; Covington 1979 [DIRS 151097]; Shimogori et al. 1985 [DIRS 159784]). Clearly, a substantial period of dry oxidation (under ventilated conditions) would be expected to improve the shield's resistance to hydrogen absorption.

This influence of the passive film in suppressing hydrogen absorption is also clearly demonstrated in the electrochemical measurements by Okada (1983 [DIRS 115556]) from whose data the value of the absorption efficiency used in the model was adopted. In this model, a value of 1.5% has been adopted for the efficiency. In reality, the actual value should be considerably less, since Okada's value was measured under cathodically polarized conditions, when the specimen potential would be very much lower than the threshold value of ~-0.6 V$_{(SCE)}$, and hence, beyond the band gap region of the oxide.

Available evidence suggests that the presence of impurity iron may increase the absorption of hydrogen by Ti Grade 2 (Cotton 1970 [DIRS 151096]; Covington and Schutz 1981 [DIRS 151098]). Observed increases in hydrogen absorption by Ti Grade 12 (Kim and Oriani 1987 [DIRS 110237]) may also be attributed to the alloying additions, especially nickel and molybdenum. By contrast, no increase in hydrogen absorption was observed for palladium-containing alloys providing the pH was greater than ~4 (Okada 1983 [DIRS 115556]). The key difference between these two categories is that the nickel in Ti Grade 12 and the iron (present as an impurity) in Ti Grade 2 can form reactive (i.e., capable of sustaining anodic and cathodic

reactions) or ß-phase intermetallics (Ti$_2$Ni, Ti$_x$Fe), or both, whereas intermetallic formation is rare in Ti Grade 7, and ß-phase formation does not occur.

Okada's electrochemical results (Okada 1983 [DIRS 115556]) show there was no difference in the hydrogen absorption efficiency for Ti Grade 2 specimens and specimens coated with noble metal (platinum) providing pH $\geq$ 4 when a passive oxide will be present. This demonstrates that any tendency for the noble metal content of alloys Ti Grades 7 and 16 to catalyze hydrogen absorption (as observed under active, acidic conditions) (Fukuzuka et al. 1980 [DIRS 151105]) is masked when a passive oxide film is present.

Based on this discussion, the assumption that the efficiency for hydrogen absorption is constant and directly proportional to the corrosion rate is clearly conservative. The adoption of a value measured under polarization conditions equivalent to galvanic coupling makes the value for the efficiency conservative, since there is no reason to fear that the palladium content of Ti Grade 7 will influence this value when the material is passive (i.e., in the neutral-to-alkaline pH range anticipated under repository conditions).

6.1.7 Comparison Between the Current Performance Assessment Conceptual Model and the Alternative Conceptual Model for Hydrogen Absorption by Titanium During General Passive Corrosion

A comparison of the current TSPA-LA conceptual model as discussed in Section 6.1.5 with the alternative conceptual model discussed in Section 6.1.6 identifies the following key differences and commonalties:

- In the TSPA-LA model, the passive corrosion rate is assumed constant with time, whereas in the alternative conceptual model it is allowed to decrease with exposure time.

- In the TSPA-LA model, all the hydrogen absorbed is retained and not re-released as the corrosion front progresses into the alloy. By contrast, in the alternative conceptual model some of the absorbed hydrogen is rereleased as the corrosion front progresses into the alloy.

- In both models, the rate of hydrogen absorption is assumed directly proportional to the passive corrosion rate and the proportionality constant is a time-independent hydrogen absorption efficiency.

- In both models, the rate of transport of hydrogen in the alloy is assumed to be very fast compared to its rate of absorption. As a consequence, hydrogen in the alloy is uniformly distributed throughout the full wall thickness.

6.2 APPLICATION OF HYDROGEN-INDUCED CRACKING MODEL TO DRIP SHIELD

6.2.1 Material

Ti Grade 7 (UNS R52400) is the material for construction of the drip shield for the waste package. As indicated in Section 1.2, this alloy consists of 0.3 wt % iron, 0.25 wt % oxygen, 0.12 to 0.25 wt % palladium, 0.1 wt % carbon, 0.03 wt % nitrogen, 0.015 wt % hydrogen, and 0.4 wt % total residuals with the balance being titanium. The chemical composition of Ti Grade 7 is identical to that of Ti Grade 16 except the palladium content. Ti Grade 16 contains 0.04 to 0.08 wt % palladium.

Crevice corrosion and general passive corrosion will be accompanied by hydrogen production and, hence, possibly by the absorption of hydrogen into the metal. It has been concluded in Section 6.1.4 that hydrogen absorption during crevice corrosion is insignificant and, as a result, is not considered in the hydrogen-induced cracking model. A passive general corrosion rate for Ti Grade 16, a material that is similar to Ti Grade 7, has been reported in Section 4.1. For the purposes of this analysis, the maximum possible general corrosion rate of the drip shield is considered to be 3.20×10^{-4} mm/yr (BSC 2004 [DIRS 169845]; DTN: LL990610605924.079 [DIRS 104994]). This value results from measurements of the corrosion rates of samples with both weight-loss and creviced geometries after one year at LTCTF. Conceptually, this general corrosion rate would be appropriate for use only on the drip shield outer surface as only the drip shield outer surface could be contacted by dripping water. Dripping water could potentially lead to the formation of scale and/or salt deposits under which crevice conditions could form. On the underside of the drip shield, no crevice conditions are possible as only condensed (hence relatively impurity-free) water could contact these regions. Therefore, the maximum possible passive general corrosion rate for the underside of the drip shield is considered to be 1.13×10^{-4} mm/yr (BSC 2004 [DIRS 169845]; DTN: LL990610605924.079 [DIRS 104994]). This value results from measurements of the corrosion rate of samples with only weight-loss geometry after one year. As the rate of hydrogen generation on the drip shield surface, and hence the rate of hydrogen absorption into the drip shield, will be proportional to the rate of drip shield corrosion, and the two surfaces of the drip shield corrode at two different rates, the average of these two maximum corrosion rates, 2.17×10^{-4} mm/yr, is appropriate for use in the hydrogen-induced cracking model.

6.2.2 Critical Hydrogen Concentration, H_C, for Ti Grade 7

Based on the literature data (Ikeda and Quinn (1998 [DIRS 144540], p. 7) and similarity between Ti Grades 16 and 7, the H_C for Ti Grade 7 is assumed to be 1,000 µg/g (Section 5.2). As discussed in Section 6.1.3, Shoesmith et al. (1997 [DIRS 112203], p. 11) concluded that a conservative value of $H_C = 500$ µg/g can be adopted as the critical hydrogen concentration in rolled plate material using Ti Grades 2 and 12 for predicting container lifetime. The lowest H_C value observed for Ti Grades 2 and 12 is ~400 µg/g. Ikeda and Quinn (1998 [DIRS 144540]) indicated that H_C for Ti Grade 16 is at least 1,000 µg/g and may be much greater.

The H_C value for Ti Grade 7 is assumed to be at least 1,000 µg/g (Section 5.2). This assumption (Section 5.2) is based on Assumption 5.1 and data reported by Ikeda and Quinn (1998

[DIRS 144540], p. 7), which, as indicated earlier, concluded that the H_C value for Ti Grade 16 is between 1,000 and 2,000 µg/g. This assumption is necessary because H_C data are not available for Ti Grade 7.

6.2.3   Determination of Hydrogen Concentration in Metal in a 10,000-Year Period

To apply the method discussed in Section 6.1.5 to drip shield, the parameters in Equation 2 are detailed as following:

$$H_A = 4 \times 10^6 f_h R_{uc} t \left[M_{Ti} (d_o - R_{uc} t) \right]^{-1}$$ Eq. 2

where

H_A = hydrogen content (µg/g)
f_h = fractional efficiency for absorption
R_{uc} = rate of general passive corrosion (mm/year)
t = duration of emplacement (years)
M_{ti} = atomic mass of titanium (g/mol) = 47.9 (Weast 1978 [DIRS 128733], p. B-177)
d_o = half of drip shield thickness (mm)

More information about the model parameters are provided in Table 6.

As seen in Table 6 and the rationalization in Section 5.6, the upper boundary fractional efficiency for hydrogen absorption (f_h = 0.015) is used in the modeling for Ti Grade 7 as a conservative approach. The rate of general passive corrosion is 2.17×10^{-4} mm/yr (average value). The reason that the average of the exterior and interior surface corrosion rates is used in the modeling is as explained in the Section 6.2.1. The duration of emplacement is $t = 10,000$ years. Half of the minimum drip shield wall thickness (15 mm) is used for d_o (i.e., $d_o = 7.5$ mm). Using half of the thickness of the drip shield in calculations is equivalent to assuming that there is twice the surface area of Ti Grade 7 available to absorb hydrogen because absorption can occur on both the exterior and inner surfaces of the drip shield.

Table 6.   Model Inputs Used in Current Performance Assessment Model for Hydrogen Absorption During Passive General Corrosion of Titanium

Input Name	Input Description	Input Source (DTN if applicable)	Value or Distribution (Units)
f_h	Fractional efficiency for hydrogen absorption	Okada (1983 [DIRS 115556]) Assumption (Section 5.6)	0.005 to 0.015 (a value of 0.015 is used in the model as a conservative approach)
ρ_{Ti}	Density of titanium	Weast 1978 [DIRS 128733], p. B-177	4.5 g/cm^3
R_{uc}	Rate of general passive corrosion (maximum)	BSC 2004 [DIRS 169845], LL990610605924.079 [DIRS 104994]	3.20×10^{-4} mm/yr 1.13×10^{-4} mm/yr (an average value 2.17×10^{-4} mm/yr is used in the modeling)
d_o	Half of drip shield thickness	BSC 2003 [DIRS 171024]	7.5 mm
t	Duration of emplacement	10 CFR 63.114(d) [DIRS 156605]	10,000 years
M_{Ti}	Atomic weight of titanium	Weast 1978 [DIRS 128733], p. B-177	47.9 g/mol

From these conservative estimates:

$R_{uc} = 2.17 \times 10^{-4}$ mm/yr
$f_h = 0.015$
$d_o = 7.5$ mm
$t = 10,000$ years

Equation 2 yields:

$$H_A = 510 \ \mu g/g < H_C = 1,000 \ \mu g/g$$

The analytical estimate presented in Section 6.2.3, based on Equation 2, provides a large margin of safety to the drip shield against the effects of hydrogen-induced cracking. The hydrogen concentration in the drip shield at 10,000 years after emplacement is 510 μg/g, resulting from a conservative estimate. The estimated hydrogen concentration is less than the critical hydrogen concentration of 1,000 μg/g for Ti Grade 7 by a factor of 2.

As discussed in Section 6.1.5, the current model is highly conservative due to several significant assumptions including that it assumes all the hydrogen absorbed during general corrosion is retained within the remaining drip shield wall thickness as the general corrosion process proceeds. It is most probable that the majority of hydrogen will be removed as corrosion progresses by conversion to the more thermodynamically stable titanium oxide. With this conservative assumption, the hydrogen concentration in the drip shield increases continuously with time as the drip shield thickness (thus the volume of the remaining drip shield) is reduced by general corrosion. This hydrogen concentration increase from the thinning of the drip shield is in addition to the hydrogen pickup from the general corrosion. With the current conservative model, the time for the hydrogen concentration in the drip shield to exceed the critical hydrogen concentration will always be less than the time to failure of the drip shield by general corrosion.

As noted in Section 6.1.3, the occurrence of hydrogen-induced cracking requires the hydrogen concentration to exceed the critical hydrogen concentration (H_C) and the stress intensity factor to exceed K_H. When the drip shield is subject to hydrogen-induced cracking, the failure will be by through-wall cracks, while the cracks are likely to be those originally generated by stress corrosion cracking (SCC). However, those cracks will be self-limited and eventually plugged by scale deposits, especially calcite and silica from groundwaters. Due to high density and the resulting low porosity or permeability of the scale deposits, the probability of water flow through plugged crack onto the waste package will approach zero (BSC 2004 [DIRS 169985], Section 6.5.5). Therefore, even if the drip shield is breached by through-wall cracks induced by hydrogen-induced cracking, the intended design function of the drip shield (i.e., preventing dripping water from directly contacting the underlying waste package) will not be compromised from the hydrogen-induced cracking failure.

6.2.4 Parameter Uncertainties

Uncertainties and Impacts on Model Output—Key input parameters in the model for hydrogen absorption during passive corrosion of titanium are R_{uc}, f_h and H_C.

R_{uc} was measured at the LTCTF of the LLNL using calibrated instruments and following quality assurance procedures that meet OCRWM requirements (DOE 2004 [DIRS 171386]). Therefore, the R_{uc} data are qualified "from origin." The maximum value of R_{uc} obtained from the weight loss plus crevice specimens (Sections 4.1, 6.2.1, and 6.2.3) was used for a conservative estimate of hydrogen concentration in the drip shield. The uncertainties in corrosion rate data are discussed in *General Corrosion and Localized Corrosion of the Drip Shield* (BSC 2004 [DIRS 169845]).

The constant value of $f_h = 0.015$ assumed in the model was determined under extremely aggressive conditions unachievable in the repository and, therefore, constitutes a conservative upper limit for this parameter (Assumption 5.6). Consequently, the model predictions obtained using this value will also be conservative. Adoption of a value of $f_h > 0.015$ (i.e., the value of 0.1 as discussed in Section 6.1.5) is not merited because it applies only to Ti Grade 12, an alloy containing β phase, while Ti Grade 7 is an α-alloy and does not undergo crevice corrosion.

The value of 1,000 µg/g assumed for H_C is a conservative lower limit as discussed in Sections 5.2 and 6.1.3. Measurements show the value could be as high as 2,000 µg/g. Adoption of a higher value, or a value distributed between 1,000 µg/g and 2,000 µg/g, would further decrease the probability of failure by hydrogen-induced cracking before 10,000 years.

The design parameters, d_0 and t, are specified. Also, M_{Ti} and ρ_{Ti} are physical constants that are established fact.

Sources of Uncertainties — A principal source of uncertainty is measurement error, particularly in the parameters R_{uc} and H_C. Another significant uncertainty is the lack of direct measurements on Ti Grade 7, leading to the adoption of parameter values measured on the similar alloy Ti Grade 16. The small database of measurements on the fracture toughness of Ti Grade 7 (Ti Grade 16) and the absence of information on the time-dependent decrease in the value of f_h have lead to the adoption of conservative limiting values for these parameters. This last uncertainty includes the uncertainty associated with variability in materials properties.

6.3 HYDROGEN-INDUCED CRACKING OF TI GRADE 7 DUE TO GALVANIC COUPLING

6.3.1 Introduction

As indicated in Section 6.1.2, the three general conditions that must exist simultaneously for the hydrogen embrittlement of α alloys are (Schutz and Thomas (1987 [DIRS 144302], p. 673):

- A mechanism for generating hydrogen on a titanium surface

- A metal temperature above approximately 80°C (175°F)

- A solution pH less than 3 or greater than 12, or impressed potentials more negative than -0.7 $V_{(SCE)}$.

According to Schutz and Thomas (1987 [DIRS 144302], p. 673), one hydrogen-generation mechanism is the coupling of active metals such as zinc, magnesium, and aluminum to titanium leading to hydrogen uptake and eventual embrittlement of the titanium if the other two conditions described above are met. A similar situation occurs when titanium is in galvanic contact with carbon steels and stainless steels. In a drip shield design without backfill, hydrogen generation may be caused by the galvanic couple between the titanium drip shield surface and ground supports (such as steel rock bolts, wire mesh, and steel liners used in the drift), which may fall onto the drip shield surface. Therefore, hydrogen-induced cracking of the drip shield due to galvanic couple needs to be considered as the conditions associated with metal temperature and water or moisture pH (or corrosion potential) as described above are attainable under Yucca Mountain conditions.

The repository design does not use carbon steel for these ground support components (Stainless Steel Type 316 will be used instead). The galvanic coupling effect between carbon steel and titanium alloys is discussed below as a conservative approach. This conservatism is explained in Section 6.3.2.

6.3.2 Qualitative Assessment

Carbon steels and stainless steels are cathodes to titanium alloys if they are galvanically coupled. Given the expected evolution of groundwaters potentially contacting the drip shield and the temperature regime within the repository (Section 1.3), the required conditions for hydrogen absorption by the titanium drip shield are clearly present when galvanically coupled to sections of the steel components. If occurring while temperatures are high ($\geq 80°C$) and concentrated groundwaters are present, then formation of local hydrided "hot spots" are possible. These "hot spots" will only occur at those sites where contact to carbon steel and the establishment of lasting (at least periodically) saturated aqueous conditions are achieved. Their formation is likely to be promoted if the contact points coincide with abraded or scratched areas of the drip shield. At higher temperature, hydrogen will be more rapidly absorbed and transported into the bulk structure to produce the hydride distribution required for extensive crack propagation. It is less likely that a hydride layer will be retained at the surface. As the temperature falls, the formation of surface hydrides becomes more likely as the rate of hydrogen transport into the bulk of the metal decreases. The formation of surface hydrides tends to reduce the efficiency of subsequent hydrogen absorption (Noel et al. 1996 [DIRS 111940]), and their presence has little effect on structural integrity.

The efficiency of iron-titanium galvanic couples to cause hydrogen-induced cracking of the titanium drip shield will be limited because:

1. The contact areas of the anode (steel) and cathode (titanium) are likely to be small and the anode-to-cathode area ratio low. Since relatively low volumes of groundwater are likely to contact both metals simultaneously, it is likely that the ratio of anode-to-cathode areas will be close to unity. If a couple with a small anode-to-cathode area ratio was established (i.e., a small piece of steel in contact with a large area of drip shield), then the couple would be more rapidly exhausted as the steel is consumed. Under these conditions, the amount of hydrogen absorbed would be limited.

2. While temperatures are high (>80°C), the intermittent nature of seepage dripping onto the drip shield should lead to only limited periods of the aqueous conditions required to sustain an active galvanic couple, thereby limiting hydrogen absorption while temperatures are high enough to drive hydrogen transport into the metal. For temperatures below 80°C, even galvanic polarization below the potential threshold of -0.6 $V_{(SCE)}$ produces only innocuous surface hydride films (Schutz and Thomas 1987 [DIRS 144302]). Also, at these lower temperatures, the small amounts of dissolved O_2 in the solutions forming the galvanic couples will make it very difficult to achieve polarization of the galvanic potential to less than -0.6 $V_{(SCE)}$. Additionally, the intermittent wetting and drying cycles anticipated on the drip shield will lead to the ready formation of calcareous and mineral deposits, which are well known to dramatically suppress galvanic currents, thereby stifling hydrogen absorption (Lunde and Nyborg 1993 [DIRS 151142]).

3. Conditions in the repository will be oxidizing, making it less likely that the couple will sustain water reduction, and hence hydrogen absorption. However, at high temperatures in concentrated saline solutions, the amount of O_2 dissolved in the solution forming the couple will probably be too low to displace water reduction as the primary cathodic reaction. However, the ferrous ion product of steel dissolution will be homogeneously oxidized to ferric species by dissolved O_2. If conditions remain neutral, this should lead to the formation of insoluble Fe(III) oxides or hydroxides, and little influence would be exerted on the galvanic couple. However, any tendency for acidification or the development of alkaline conditions will increase the ferric ion solubility. Under evaporative conditions, this could lead to quite high dissolved ferric ion concentrations and the establishment of a galvanic potential sufficiently positive to avoid hydrogen absorption into the titanium. It is well documented that only parts per million concentrations of multivalent transition metal cations such as Fe(III) are required to polarize titanium to passive conditions (Covington and Schutz 1981 [DIRS 151098]; Schutz and Thomas 1987 [DIRS 144302]) and ferric oxide deposits are passivating to titanium (Covington and Schutz 1981 [DIRS 151098]). Also, experimental evidence exists to show that galvanic currents and the rate of hydrogen absorption will decrease with time as deposits (calcite from atmospheric CO_2 and silicates from groundwaters) accumulate (Lunde and Nyborg 1993 [DIRS 151142]; Hodgkiess et al. 1987 [DIRS 159787]).

4. In the repository environment, the titanium drip shield and steel component surfaces will experience a considerable period of dry high temperature ($\geq$ 85°C depending on whether the higher- or lower-temperature operating mode is adopted). This will leave titanium and steel passivated (especially titanium) and avoid galvanic contact. While passivity on the steel may be subsequently disrupted, loss of passivity of the titanium drip shield will not be so readily achieved. Experimental evidence exists to show that air oxidation prevents hydrogen absorption by titanium even in aggressive (0.5 percent to 6 percent HCl) solutions at elevated temperatures (70°C to 250°C) (Mon 2002 [DIRS 160876], Attachment III).

Titanium has a large tolerance for hydrogen (Section 6.1.3 for critical hydrogen concentration), and substantial concentrations must be achieved before any degradation in fracture toughness is observed. This concentration level, as indicated in Section 6.1.3, has been measured to be in the range of 400 to 1,000 µg/g for Ti Grades 2 and 12. Recent measurements suggest that the tolerance for hydrogen of the Ti Grade 16 (a titanium alloy very similar to Ti Grade 7 in chemical composition) may be between 1,000 to 2,000 µg/g (Ikeda and Quinn 1998 [DIRS 144540], p. 7). According to Section 6.1.3, the critical hydrogen concentration for Ti Grade 7 is assumed to be 1,000 µg/g.

Given the high critical hydrogen concentration, the large volume of available titanium in the drip shield into which absorbed hydrogen can diffuse, and other reasons stated above, hydrogen-induced cracking of the titanium drip shield has a very low probability.

Moreover, Figure 6 shows the galvanic series of metals in seawater (ASM International 1987 [DIRS 103753], p. 235, Figure 1). As indicated in Figure 6, the potential of stainless steel, even in its active state (indicated by the open arrow), is much closer to that of titanium alloys. The less the potential difference between two metals, the less the driving force for galvanic corrosion. Therefore, the analysis of galvanic effect based on carbon steel is a conservative approach when the actual components will be made of stainless steel. The mathematical modeling discussed in Section 6.3.3 is based on the galvanic coupling between carbon steel and titanium alloy.
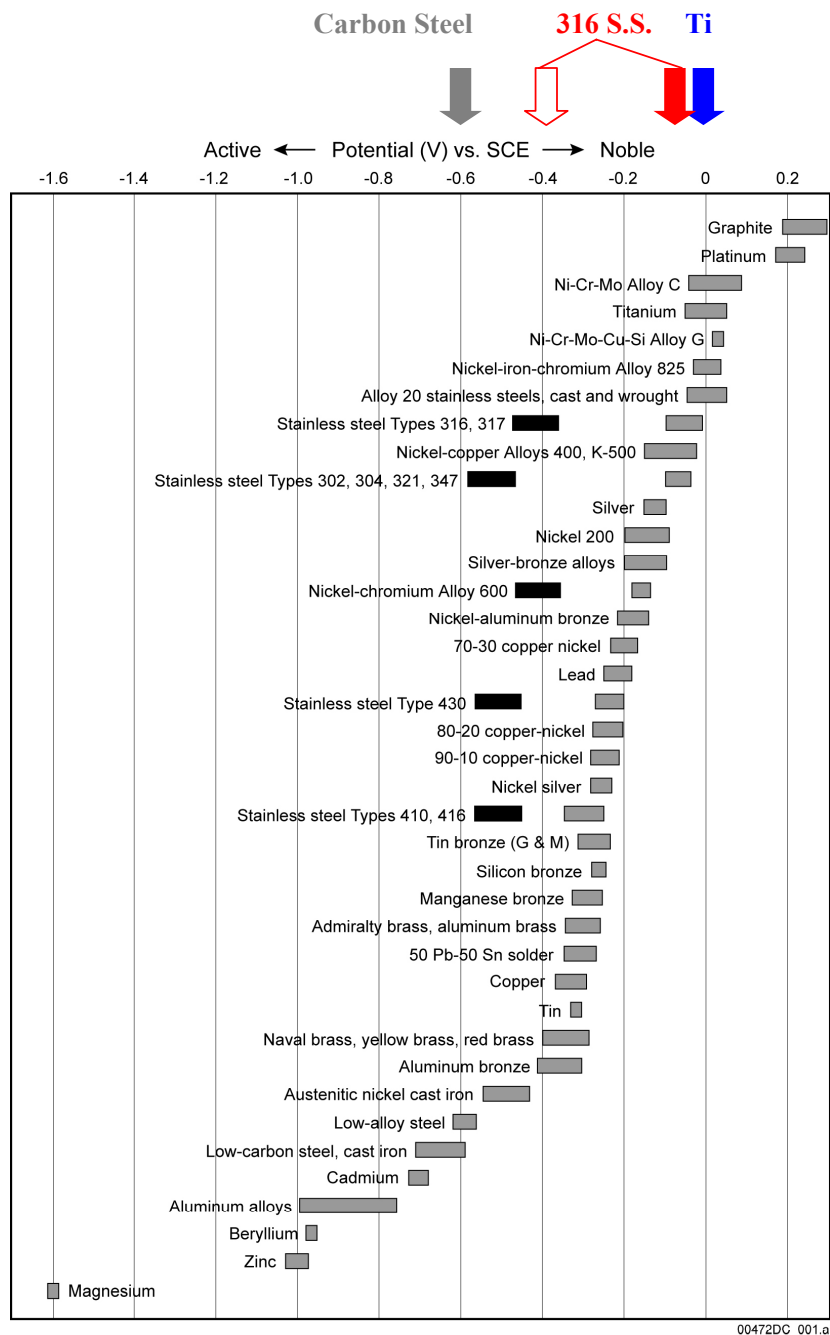
Source: ASM International 1987 [DIRS 103753], p. 235, Figure 1

NOTE: Open Arrow Indicating Active Behavior of Stainless Steel Type 316

Figure 6. Galvanic Series for Seawater

6.3.3 Mathematical Model for Hydrogen Absorption and Diffusion in Drip Shield Galvanic Couple

As described in Section 6.3.2, hydrogen absorbed in the Ti Grade 7 drip shield due to galvanic coupling with carbon steel may diffuse to the rest of the drip shield. A mathematical model is

proposed in this section to predict the hydrogen concentration in the drip shield due to a galvanic couple between the drip shield and a carbon steel segment. The absorption and diffusion of hydrogen in the drip shield is a complex process. A mathematical model is developed by making the following assumptions:

- The drip shield is treated as an infinite plate. The thickness of the plate is denoted by H.

- The area of galvanically coupled wetted surface is circular. While the actual geometry of the wetted area have a more complex geometry, its representation by an equivalent circular area does not significantly alter the calculations described below. The radius of this circular wetted area is denoted by r_o.

- Hydrogen is absorbed into the drip shield through the contact plane and immediately reaches the other surface. The initial region of the drip shield with hydrogen absorption is a circular disk with a radius, r_o, and thickness, H.

- As hydrogen starts to diffuse in the drip shield, the radius of the circular region will expand at a constant speed v. As a result, the radius, r(t), of the circular disk at a time, t, is expressed by the following equation:

$$r(t) = r_o + v\, t \qquad\qquad (\text{Eq. 4})$$

The amount of hydrogen (in g or mg, for example), Q(t), absorbed in the drip shield at a time, t, therefore, is:

$$Q(t) = \lambda\left(\rho_{Ti}\pi r_o^2\right)Ht + \int_{\tau=0}^{\tau=t}\lambda\rho_{Ti}\left[2\pi r(\tau)\right]H(t-\tau)dr(\tau) \qquad\qquad (\text{Eq. 5})$$

where λ is the hydrogen absorption rate, in ppm (or μg/g) /day, for example, and ρ_{Ti} is the mass density of the Ti Grade 7 drip shield (Section 6.1.5) and τ is time.

Based on the reaction: $2Fe + 3H_2O \rightarrow Fe_2O_3 + 3H_2$, the maximum amount of hydrogen (formed by corrosion of the carbon steel) that can be absorbed by titanium is:

$$Q_{max} = f_{Fe}3W / M_{Fe} \qquad\qquad (\text{Eq. 6})$$

where W is the mass of the carbon steel segment, f_{Fe} is the fraction of hydrogen produced by oxidation of the total mass of carbon steel, and M_{Fe} is the atomic weight of iron.

If t_{max} is the time when Q(t) reaches Q_{max}, t_{max} can be obtained by solving for the following equation:

$$Q_{max} = \lambda\left(\rho_{Ti}\pi r_o^2\right)Ht_{max} + \int_{\tau=0}^{\tau=t_{max}}\lambda\rho_{Ti}\left[2\pi r(\tau)\right]H(t_{max}-\tau)dr(\tau) \qquad\qquad (\text{Eq. 7})$$

Using Equation 4, Equation 7 can be written as:

$$Q_{max} = \lambda \rho_{Ti} \pi H \left(r_o^2 t_{max} + r_o v t_{max}^2 + \frac{v^2 t_{max}^3}{3} \right) \qquad \text{(Eq. 8)}$$

The maximum hydrogen concentration $H_A(r_o)$ in ppm (or µg/g), for example, will be in the region of the drip shield beneath the initial contact area and at the time t_{max}, i.e.:

$$H_A(r_o) = \lambda t_{max} \qquad \text{(Eq. 9)}$$

The hydrogen concentration $H_A(r)$ tends to be reduced at locations with a radius, r, from the center of the initial contact area, i.e.:

$$H_A(r) = \lambda \left(t_{max} - \frac{r - r_o}{v} \right) \quad \text{for} \quad r_o \leq r \leq r(t_{max}) \qquad \text{(Eq. 10)}$$

At $t > t_{max}$, $H_A(r)$ will start to decline as the hydrogen diffusion continues and the source of hydrogen becomes exhausted.

As a numerical example, the following input data are considered:

H   = Ti Grade 7 plate thickness   = 15 mm
r_o = radius of the initial contact area = 50.8 mm (2 in.)
ρ_{Ti} = density of Ti Grade 7   = 4.5×10^6 µg/cm^3
f_{Fe} = fraction of hydrogen available for absorption by Ti Grade 7 drip shield (refers to Assumption 5.6)   = 0.015
W   = mass of carbon steel   = 22.73×10^3 g (50 lb.)
M_{Fe} = atomic weight of Fe   = 55.847 (Weast 1978 [DIRS 128733], p. B-177)

The corrosion potential of carbon steel is estimated to be about -0.6 $V_{(SCE)}$, and a galvanic couple would polarize titanium down to that level. Based on Shoesmith et al. (1995 [DIRS 117892], Figure 19) and Murai et al. (1977 [DIRS 111926], Figure 5), the hydrogen absorption rate, λ, for Ti Grade 7 would be about 0.5 µg/g/day. Inspection of Figure 5 in Murai et al. (1977 [DIRS 111926]) shows that the maximum value of λ measured in the potential range -0.6 $V_{(SCE)}$ to −1.0 $V_{(SCE)}$ is ~0.7 µg/g/day. Therefore, this value is adopted as the maximum λ value in this sensitivity study. No data are available for the hydrogen diffusion rate, v, of Ti Grade 7. For the base case of the numerical example, the values used for λ and v are, respectively, 0.5 µg/g/day and 1 mm/day. For the parametric study, λ = 0.5, 0.7 µg/g/day, and v = 1, 2, 3 mm/day are considered, and plots of hydrogen concentration versus distance from the original contact area are shown in Figure 7. It can be seen that, in all cases of the parametric study, the hydrogen concentration does not exceed about 50 percent of the assumed critical hydrogen concentration of 1,000 µg/g for Ti Grade 7 (Assumption 5.2). The results of the parametric study are consistent with the qualitative assessment presented in Section 6.3.2. The choice of the mathematical model and the value of λ are reasonable and conservative. The value of v is high but is also reasonable, as it ignores the probability that the hydrogen will be retained at the

titanium surface and the efficiency of absorption would then decrease. The calculation can be considered bounding since all the features likely to suppress hydrogen absorption are ignored in the calculation. These features are summarized in Section 6.3.2.
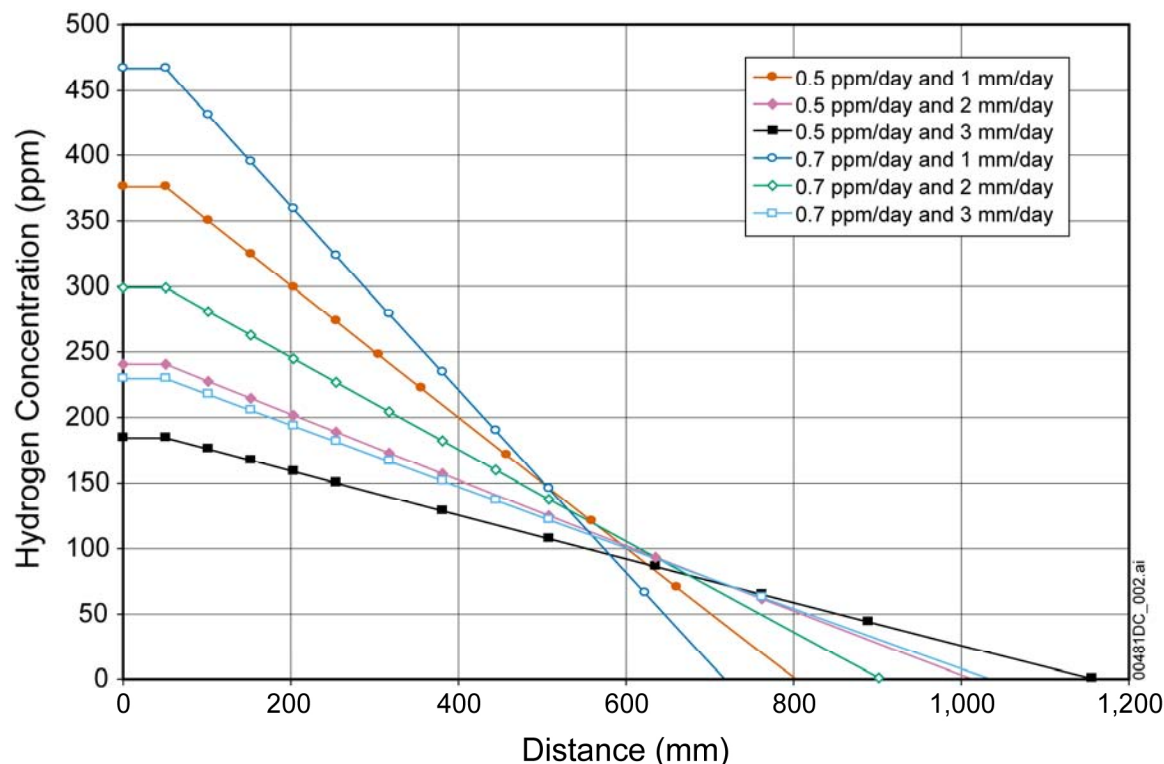
Figure 7. Hydrogen Concentration in Drip Shield Versus Distance from Contact Area

6.3.4 Parameter Uncertainties and Sensitivity Analyses

Uncertainties and Impacts of Uncertainties on Model Outputs—The key parameters in this model are the mass of steel (W), the radius of the initial contact area (r_o), the fraction of hydrogen absorbed (f_{Fe}), the critical hydrogen concentration (H_C), the hydrogen absorption rate (λ), the hydrogen diffusion rate (v), and the corrosion rate (R_{uc}).

The values of W and r_o adopted will influence the analysis but include uncertainties treated below:

- The value of W = 22.73 kg (50 lbs) for the mass of steel available for consumption in a single galvanic couple is a conservative limit, since it ignores the stifling of coupled conditions by the evolving local environment at the coupled site, as discussed in Section 6.3.2.

- The choice of a value of $r_o \sim 50.8$ mm (2 in.) is a realistic but uncertain value. The size of the contact area is decided by the amount and distribution of aqueous solution trapped at the carbon steel/Ti Grade 7 contact site, not the actual metal-to-metal contact area. The loss of wet contact by evaporation, gravitational flow and capillary absorption into accumulating corrosion products will be the primary influence limiting r_o. The value of

λ, the hydrogen absorption rate, is a very conservative upper limit as it ignores the observed decrease in absorption rate with time as discussed in Section 6.3.6. As a consequence, the model predicts a conservative rapid accumulation of hydrogen. To be consistent with this constant high rate of hydrogen absorption it was necessary to also assume a fast rate of hydrogen transport (v) within the Ti Grade 7 (Assumption 5.7). The values of v chosen were arbitrary, but much higher than the transport rates that would be calculated from measured diffusion coefficients of hydrogen in titanium. This conservatism is partially offset by allowing lateral hydrogen transport away from the contact area. The uncertainties in corrosion rate, R_{uc}, are discussed in *General Corrosion and Localized Corrosion of the Drip Shield* (BSC 2004 [DIRS 169845]).

Sources of Uncertainties—Any event sequence(s) causing variations in the mass of the steel anode, and the anode and cathode areas may alter the model output and serve as sources of uncertainty.

6.3.5 Worst-Case Considerations

As a worst-case scenario, it is considered that the majority of the hydrogen generated by the section of carbon steel will be absorbed by the drip shield and that the absorbed hydrogen will be retained in the vicinity of the contact area and not diffused to the rest of the drip shield. In this case, there may be a local embrittlement of the drip shield in the contact area. It is further considered that the contact area is impacted by rockfall and residual stress to initiate a crack. As a result, a fast brittle fracture is possible if the stress intensity factor calculated from the residual stress and the crack size exceeds the fast fracture stress intensity factor, K_H. This fast fracture stress intensity factor tends to have a lower value than the critical slow crack growth stress intensity factor, K_S (also called fracture toughness), as indicated in Figure 3.

Calculated stress intensity factors due to rockfall in the drip shield for various crack sizes (depths) are listed in *Stress Corrosion Cracking of the Drip Shield, the Waste Package Outer Barrier, and the Stainless Steel Structural Material* (BSC 2004 [DIRS 169985], Attachment II). Section 6.5.2 of that document (BSC 2004 [DIRS 169985]) indicates an initial crack depth of 50 μm (i.e., the maximum incipient crack size) is considered. The equivalent stress intensity factor is still <5 MPa·m$^{1/2}$, although the maximum stress has increased from 157.5 MPa to 180 MPa. This document indicates that the fracture toughness K_S for Ti Grade 7 should be at least 30 MPa·m$^{1/2}$. Noting that K_H equals approximately one third K_S from Figure 8 in a report by Clarke et al. (1994 [DIRS 151092]), brittle fracture of the drip shield would require a value of $K_H = 10$ MPa·m$^{1/2}$. Because this value of K_H is greater than 5 MPa·m$^{1/2}$, brittle fracture due to hydrogen-induced cracking would not be a problem for the drip shield subjected to galvanic coupling with a section of the carbon steel ground support.

Finally, hydrogen generations due to either general corrosion or to galvanic corrosion are considered separately, not combined, in this report. This approach is reasonable and can be rationalized as follows:
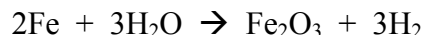
When the drip shield is galvanically coupled to less-noble metals such as carbon and stainless steels, the drip shield becomes a cathode (otherwise, there will be no enhanced galvanic corrosion of carbon or stainless steel). This process, however, will suppress the general corrosion

of the drip shield to an insignificant level. An alternative approach could be assuming the general corrosion rate of the drip shield remains the same while the corrosion of the less noble metal is enhanced. This is an overly conservative approach, adding to other already adopted conservatisms in this report. In addition, as mentioned in Section 6.3.2, items 1 and 3, hydrogen absorption due to galvanic coupling will be self-limiting due to the formation of mineral deposits and corrosion products on the surface of the contact area. Therefore, combining the effects of general and galvanic corrosion effects is overly conservative and unrealistic. However, even if the hydrogen pick up from the galvanic coupling and general corrosion were assumed to be additive, the total estimated hydrogen concentration is well below the threshold level of 1,000 ppm. On the other hand, hydrogen may evolve on the surface of the drip shield if it becomes a cathode. This, based on the basic knowledge of thermodynamics and electrochemistry, will not occur unless the potential of the drip shield surface is polarized to below about 0.7 $V_{(SCE)}$, a value that galvanic coupling to carbon steel cannot achieve. Based on the above analysis, the concern that a combination of general corrosion and galvanic corrosion will result in exceeding the critical hydrogen concentration is unwarranted.

6.3.6 Alternative Conceptual Model For Hydrogen-Induced Cracking Under Galvanically Coupled Conditions

Wet contact between the drip shield and carbon steel ground supports components (e.g., rock bolts, wire mesh, and steel drift liners) within the repository drifts is an additional source of hydrogen that could lead to its absorption by the drip shield and, hence, possibly to drip shield failure by hydrogen-induced cracking.

In the primary model, as noted in Section 6.3.3, the galvanic coupling supports corrosion of the carbon steel according to the reaction:

$$2Fe + 3H_2O \rightarrow Fe_2O_3 + 3H_2$$

and a certain fraction of the hydrogen, produced on the drip shield surface, is then absorbed into the titanium. This fraction, expressed as an absorption efficiency, is the same as that absorbed under nongalvanically coupled conditions and used in the model for hydrogen absorption during general passive corrosion. This is appropriate since the absorption efficiency was measured under cathodically polarized conditions similar to those that will prevail when the titanium is galvanically coupled. While this makes the use of this efficiency very conservative for general passive corrosion, it is more realistic for galvanically coupled conditions.

Once absorbed, the hydrogen rapidly diffuses through the full wall thickness of the drip shield and, with time, diffuses laterally within the drip shield wall to adjacent locations not in direct galvanic contact with the steel. Corrosion of the carbon steel and, hence, hydrogen absorption by titanium, stop once all the available contacting steel has been consumed. The criterion for failure is the same as that used in the general passive corrosion hydrogen-induced cracking model (i.e., failure by hydrogen-induced cracking is instantaneous once the concentration of hydrogen in the titanium exceeds the critical value, H_C).

This model contains a number of key conservatisms mentioned below:

1. The possible extent of galvanic corrosion will be limited by the small area of contact between the two metals; the low cathode-to-anode ratio (titanium/iron), which is likely to approach one; the low probability that the point of galvanic contact will simultaneously experience seepage drips; the inability of the site to remain wet due to runoff; and the stifling of steel corrosion by the accumulation of iron oxide corrosion products. In view of these limitations, the assumption that a considerable mass of steel (up to 50 lbs) could be consumed by galvanic corrosion is very conservative (Assumption 5.7).

2. Once absorbed, hydrogen diffuses rapidly within the metal (Assumption 5.7). However, practically measured diffusion coefficients for hydrogen in α-titanium are low and thermally activated in the normal Arrhenius manner (Phillips et al. 1974 [DIRS 151152]).

3. The absorption efficiency for hydrogen remains constant throughout the duration of the galvanic corrosion process (Assumption 5.6). Considerable evidence exists to show that, under galvanically coupled conditions, a surface hydride layer is formed (Noel et al. 1996 [DIRS 111940]; Mon 2002 [DIRS 160876], Attachment II; Tomari et al. 1999 [DIRS 159786]) and, as a consequence, the efficiency for hydrogen absorption decreases substantially with time.

An alternative, less conservative and, hence, more realistic model can be defined by incorporating a flux term for hydrogen absorption in the alloy and using a time-dependent absorption efficiency. This is equivalent to relaxing the conservatisms in (2) and (3) above.

The rate of hydrogen production is taken as constant and equal to the rate of carbon steel corrosion until the amount of available steel is consumed, after which no further hydrogen absorption due to galvanic coupling occurs. However, since a considerable literature exists to show that the rate of hydrogen absorption follows a parabolic relationship (e.g., Tomari et al. 1999 [DIRS 159786]), the absorption efficiency is taken to decrease with time. This acknowledges that the amount of hydrogen that can absorb is limited to the amount required to form a surface hydride layer.

The flux of hydrogen within the material is calculated using Fick's laws with a diffusion coefficient, as J_H, which is dependent on temperature according to Arrhenius' Law as shown in Figure 8. As a consequence, a steady state is eventually established in which the rate of hydrogen absorption into the surface of the titanium is controlled by the temperature-dependent flux of hydrogen from the surface into the bulk of the material. Lateral diffusion of hydrogen to sites not in direct galvanic contact with the titanium is ignored.

A schematic comparison of these two models is given in Figure 8 and Figure 9. This comparison emphasizes the conservatisms in the TSPA-LA model compared to the alternative conceptual model. The additional terms are defined as follows:

$(R_{Corr})_{CS}$ = Corrosion rate of carbon steel galvanically coupled to titanium
$(f_h)_t$ = Time-dependent fractional absorption efficiency for hydrogen in to titanium
n_2 = Time exponent for the decrease in $(f_h)_t$ as a function of time

D_H	=	Temperature-dependent diffusion coefficient of hydrogen in α-titanium
D_0	=	Diffusion coefficient of hydrogen in α-titanium at 25°C
$\Delta c/\Delta x$	=	Concentration gradient of hydrogen in the titanium defined by Fick's laws
$E_A^{\#}$	=	Activation energy for hydrogen diffusion in α-titanium
V_m	=	Volume of titanium containing hydrogen
R	=	Gas constant
T	=	Temperature.

A number of studies have been published that clearly show the rate of hydrogen absorption decreases parabolically with time (Kim and Oriani 1987 [DIRS 110237]; Noel et al. 1996 [DIRS 111940]; Phillips et al. 1974 [DIRS 151152]; Tomari et al. 1999 [DIRS 159786]; Foroulis 1980 [DIRS 159837]). Since all of these studies were conducted under cathodically polarized conditions similar to, or much more polarized than, those anticipated as a consequence of galvanic coupling to carbon steel, the use of a decreasing absorption efficiency in the adopted model is appropriate. In all cases, the storage of hydrogen in the surface of the titanium was clearly demonstrated by the identification of a surface hydride layer. As the majority of these studies were performed in acidic solutions with large applied current densities, the hydride layers were much thicker (many microns) than would be anticipated for galvanic coupling conditions under Yucca Mountain conditions.

Tomari et al. (1999 [DIRS 159786]) and Phillips et al. (1974 [DIRS 151152]) showed that the parabolic relationship for hydrogen absorption possessed a $t^{1/2}$ time-dependence consistent with the form adopted in the model (i.e., the hydrogen absorption process is controlled by the transport of hydrogen from the surface layer into the bulk of the alloy). The presence of the surface hydride, or the storage of hydrogen in a concentrated surface layer, was confirmed optically (Noel et al. 1996 [DIRS 111940]; Phillips et al. 1974 [DIRS 151152]) by glow discharge spectroscopy (Mon 2002 [DIRS 160876], Attachment II) and by SIMS depth profiling (Tomari et al. 1999 [DIRS 159786]). Glow discharge spectroscopy was also used to show the change in distribution of hydrogen in the alloy as a consequence of transport over time.

Tomari et al. (1999 [DIRS 159786]) showed that Ti Grades 2 and 17 (Ti Grade 16 with a slightly higher oxygen concentration) exhibited effectively identical parabolic relationships for hydrogen absorption, indicating that the palladium alloy content had no measurable influence on either hydrogen absorption or its subsequent transport within the alloy. This is consistent with the conclusion (above) that any possible influence of the palladium content of the titanium is masked under passive conditions.
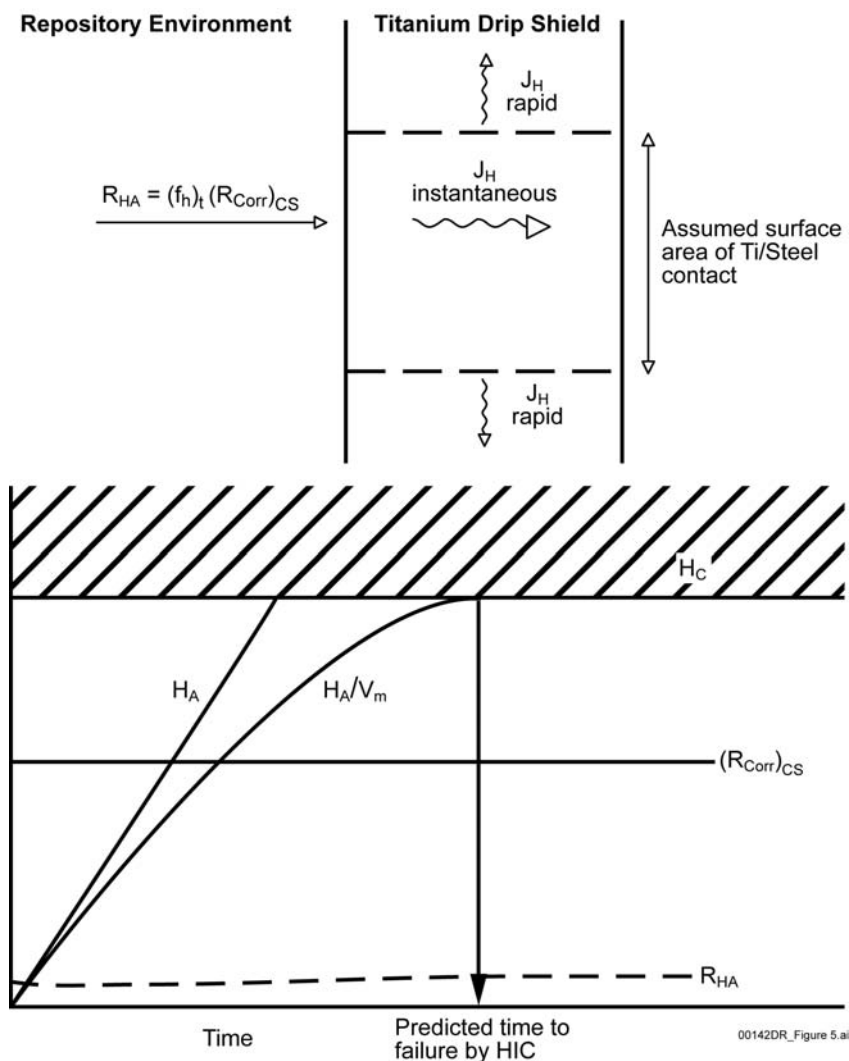
NOTE: This representation refers to the mathematical model described in Section 6.3.3

CS = carbon steel

Figure 8. A Schematic Representation of the Performance Assessment Conceptual Model for Hydrogen Absorption (HA) During Galvanic Coupling of Titanium ()

Based on similar studies performed as a function of temperature by Phillips et al. (1974 [DIRS 151152]) and Mon (2002 [DIRS 160876], Attachment II), a diffusion coefficient for hydrogen transport in titanium (2 to 4×10^{-12} cm^2/s) and an activation energy of 60 ± 3.4 kJ/mol were determined.

Based on this discussion, the use of a time-dependent hydrogen absorption efficiency, which decreases with time, is appropriate. The use of a constant absorption efficiency in the primary model makes it conservative by comparison to this alternative model. The adoption of a $t^{-1/2}$ time dependency for this efficiency is also justified. As well-documented values exist for the diffusion coefficient of hydrogen in titanium and the activation energy for this diffusion process, the form of the model is appropriate.
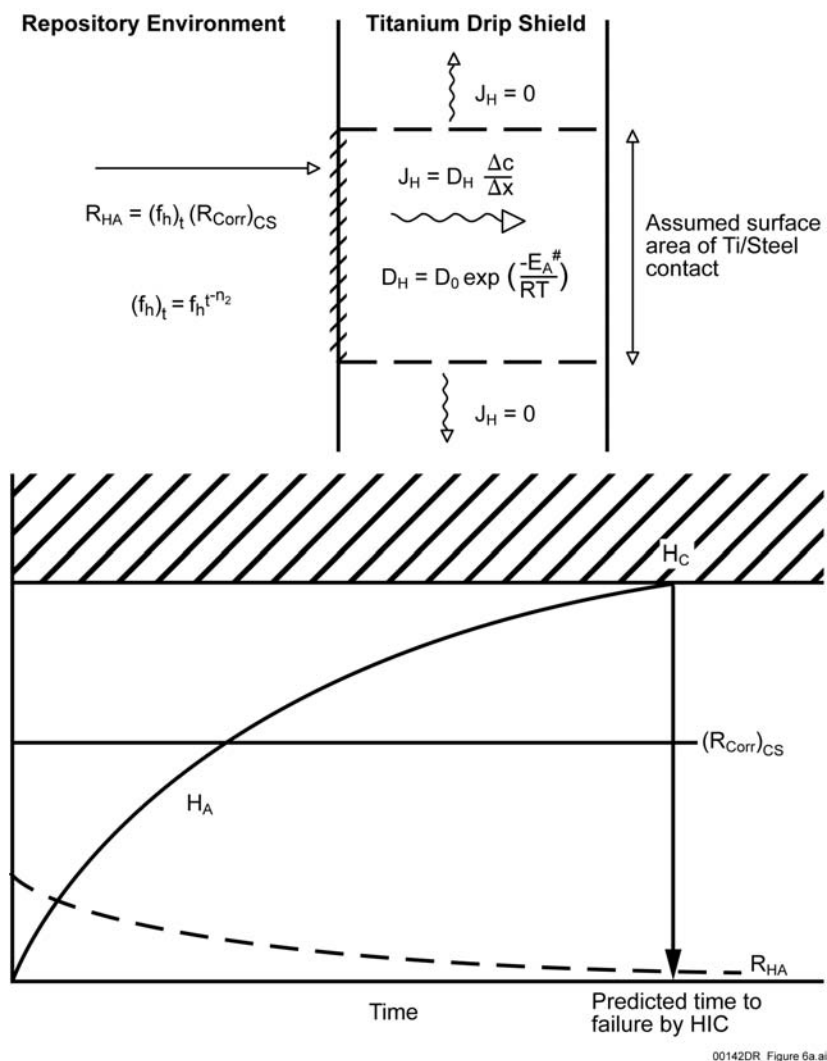
NOTE: CS = carbon steel

Figure 9.   A Schematic Representation of the Alternate Performance Assessment Conceptual Model for Hydrogen Absorption During Galvanic Coupling of Titanium

6.3.7   Comparison between the Primary Conceptual Model and the Alternative Conceptual Model for Hydrogen Absorption During Galvanic Coupling

A comparison of the primary conceptual model for hydrogen absorption as discussed in Section 6.3.3 with the alternative conceptual model discussed in Section 6.3.6 reveals the following commonalities:

- The rate of hydrogen absorption is directly proportional to the rate of carbon steel corrosion.

- The extent of carbon steel corrosion is limited by assuming a limited mass of steel is available by galvanic coupling.

- An arbitrary, but reasonable, area of wetted contact between the steel and the Ti Grade 7 is assumed.

The same comparison also reveals differences between the two models where in the primary model:

- The efficiency for hydrogen absorption is assumed to be constant with time, while the alternative conceptual model allows hydrogen absorption to decrease with time as hydrogen accumulates in the surface of the titanium.

- The absorbed hydrogen is rapidly transported through the full wall thickness. In the alternative conceptual model, hydrogen diffuses through the Ti Grade 7 at a rate controlled by the measured temperature dependent diffusion coefficient.

- Hydrogen is allowed to diffuse laterally along the wall of the drip shield. In the alternative conceptual model, lateral diffusion is not allowed.

These differences make the primary model more conservative than the alternative conceptual model.

6.4 ESTIMATE OF CRITICAL HYDROGEN CONCENTRATION FOR TITANIUM GRADE 24

Ti Grade 24, an alloy with ~ 6 wt % aluminum and 4 wt % vanadium with and addition of ~ 0.04 to 0.08 wt % palladium, is used as the structural material in the design of the drip shield. Ti Grades 5 and 24 are high strength titanium alloys and their chemical compositions are shown in Table 1. The experimentally obtained critical hydrogen concentration for Ti Grade 24 is not available at this time. However, the comparative corrosion behavior of this alloy and its approximate H_C value can be estimated based on available information on other titanium alloys, including Ti Grade 5, and on the relationship between Ti Grades 2, 16, and 7.

ASTM B 265-02 [DIRS 162726] specifications list identical minimum tensile and yield strengths for Ti Grades 5 and 24 (895 and 828 MPa, respectively). Ti Grades 5 and 24 contain 5.5 to 6.75 wt % of aluminum and 3.5 to 4.5 wt % of vanadium. The only difference between these alloys is the palladium content of Ti Grade 24 (0.04 to 0.08 wt %). Ti Grades 9 and 18 are similar to Ti Grades 5 and 24 in that Ti Grade 18 contains 0.04 to 0.08 wt % palladium, while both contain 2.5 to 3.5 wt % aluminum and 2.0 to 3.0 wt % vanadium. The chemical compositions and mechanical properties of Ti Grades 9 and 18, with leaner aluminum and vanadium, are also listed in Table 1. From Table 1 and Table 2, addition of palladium to titanium alloys does not influence their mechanical properties, but addition of aluminum and vanadium contents do. Three groups of titanium alloys listed in Table 1 and Table 2 (Ti Grades 2, 16, and 7; Ti Grades 5 and 24; and Ti Grades 9 and 18) have identical tensile and yield strengths, and share other mechanical properties within their respective group. On the other hand, other alloying elements alter their mechanical properties, implying that addition of palladium to the level of interest does not modify the microstructure of titanium alloys.
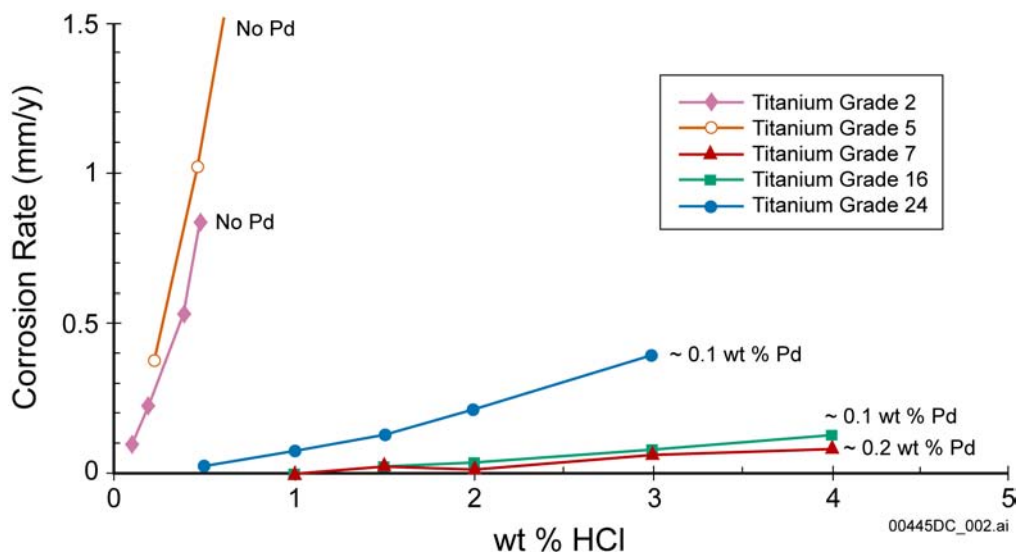
Source: Schutz 1995 [DIRS 102790] (Reproduced from Figures 4 and 7)

NOTE: This figure shows the significant improvement in corrosion resistance due to addition of palladium.

Figure 10. Corrosion Rates of Ti Grades 2, 5, 7, 17, and 24 in Boiling HCl

Addition of 0.04 to 0.08 wt % of palladium (to produce Ti Grades 16 and 24) significantly improves the corrosion resistance of the alloy as demonstrated in Figure 10. Testing of Ti Grade 5 and its palladium-modified version, Ti Grade 24, showed the addition of palladium improves the alloy's corrosion resistance in an analogous manner to that observed when palladium is added to the Ti Grade 2 alloy to produce Ti Grade 16 (Schutz 1995 [DIRS 102790]; Schutz and Xiao 1993 [DIRS 151167]; Kitayama et al. 1992 [DIRS 159803]). The mechanism by which palladium improves the corrosion resistance of Ti Grade 24 as compared to Ti Grade 5 is expected to be similar to that for Ti Grade 7 as compared to Ti Grade 16, where the accumulation of palladium in the corroding surface ennobles the corrosion potential of the alloys and increases the hydrogen solubility in the metal.

The H_C has been established for Ti Grade 5 by using similar experimental techniques as those used to determine the critical hydrogen concentrations for Ti Grades 2, 12, and 16 (Hardie and Ouyang 1999 [DIRS 159757]). Using the slow strain-rate technique on precracked compact tension specimens precharged with known amounts of hydrogen, Hardie and Ouyang (1999 [DIRS 159757]) showed that the fracture toughness of Ti Grade 5 was not significantly altered until the hydrogen level in the alloy exceeded 200 µg/g. For smooth tensile specimen, the authors showed that the reduction in area and elongation of Ti Grade 5 did not decrease until the hydrogen concentration reached about 1,500 ppm (Hardie and Ouyang 1999 [DIRS 159757]).

Based this, it is clear that the addition of palladium should lead to a higher value of H_C in Ti Grade 24. A similar increase in H_C was observed when Ti Grade 2 was alloyed with same amount of palladium to produce Ti Grade 16. A modest improvement to 600 µg/g, if not higher, is not an unreasonable H_C value assumed for Ti Grade 24. However, considering the higher strength of Ti Grade 24 than Ti Grades 16 and 7, it can be estimated conservatively, based on the above analysis, that the H_C of Ti Grade 24 is at least in the range of 400 to 600 µg/g, if not higher. This estimated value of H_C is realistic and conservative. To support this assertion,

Kitayama et al. (1992 [DIRS 159803]) evaluated the effect of palladium added to Ti-6Al-4V (Ti Grade 5) and Ti-3Al-2.5V (Ti Grade 9) on their hydrogen-induced cracking behavior. By cathodically charging hydrogen to palladium-containing Ti-6Al-4V (an equivalent to Ti Grade 24) to a level of approximately 1,000 and 1,100 ppm, the 0.2 percent proof stress was found to be 175 and 145 ksi, respectively (Kitayama et al. 1992 [DIRS 159803]), suggesting that there was no degradation in mechanical properties.

7. VALIDATION

7.1 MODEL VALIDATION ACTIVITIES AND CRITERIA

Models described in this report are expected to predict accurately and conservatively the hydrogen concentration in the Ti Grade 7 drip shield for a period of at least 10,000 years. This extraordinarily long time factor makes it difficult to validate these models in the usual way (i.e., by comparison of model predicted values with those observed experimentally for the whole range of time (ASTM C 1174-74 [DIRS 105725], Sections 19.3 and 20.4)). Therefore, the following validation activities have been adopted in the technical work plan (BSC 2004 [DIRS 169944], Table 2-1) for the model validation.

> *Criterion 1: Is the critical hydrogen content of the Grade-7 titanium alloy consistent with the literature?*
>
> *Criterion 2: Are the general corrosion rates in the model consistent with the literature?*
>
> *Criterion 3: Are the hydrogen contents for Grade-7 titanium and similar alloys predicted by the model consistent with the literature?*

The technical work plan (BSC 2004 [DIRS 169944], Table 2-1) also specifies that "corroborating data must match qualitatively" to achieve the required level of confidence (Level I in this case). The models are validated by validating the input parameter values used and comparing these parameters and model predictions to available peer-reviewed and qualified project data. The low level of confidence in the titanium hydrogen-induced cracking models, as classified as Level I in the technical work plan (BSC 2004 [DIRS 169944]), was obtained by validating three key model parameters (e.g., the passive corrosion rate, the critical hydrogen concentration, and the hydrogen absorption efficiency).

7.2 CONFIDENCE-BUILDING DURING MODEL DEVELOPMENT TO ESTABLISH SCIENTIFIC BASIS AND ACCURACY FOR INTENDED USE

For Level I validation, the development of the model should be documented in accordance with the requirements of Section 5.3.2(b) of AP-SIII.10Q. The development of the hydrogen-induced cracking was conducted according to these criteria, as discussed below:

> *1. Selection of input parameters and/or input data, and a discussion of how the selection process builds confidence in the model.*

The inputs to the hydrogen-induced cracking modeling have all been obtained from controlled sources (Table 4, Section 4.1), including discussion about selection of input and design parameters. Model assumptions have been described in Section 5. Detailed discussion about model concepts can be found in Sections 5 through 8. Thus, this requirement can be considered satisfied.

2. Description of calibration activities, and/or initial boundary condition runs, and/or run convergences, simulation conditions set up to span the range of intended use and avoid inconsistent outputs, and a discussion of how the activity or activities build confidence in the model. Inclusion of a discussion of impacts of any non-convergence

Discussion of initial and boundary conditions are described in Sections 1.5, 6, and 8 where hydrogen-induced cracking modeling and ranges of application are discussed. Discussion about nonconvergence runs is not applicable to this report because none were encountered. Thus, this requirement can also be considered satisfied.

3. Discussion of the impacts of uncertainties to the model results including how the model results represent the range of possible outcomes consistent with important uncertainties.

Uncertainties associated with the hydrogen-induced cracking modeling are discussed in Section 6.2.4 and partially in Section 6.3.4. Thus, this requirement can be considered satisfied.

4. Formulation of defensible assumptions and simplifications. [AP-2.27Q, Attachment 3, Level I (b)].

Discussion of assumptions and simplifications are provided in Section 5 with appropriate technical bases for their use. Thus, this requirement can also be considered satisfied.

5. Consistency with physical principles, such as conservation of mass, energy, and momentum.

Consistency with physical principles is demonstrated by the conceptual and mathematical formulation in Section 6. Information available in the peer reviewed scientific literature and those that is recently acquired at the LTCTF. Thus, this requirement can also be considered satisfied.

7.3 CONFIDENCE BUILDING AFTER MODEL DEVELOPMENT TO SUPPORT THE SCIENTIFIC BASIS OF THE MODEL

The technical work plan (BSC 2004 [DIRS 169944], Table 2-1) specifies the following criteria for the model validation.

Criterion 1: *Is the critical hydrogen content of the Grade-7 titanium alloy was consistent with the literature?*

Criterion 2: *Are the general corrosion rates in the model consistent with the literature?*

Criterion 3: *Are the hydrogen contents for Grade-7 titanium and similar alloys predicted by the model consistent with the literature?*

The technical work plan (BSC 2004 [DIRS 169944], Table 2-1) also specifies "corroborating data must match qualitatively" to achieve the required level of confidence (Level I in this case). Based on these criteria, the following model validation activities are performed.

7.3.1 Information Used for Model Validation

The supporting or corroborative information used in the model validation in this section is listed below. As specified in the technical work plan (BSC 2004 [DIRS 169944], Table 2-1), the use of the information contained in the following references for model validation is corroborative and qualitative. The input status of the corroborating information in this section is detailed in the corresponding DIRS report (Column 5) and throughout this section.

- "Recent Titanium Alloy and Product Developments for Corrosive Industrial Service" (Schutz 1995 [DIRS 102790])

- "Brine Radiolysis and its Effect on the Corrosion of Grade 12 Titanium (1)" (Kim and Oriani 1987 [DIRS 110236])

- "Corrosion Properties of the Oxide Film Formed on Grade 12 Titanium in Brine Under Gamma Radiation" (Kim and Oriani 1987 [DIRS 110237])

- "Analysis of Oxide Formed on Ti During Exposure in Bentonite Clay-I. The Oxide Growth" (Mattsson and Olefjord 1990 [DIRS 111885])

- "The Absorption of Hydrogen into Titanium Under Cathodic Polarization" (Murai et al. 1977 [DIRS 111926])

- *Hydrogen Absorption by Grade-2 Titanium* (Noel et al. 1996 [DIRS 111940])

- *A Model for Predicting the Lifetimes of Grade-2 Titanium Nuclear Waste Containers* (Shoesmith et al. 1995 [DIRS 117892])

- "Corrosion Behaviour of Container Materials for the Disposal of High-Level Wastes in Rock Salt Formations" (Smailos et al. 1986 [DIRS 119592])

- "Corrosion of Titanium and Titanium Alloys" (Schutz and Thomas 1987 [DIRS 144302])

- "Stability and Open Circuit Breakdown of the Passive Oxide Film on Titanium" (Blackwood et al. 1988 DIRS 151090])

- "The Effect of Hydrogen Content on the Fracture of Pre-Cracked Titanium Specimens" (Clarke et al. 1994 [DIRS 151092])

- *Hydrogen Induced Cracking of Grade-2 Titanium* (Clarke et al. 1995 [DIRS 151093])

- "The Influence of Surface Condition and Environment on the Hydriding of Titanium" (Covington 1979 [DIRS 151097])

- "Role of Palladium in Hydrogen Absorption of Ti Grade Pd Alloy" (Fukuzuka et al. 1980 [DIRS 151105])

- Hydrogen Absorption of Titanium Alloys During Cathodic Polarization (Lunde and Nyborg 1993 [DIRS 151142])

- "Hydride Formation During Cathodic Polarization of Ti–II. Effect of Temperature and pH of Solution on Hydride Growth" (Phillips et al. 1974 [DIRS 151152])

- "Hydrogen Absorption and Crevice Corrosion Behaviour of Titanium Grade-12 During Exposure to Irradiated Brine at 150°C" (Westerman 1990 [DIRS 151188])

- *A Preliminary Examination of the Effects of Hydrogen on the Behaviour of Grade-16 Titanium at Room Temperature* (Ikeda and Quinn 1998 [DIRS 152481])

- *Review of the Expected Behavior of Alpha Titanium Alloys Under Yucca Mountain Conditions* (CRWMS M&O 2000 [DIRS 154666])

- "Effect of Hydrogen and Strain Rate Upon the Ductility of Mill-Annealed Ti6Al4V" (Hardie and Ouyang 1999 [DIRS 159757])

- "Hydrogen-Induced Cracking of Commercial Purity Titanium" (Clarke et al. 1997 [DIRS 159758])

- "Hydrogen Absorption and the Lifetime Performance of Titanium Nuclear Waste Containers" (Shoesmith et al. 2000 [DIRS 159759])

- "The Hydrogen-Induced Cracking and Hydrogen Absorption Behaviour of Grade-16 Titanium" (Ikeda et al. 2000 [DIRS 159760])

- "Titanium and Titanium Alloys" (Been and Grauman 2000 [DIRS 159767])

- "Corrosion Studies on Selected Packaging Materials for Disposal of High Level Wastes" (Smailos and Köster 1987 [DIRS 159774])

- "Analysis of Passive Film on Titanium Formed in Dilute HCl Solutions at Elevated Temperatures" (Shimogori et al. 1982 [DIRS 159778])

- "Investigation of Hydrogen Absorption-Embrittlement of Titanium Used in the Actual Equipment" (Shimogori et al.1985 [DIRS 159784])

- "Hydrogen Absorption of Titanium for Nuclear Waste Container in Reducing Condition" (Tomari et al.1999 [DIRS 159786])

- "Galvanic Studies Related to the Use in Desalination Plant of Corrosion-Resistant Materials" (Hodgkiess et al.1987 [DIRS 159787])

- "Hydrogen Influence Cracking Inputs for TSPA-LA" (Mon 2002 [DIRS 160876])

- Titanium (Ti) Grade 16 Corrosion Rate Data in Simulated Diluted and Concentrated Well Water (SDW and SCW) (DTN: LL030205912251.016 [DIRS 161755])

- "2003 F.N. Speller Award Lecture: Platinum Group Metal Additions to Titanium: A Highly Effective Strategy for Enhancing Corrosion Resistance" (Schutz 2003 [DIRS 168772])

- *General Corrosion and Localized Corrosion of the Drip Shield* (BSC 2004 [DIRS 169845]).

In addition, the 5-year corrosion rate data obtained at LTCTF for Ti Grade 16 (BSC 2004 [DIRS 169845]) will be used to validate the conservatism of the currently developed model. The data used in this section are shown in Table 7.

Table 7. 5-Year Corrosion Rates Used for Model Validation

Input Name	Input Description	Input Source (DTN if applicable)	Value or Distribution (Units)
R_{uc}	5-year general passive corrosion rates for model validation	BSC 2004 [DIRS 169845], LL030205912251.016 [DIRS 161755]	0.77×10^{-4} mm/yr 0.58×10^{-4} mm/yr (average 0.675×10^{-4} mm/yr)

Furthermore, recently obtained 2.5-year corrosion rate data for Ti Grade 7 at LTCTF are also used as the corroborative information for model validation. The corroborative data are from *General Corrosion and Localized Corrosion of the Drip Shield* (BSC 2004 [DIRS 169845], Section 7.2, Table 21). These corroborative 2.5-year data are used in Table 8 and Figure 11.

7.3.2   Validation of the Values of H_C for Ti Grades 7 and 24

Although this assumption has been validated in Section 5.2, the critical hydrogen concentration is further discussed below according to the technical work plan (BSC 2004 [DIRS 169944].

> *Criterion 1: Is the critical hydrogen content of the Grade-7 titanium alloy was consistent with the literature?*

Using the slow strain rate technique on precracked compact tension specimens precharged with known amounts of hydrogen, it has been shown that the fracture toughness of Ti Grades 2, 12, and 16 are not significantly altered until their hydrogen levels exceed critical values 400 µg/g, 400 µg/g, and >1,000 µg/g, respectively (Clarke et al. 1994 [DIRS 151092]; Clarke et al. 1997 [DIRS 159758]; Shoesmith et al. 2000 [DIRS 159759]; Ikeda et al. 2000 [DIRS 159760]). These values are lower-limiting values, not mean values and, hence, are conservative. These values, and the details of their measurement, are published in the peer-reviewed literature (Clarke et al.

1994 [DIRS 151092]; Clarke et al. 1997 [DIRS 159758]; Shoesmith et al. 2000 [DIRS 159759]; Ikeda et al. 2000 [DIRS 159760]). The model assumes, for Ti Grade 7, the minimum H_C value of 1,000 μg/g is conservative. While this value was measured on Ti Grade 16, as rationalized in Section 5.2 and discussed in Section 6.1.3, the critical hydrogen concentration of Ti Grade 7 is at least equal, if not superior, to that of Ti Grade 16.

The value of H_C is the hydrogen concentration above which slow crack growth is no longer observed in these tests and only fast crack growth occurs. It is sensitive to the microstructure and texture of the material with respect to the orientation of the crack and the applied stress. The hydride precipitation in the α-phase, which for $H_A > H_C$ can lead to the decrease in fracture toughness, is favored close to the basal planes (Clarke et al. 1997 [DIRS 159758], p. 1,550). For Ti Grade 12, β-phase laminations are introduced into the material through the manufacturing process (rolling) leading to a preferential pathway for cracking along these laminations. These can be easily seen in the metallographic cross sections presented in the work of Clarke et al. (1994 [DIRS 151092]). Thus, the measured value of H_C for cracks propagating along these laminations is ~400 to 600 μg/g compared to a measured value of ≥ 1,800 μg/g for cracks propagating perpendicular to them (compare Figures 10 and 12 to Figure 14 in the work of Clarke et al. 1994 [DIRS 151092]). Heat treatments to remove these laminations lead to a value of H_C ~400 μg/g, irrespective of the direction of crack propagation, since a preferential direction of orientation for hydride precipitates no longer exists. The H_C values for Ti Grade 2 varied between 400 and 1,000 μg/g depending on the crack orientation. Heat treatments associated with welding did not significantly reduce these values (Clarke et al. 1995 [DIRS 151093]).

Measurements with the palladium-containing Ti Grade 16, a material with very similar properties to Ti Grade 7, show that the value of H_C is between 1,000 and 2,000 μg/g (Ikeda et al. 2000 [DIRS 159760]; Ikeda and Quinn 1998 [DIRS 144540]; Ikeda and Quinn 1998 [DIRS 152481]). This is thought to be due to the increased solubility of hydrogen in this material (Ikeda et al. 2000 [DIRS 159760; Ikeda and Quinn 1998 [DIRS 152481]). Because no β-phase laminations are present in Ti Grade 16, its hydrogen-cracking behavior is not expected to be directional in the manner shown for Ti Grade 12. Since Ti Grade 7 possesses similar mechanical properties to Ti Grade 16, the adoption of a model value of H_C of 1,000 μg/g is reasonable. This similarity in properties is illustrated by the equal minimum yield and ultimate tensile strengths for Ti Grades 2, 16, and 7 (Been and Grauman 2000 [DIRS 159767]; Schutz 1995 [DIRS 102790]).

The values of H_C adopted in the model are also conservative for other reasons. Slow cracking in the α-alloy Ti Grade 2 is dominated by creep and plastic deformation at the crack tip leading to blunting (Clarke et al. 1997 [DIRS 159758]) (i.e., there is no sustained load cracking, as could be the case for the stronger Ti Grade 12 (Clarke et al. 1994 [DIRS 151092]). This inability to achieve a sufficient stress intensity factor for fast fracture is most evident at low strain rates indicating that crack blunting should dominate under the very slow straining conditions expected under repository conditions. The value of H_C has also been shown to increase markedly with temperature. At 90°C, the value of H_C for Ti Grade 2 has been measured to be >1,000 μg/g (Clarke et al. 1995 [DIRS 151093]). Whether sustained load cracking or creep or plastic deformation will occur in slow strain rate tests prior to fast fracture depends on the strength of

the alloy. Since Ti Grades 16 and 7 are α-alloys with very similar strengths (the minimum yield strengths of the two materials are around 275 MPa (Been and Grauman 2000 [DIRS 159767])), they would be expected to exhibit similar cracking behavior. By contrast, Ti Grade 12 has a minimum yield strength of 345 MPa.

To date, a critical hydrogen concentration has not been measured for Ti Grade 24, proposed for use in the support structure for the drip shield. This alloy is a much stronger material than the Ti Grade 7 (minimum yield strength of 828 Mpa) (Schutz 1995 [DIRS 102790]) and would be expected to experience sustained load cracking at lower hydrogen concentrations. A value of H_C for an alloy identical to Ti Grade 24 except for the absence of palladium (i.e., Ti Grade 5) has been measured to be ~200 µg/g using the identical experimental procedure to that employed for the other titanium alloys discussed above (Hardie and Ouyang 1999 [DIRS 159757]). If the influence of palladium addition is taken to have a similar effect on Ti Grade 5 (to yield Ti Grade 24) as its addition to Ti Grade 2 (to yield Ti Grade 16) did, then it is not unreasonable to expect that H_C for Ti Grade 24 will be increased to 400 µg/g or greater.

Based on the above discussion, it can be concluded that the Criterion 1 is met.

7.3.3 Validation of Model For Hydrogen Absorption During General Passive Corrosion of titanium

Criterion 2. Are the general corrosion rates in the model consistent with the literature?

The corrosion rates used in the model are those based on weight loss measurements conducted at the LTCTF on specimens of Ti Grade 16 exposed to environments chosen to simulate those anticipated within the repository (BSC 2004 [DIRS 169845], Section 6.5). The 1-year corrosion rate data from Ti Grade 16 weight-loss plus crevice specimens set fit a Weibull distribution with 50, 90, and 100 percentile values of 25, 100, and 320 nm/yr, respectively. These rates were independent of solution composition, pH over the range 2.7 to 8.0, and temperature over the range 60°C to 90°C. The above-mentioned 1-year data have been used as direct inputs to the hydrogen-induced cracking model developed in this report. A more recent data set on general passive corrosion rates of Ti Grade 16 (5-year data set) show significantly lower values of 58 nm/yr and 77 nm/yr (DTN: LL030205912251.016 [DIRS 161755]), respectively, for weight-loss only and weight loss and creviced specimens tested in the LTCTF and is used for model validation in this report (Section 7.3.5).

Mattsson and Olefjord (1990 [DIRS 111885]) measured rates in the range 0.5 to 4 nm/yr on Ti Grades 2 and 7 in compacted clays saturated with saline solutions (95°C). Rates of 40 to 60 nm/yr can be obtained from the plots of oxide film thickness as a function of time published by Kim and Oriani (1987 [DIRS 110236]). These authors also found only a marginal increase in rate with increasing temperature between 25°C and 108°C (the boiling point of the brine). A similar absence of a temperature dependence (90°C to 200°C) was observed by Smailos and Koster (1987 [DIRS 159774]) and Smailos et al. (1986 [DIRS 119592]) for Ti Grade 7 in aggressive manganese-dominated brines[1] over an exposure period of ~3.5 years. For this last set

---

[1] Q-brine (wt %) – 1.4 NaCl; 4.7 KCl; 26.8 $MgCl_2$; 1.4 $MgSO_4$; 65.7 H_2O (pH = 4.9 at 25°C)

of results the rates were < 100 nm/yr. Blackwood et al. (1988 [DIRS 151090]) measured rates in acidic (pH = -1 to 1) and alkaline solutions (pH =14). Since they also measured pH dependence over the acidic pH range, it was possible to estimate (by extrapolation to more neutral pH values) that the rates in more neutral environments should be in the range 15 to 20 nm/yr for Ti Grade 2.

Because these rates were measured using electrochemical (Blackwood et al. 1988 [DIRS 151090]), surface analytical (Mattsson and Olefjord 1990 [DIRS 111885]; Kim and Oriani 1987 [DIRS 110236]), and weight change techniques (Smailos and Koster 1987 [DIRS 159774]; Smailos et al. 1986 [DIRS 119592]), they validate not only the values but also the weight-change method used to determine the rates on the LTCTF specimens.

> *Criterion 3: Are the hydrogen contents for Grade-7 titanium and similar alloys predicted by the model consistent with the literature?*

The amount of hydrogen absorbed is determined in the model using the general corrosion rates (discussed above) multiplied by an electrochemically measured absorption efficiency taken from the published literature (Okada 1983 [DIRS 115556]). This value was measured for commercially pure titanium (equivalent to Ti Grade 2) at pH values from 3.5 to 4.5, but only a marginally higher value was obtained under the same conditions for titanium plated with the noble metal platinum (Okada 1983 [DIRS 115556]). This clearly indicates that the primary controlling factor is the presence of oxide films, not the noble metal content of the electrode surface. In fact, according to Schutz (2003 [DIRS 168772] and references therein), alloy hydrogen absorption measured after corrosion in hot reducing acid media mostly tends to support the slightly beneficial influence of platinum group metals in titanium. Therefore, the palladium-containing Ti Grade 7 alloy would be expected to exhibit similar absorption efficiency. This similarity between the absorption behavior of commercially pure titanium (Ti Grade 2) and Ti Grade 7 is supported by the measurements of Fukuzuka et al. (1980 [DIRS 151105]), who showed, even under nonpassive conditions (boiling HCl), the rate of hydrogen absorption by Ti 0.15%Pd (equivalent to Ti Grade 7) was only a factor of two greater than for commercially pure titanium (Ti Grade 2). Since surface analytical evidence shows the oxide film formed on Ti 0.15%Pd (1.25% HCl at 125°C) becomes more passive (i.e., thickens more slowly) with time than that on titanium (Shimogori et al. 1982 [DIRS 159778]), its ability to prevent hydrogen formation and absorption will improve more with time than that of titanium. This justifies the adoption of a hydrogen absorption efficiency measured on titanium for use in the model with Ti Grade 7.

There are published grounds to believe that the absorption efficiency used in the model is conservative. Thermally grown oxides (and oxides grown under pickling conditions) have been shown to increase the resistance to hydrogen absorption (Been and Grauman 2000 [DIRS 159767]; Covington 1979 [DIRS 151097]), and the hydrogen absorption observed in deaerated HCl ($2 \le pH \le 4$; 50°C to 250°C) was exceedingly low under aerated conditions (Shimogori et al. 1985 [DIRS 159784]).

Calculations of the diffusive fluxes within the α-modification of titanium using published values of diffusion coefficients (Phillips et al. 1974 [DIRS 151152]) indicate that any hydrogen absorbed should be transported into the bulk of the alloy. However, the accumulation of

experimental evidence shows that the amount of hydrogen absorbed increases parabolically (i.e., the rate of absorption decreases) with time. This suggests that the hydrogen accumulates in the surface region and not transported deep into the alloy. This is particularly clear in the results provided by Kim and Oriani (1987 [DIRS 110236]) for Ti Grade 12. These results are particularly pertinent since they were measured in 25°C to 108°C saturated brines (conditions close to those anticipated in the repository). It should be noted that the β-phase in Ti Grade 12 leads to higher hydrogen absorption rates than would be expected in Ti Grade 2 (Lunde and Nyborg 1993 [DIRS 151142]) and other α-alloys. Westerman (1990 [DIRS 151188]) showed that the susceptible Ti Grade 12 absorbed only small amounts of hydrogen over an 18-month exposure to concentrated brines at 150°C, in which absorption stopped after ~6 months.

These results show that hydrogen will accumulate in the surface of titanium alloys. This is likely to be more marked in Ti Grade 7 than in Ti Grade 12, since the former alloy does not contain the β-phase ligaments that facilitate diffusion into the alloy bulk (CRWMS M&O 2000 [DIRS 154666], Section 3.4). Accumulation of hydrogen in the surface of the alloy in this manner would mean that it was rereleased as corrosion progressed. As a consequence, the hydrogen content of the alloy would increase more slowly than predicted by the model. This makes it very conservative to assume in the model that all the hydrogen absorbed due to general corrosion accumulates until the critical hydrogen concentration for a decrease in fracture toughness is achieved.

The majority of hydrogen absorption measurements have been performed under aggressive conditions not relevant to Yucca Mountain (i.e., under acidic conditions or with a large cathodic potential applied to simulate cathodic protection conditions). For more-relevant conditions (concentrated brines at 150°C), Westerman (1990 [DIRS 151188]) measured only marginal hydrogen absorption (10 to < 30 µg/g) by Ti Grade 12 (an alloy more susceptible to hydrogen absorption than Ti Grades 16 and 7) over 12 to 18 months of exposure. The majority of the absorption appeared to occur in the first 6 months and then stopped. These measurements were made in the presence of a radiation field (3×10^4 Rad/h) and it is possible that the hydrogen permeability of the oxide films was reduced. An improvement in resistance of the passive film on Ti Grade 12, to hydrogen absorption in the presence of a radiation field, was also observed by Kim and Oriani (1987 [DIRS 110237]). Under cathodic polarization conditions in NaCl (pH = 1) negligible amounts of hydrogen were absorbed into Ti Grade 16 for applied potentials ≤ -600 mV$_{(SCE)}$ (Ikeda et al. 2000 [DIRS 159760]; Ikeda and Quinn 1998b [DIRS 152481]). In the absence of galvanic coupling, such negative potentials should be unattainable under repository conditions.

Of particular relevance are the results of Shimogori et al. (1985 [DIRS 159784]) who measured the amount of hydrogen absorbed in dilute HCl as a function of pH (2 to 4), temperature (50°C to 250°C), and degree of aeration (deaerated and aerated). Over an exposure period of 10 days the amount of hydrogen absorbed increased with a decrease in pH and an increase in temperature for deaerated conditions. For the most relevant condition (pH = 4), absorption was immeasurable at 50°C and only 1-2 µg/g at 250°C. For aerated conditions, essentially no measurable hydrogen was absorbed irrespective of the pH or temperature over a similar exposure period. There is also experimental evidence that aeration suppresses hydrogen absorption by Ti-0.15Pd (equivalent to Ti Grade 7) more than it does to titanium (1% HCl, 70°C) (Fukuzuka et al. 1980

[DIRS 151105]). Because conditions within Yucca Mountain are expected to be oxidizing these results are consistent with the expectation that hydrogen absorption by the drip shield will be minor.

Two attempts to predict the hydrogen absorption rates of titanium nuclear waste containers have been published. The model adopted for the drip shield was used to predict the hydrogen absorption rates for Canadian waste containers (Shoesmith et al. 2000 [DIRS 159759]). In these calculations the very low corrosion rates expected in the compacted clay buffer environment proposed for the repository (0.4 to 3.3 nm/yr) were used with a little higher hydrogen absorption efficiency than that used in the Yucca Mountain Project drip shield model. It was predicted that the critical hydrogen concentration of 500 µg/g would not be exceeded in less than 1,000,000 years. These calculations are compared with the current primary model prediction of 510 µg/g after 10,000 years. Based on cathodic polarization measurements as a function of applied potential, pH and duration of polarization (60 days), a parabolic hydrogen absorption relationship was adopted, and it was calculated that only 17 µg/g of hydrogen would be absorbed in 1,000 years (Tomari et al. 1999 [DIRS 159786]). Given that this model is based on a parabolic relationship compared to the linear relationship used in the current primary model, it strongly supports the model prediction that critical hydrogen concentrations will not be exceeded in less than 10,000 years.

In light of the above discussion, it can be concluded that the input parameter values used in the hydrogen-induced cracking model of titanium during passive general corrosion, and the model output corroborate extremely well with those reported mostly in the peer-reviewed scientific literature. It is also clear from the above discussion that the validation activities performed for building confidence in the model have sufficiently strong scientific bases, and that all of the four criteria, used to determine that the required level of confidence in the model has been achieved, have been met. Recent publication of this model in a peer-reviewed scientific journal (Shoesmith et al. 2000 [DIRS 159759]) has further increased the level of confidence in this model.

Therefore, Criterion 2 and Criterion 3 are met.

7.3.4 Validation Of The Model For Hydrogen Absorption by titanium Under Galvanically Coupled Conditions

Criterion 1: Is the critical hydrogen content of the Grade-7 titanium alloy was consistent with the literature?

The critical hydrogen concentration used in this model is the same as that used in the general passive corrosion model for hydrogen-induced cracking. Since the difference between the primary model and that for hydrogen-induced cracking under galvanically coupled conditions is in the processes leading to hydrogen absorption, not in the materials properties defining the resistance to cracking, the use of an identical value of H_C is appropriate. Consequently, the arguments used to validate the values of H_C used in the general passive corrosion model are equally applicable to this model.

The value of H_C used is the minimum absorbed hydrogen concentration for which a reduction in fracture toughness is observable. For general passive corrosion, this concentration would be achieved universally throughout the drip shield making it vulnerable to fracture over a wide area. By contrast, in the case of galvanic coupling, hydrogen absorption will be confined to a relatively small area of the shield (~1,000 to 2,000 cm^2 affected area for the Fe/Ti contact area of ~75 cm^2 assumed (Assumption 5.7) in the model). Hence, fracture would be expected to occur over a much smaller area of the drip shield, making the consequences of failure in the galvanically coupled case much less severe.

> *Criterion 2: Are the general corrosion rates in the model consistent with the literature?*

In the galvanically coupled case, the rate of hydrogen absorption by the Ti Grade 7 is the key rate used in the model. This absorption rate is supported by the corrosion rate of the coupled steel. The value used for the rate of hydrogen absorption is taken from the measurements by Murai et al. (1977 [DIRS 111926]) and discussed by Shoesmith et al. (1995 [DIRS 117892]). A rate of 0.5 µg/g/day was used. This value was measured in artificial seawater (30°C) at a potential of -800 mV$_{(SCE)}$. This is an appropriate value since the corrosion potential of a galvanic couple between carbon steel and titanium in neutral seawater has been measured to be in the ranges -662mV to -766mV at 18°C and -736mV to -763mV at 60°C (Hodgkiess et al. 1987 [DIRS 159787]).

This value of absorption rate is conservative for a number of reasons. The rate is calculated from the total amount of hydrogen absorbed over the 180-day exposure time employed and, hence, is an average linear rate over that period. A simple linear extrapolation of this rate indicates that the galvanic couple would have to persist, without any decrease in rate, for 2,000 days to achieve the critical H_C value of 1,000 µg/g. Actually, since the model allows a considerable amount of hydrogen to diffuse laterally within the shield (i.e., to adjacent sites not in galvanic contact with the steel), the period required to exceed H_C would be greater. However, considerable published evidence exists to show that the rate of hydrogen absorption under galvanically coupled conditions decreases parabolically with time (Phillips et al. 1974 [DIRS 151152]; Noel et al. 1996 [DIRS 111940]; Tomari et al. 1999 [DIRS 159786]). This is equivalent to a decrease in the hydrogen absorption efficiency since the carbon steel corrosion rate and, hence, the rate of hydrogen production would not necessarily also decrease with time. This parabolic decrease indicates the lower actual absorption rate beyond 180 days than used by Murai et al. (1977 [DIRS 111926]). The constant hydrogen-absorption rate used in the model, therefore, applies conservatively well beyond the 180 days over which it was measured. As a consequence, the amount of hydrogen absorbed for the assumed amount of carbon steel corroded over the duration of the galvanic couple will be less than calculated by the model.

Hodgkiess et al. (1987 [DIRS 159787]) measured the current flowing in a carbon steel/titanium galvanic couple with a 1:1 contact area (1 cm^2) in seawater (pH = 8.1; 60°C; 36 to 45 days exposure) to be in the range 14 to 22 µA. The results of Mon (2002 [DIRS 160876]) show the steel corrosion rate in a galvanic couple is approximately proportional to the contact area. If this proportionality is accepted, and the current measured by Hodgkiess et al. (1987 [DIRS 159787]) is taken to be representative of that anticipated under repository conditions, then for the assumed

contact area in the model ($\sim$75 cm^2), the galvanic current would be 1,650 µA (1.65 mA). Application of Faraday's Law then estimates that such a current would not produce, by a large margin, sufficient hydrogen to maintain an absorption rate of 0.5 µg/g/day at a fractional absorption efficiency of 0.015, the value used in the model.

The key point in this conservative argument is the applicability of the Hodgkiess et al. (1987 [DIRS 159787]) data to repository conditions. Higher temperatures and more-aggressive exposure environments, especially those containing Fe(II) corrosion products (Mon 2002 [DIRS 160876], Attachments I and IV), could lead to the production of considerably larger amounts of hydrogen and, hence, to higher absorption rates. However, such rates would be prevented by the production of Fe(III) species under oxidizing repository conditions, which are known to reinforce the passivation of titanium (Schutz and Thomas 1987 [DIRS 144302]; Covington and Schutz 1981 [DIRS 151098]), or the presence of thermal oxides grown during the ventilation period, or both; or while temperatures are high prior to the formation of aqueous conditions. Substantial published evidence exists to show that thicker oxide films grown thermally prevent hydrogen absorption to temperatures approaching 120°C (Mon 2002 [DIRS 160876], Attachment III) or in a pickling solution (Mon 2002 [DIRS 160876], Attachment IV). The results reported by Mon (2002 [DIRS 160876], Attachment III) show that a 40-nm-thick thermally grown oxide maintains its thickness and prevents hydrogen absorption even in 2% HCl at 70°C.

> *Criterion 3: Are the hydrogen contents for Grade-7 titanium and similar alloys*
> *predicted by the model consistent with the literature?*

Unlike the case for general passive corrosion the titanium drip shield wall is not thinned by material loss during the galvanically coupled corrosion process. In this latter case, the titanium maintains its wall thickness while cathodically absorbing hydrogen-coupled to anodically corroding carbon steel. Thus, the assumption that all absorbed hydrogen remains in the alloy is realistic, not conservative.

The majority of hydrogen absorption measurements under galvanically coupled conditions (or in the presence of cathodic polarization to simulate such conditions) have been made in aggressive environments not relevant to Yucca Mountain (i.e., in acidic environments or with a large potential that simulates cathodic protection conditions).

By comparison to hydrogen absorption rates measured by Tomari et al. (1999 [DIRS 159786]) (neutral carbonate solutions of pH 8 containing 1,000 µg/g of chloride at 25°C) at –750 mV$_{(SCE)}$, the absorption rate used in the model is very conservative. Based on the parabolic relationships measured by Tomari et al. (1999 [DIRS 159786]), only a few tens of µg/g of hydrogen would be absorbed by Ti Grade 2 (or Ti Grade 17; Ti Grade 16 with a little extra oxygen content) over thousands of years. By contrast, the rate used in the model would predict that the critical hydrogen concentration would be exceeded in $\sim$5 to 10 years, providing the galvanic coupling is maintained. The model rates are also conservative compared to those measured by Lee et al. (1986 [DIRS 159788]) in seawater (pH = 8, 25°C), which are approximately one order of magnitude lower.

Additional features should also be noted:

- While the rate of hydrogen absorption is higher at higher temperatures (in the absence of a thermally grown oxide), a very large majority of the hydrogen is stored in a surface hydride layer (Noel et al. 1996 [DIRS 111940]; Mon 2002 [DIRS 160876], Attachment II), which drastically limits the absorption rate (Noel et al. 1996 [DIRS 111940]). This makes the use in the model of a constant absorption efficiency of 0.015 conservative. Even for large applied potentials or applied currents (equivalent to galvanic currents well in excess of those sustainable on the drip shield [$>10^5$ μA through the galvanic contact area assumed in the model]) the thickness of the surface hydride layer would be only tens of μm thick. This is insufficient to threaten the full-wall integrity of the drip shield.

- Experimental evidence shows that the rate of hydrogen absorption (Lunde and Nyborg 1993 [DIRS 151142]) will decrease with the accumulation of deposits—calcite from atmospheric CO_2 and silicates from groundwater. The accumulation of silicate deposits has been well characterized in LTCTF specimens.

In light of the above discussion, it can be concluded that the input parameter values used in the hydrogen-induced cracking model of titanium under the galvanically coupled condition and the model output corroborate extremely well with those reported in the peer-reviewed scientific literature. It is also clear from the above discussion that the validation activities performed for building confidence in the model have sufficiently strong scientific bases and that all four criteria have been met.

It can be, therefore, concluded that the criteria specified in the technical work plan are met in the case of modeling hydrogen absorption by titanium alloys under galvanically coupled conditions.

7.3.5 Validation for the Conservatism in Using 1-Year Corrosion Rates for H_A Modeling

This report emphasizes using the LTCTF 1-year corrosion rate data for modeling hydrogen content in metal is conservative. This is further supported based on the more recently acquired 5-year corrosion rate data at LTCTF for Ti Grade 16.

More recently acquired 5-year passive general corrosion rates for Ti Grade 16 are reported in *General Corrosion and Localized Corrosion of the Drip Shield* (BSC 2004 [DIRS 169845]) as the corroborative information for model validation only. For the purposes of this analysis, the maximum possible general corrosion rate of the drip shield is considered to be 3.20×10^{-4} mm/yr (1-year data, BSC 2004 [DIRS 169845]). This value results from measurements of the corrosion rates of samples with both weight-loss and creviced geometries after one year.

The general corrosion rates resulted from measurements of the corrosion rate of samples after five years showed much lower corrosion rates (BSC 2004 [DIRS 169845]). The maximum 5-year corrosion rates are 0.77×10^{-4} mm/yr and 0.58×10^{-4} mm/yr for crevice specimens and weight loss specimens, respectively (BSC 2004 [DIRS 169845]). The average of these two maximum corrosion rates is 0.675×10^{-4} mm/yr as shown in Table 7.

Using the same method of Section 6.2.3 (Equation 2) and the corrosion rate shown in Table 7, the following value of the hydrogen concentration in metal can be obtained:

$$H_A = 124 \text{ µg/g} < H_C = 1,000 \text{ µg/g}$$

Where $R_{uc} = 0.675 \times 10^{-4}$ mm/yr, $f_h = 0.015$, $d_o = 7.5$ mm and $t = 10,000$ years are used in the calculation (Equation 2). Assuming that the corrosion rates are constant over the time period when the drip shield is exposed in the repository environments and using the 1-year corrosion rate data to calculate the H_A in Ti Grade 7 is conservative.

Further, LTCTF has recently acquired the 2.5-year corrosion rate data for Ti Grade 7 under same test conditions as those obtained after 1- and 5-years for Ti Grade 16 (BSC 2004 [DIRS 169845]). The maximum and median values of 1-, 2.5-, and 5-year corrosion rate data are summarized in Table 8 (BSC 2004 [DIRS 169845], Table 21).

Table 8. Summary of 1-, 2.5-, and 5-Year Corrosion Data Comparison

	One -Year (nm/yr)		2.5-Year (nm/yr)		5-Year (nm/yr)	
Specimen Type	Weight-Loss	Crevice	Weight-Loss	Crevice	Weight-Loss	Crevice
Median	0	0	6	3	5	10
Maximum	113	319	50	38	58	77

Source: BSC 2004 [DIRS 169845], Section 7.2, Table 21

A more direct comparison of the 1-, 2.5-, and 5-year maximum corrosion rate data is presented in Figure 11. From Figure 11, there are three important conclusions can be drawn. First, the 1-year corrosion rates are higher than the 5-year corrosion rates both obtained from Ti Grade 16. This observation confirms that the corrosion rate of titanium alloys decreases with time. Secondly, the 2.5-year maximum corrosion rate, obtained from Ti Grade 7, is apparently lower than general corrosion resistance of Ti Grade 16 tested for five years, further confirming that the corrosion resistance of Ti Grade 7 is superior to that of Ti Grade 16. Lastly, the difference between the corrosion rates obtained from the weight loss specimens and crevice specimens diminishes at the prolonged exposure times, confirming the excellent resistance to crevice corrosion of titanium alloys in environments relevant to repository conditions.
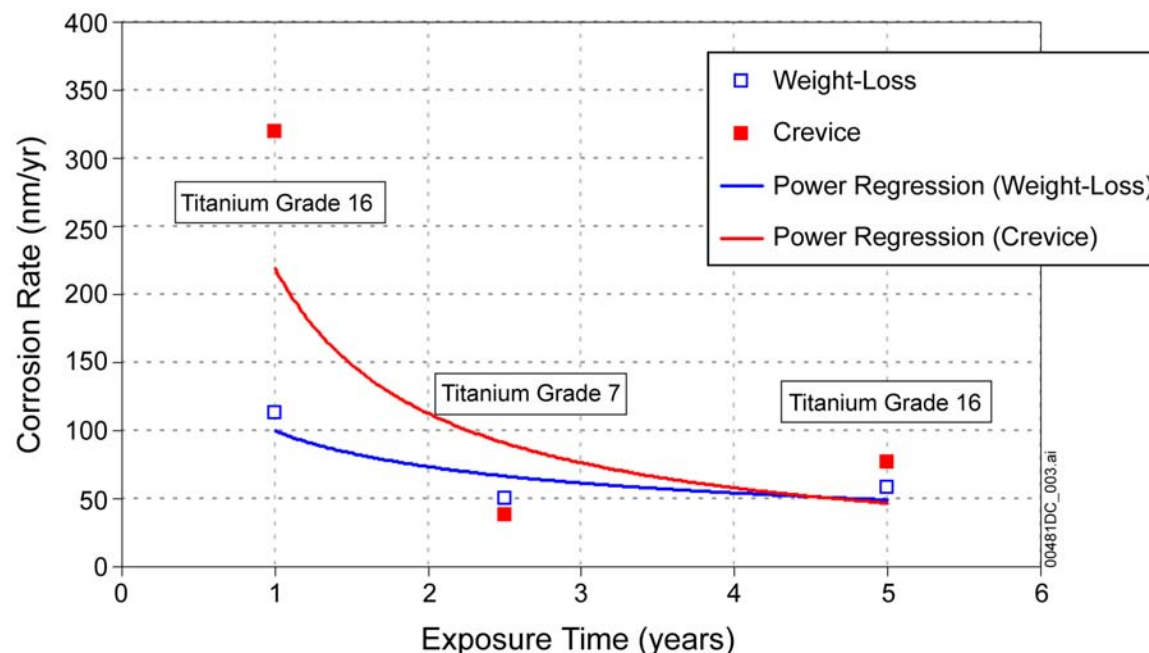
Source: BSC 2004 [DIRS 169845], Section 7.2, Figure 25

Figure 11. A Comparison of 1-Year (Ti Grade 16), 2.5-Year (Ti Grade 7), and 5-Year (Ti Grade 16) Corrosion Rates Obtained from Weight-Loss Specimens and Crevice Specimens, Showing the Decreasing Trend in Corrosion Rate

As the rate of hydrogen generation on the drip shield surface and, hence, the rate of hydrogen absorption into the drip shield, is proportional to the rate of drip shield corrosion, the hydrogen content will be lower according to the 5-year corrosion rate data than that estimated by using the 1-year corrosion rate data.

Therefore, the current model is highly conservative because it assumes all the hydrogen absorbed during general corrosion is retained within the remaining drip shield wall thickness as the general corrosion proceeds. It is most likely that some of the hydrogen will be removed as corrosion progresses. With this conservative assumption, the hydrogen concentration in the drip shield increases continuously with time as the drip shield thickness (thus, the volume of the remaining drip shield) reduces by general corrosion. This hydrogen concentration increase from the thinning of the drip shield is in addition to the hydrogen pickup from the general corrosion. With the current conservative model, the time for the hydrogen concentration in the drip shield to exceed the critical hydrogen concentration will always be less than the time to failure of the drip shield by general corrosion.

INTENTIONALLY LEFT BLANK

8. CONCLUSIONS

A simple conservative model has been developed to evaluate the effects of hydrogen-induced cracking on the drip shield. The basic premise of the model is that failure will occur once the hydrogen content exceeds a critical value, H_C. Quantitative evaluation based on the hydrogen-induced cracking model described in Section 6 indicates that the drip shield material (Ti Grade 7) is able to sustain the effects of hydrogen-induced cracking.

8.1 SUMMARY OF MODEL OUTPUT

The hydrogen content in Ti Grade 7 drip shield with a half thickness, d_o, after time, t, with a fractional hydrogen absorption efficiency, f_h, in environments where the maximum corrosion rate, R_{uc}, is evaluated by Equation 2 (Section 6.1.5):

$$H_A = 4x10^6 f_h R_{uc} t [M_{Ti}(d_o - R_{uc}t)]^{-1} \qquad \text{(Eq. 2)}$$

where

H_A = hydrogen content (μg/g) = 510 μg/g (based on the 1-year corrosion rates)

f_h = fractional efficiency for absorption = 0.015

R_{uc} = *rate* of general passive corrosion (mm/year) = 2.17×10^{-4} (which is the average of 3.20×10^{-4} and 1.13×10^{-4}, the highest corrosion rates from weight-loss plus crevice samples, and from weight-loss samples, respectively (BSC 2004 [DIRS 169845], Section 6.3.5))

t = duration of emplacement (year) = 10,000

M_{Ti} = atomic mass of Ti (g/mol) = 47.9

d_o = half of drip shield thickness (mm) = 7.5

Using the 1-year corrosion rate data, the hydrogen concentration in the drip shield at 10,000 years after permanent closure is 510 μg/g, resulting from a conservative estimate. The estimated hydrogen concentration is a factor of two less than the critical hydrogen concentration of 1,000 μg/g for Ti Grade 7, a conservative value estimated in Sections 5.2 and 6.1.3. The model output is shown in Table 9.

Table 9. Output of Model for Hydrogen Absorption During Passive General Corrosion of Titanium

| Output Name | Output Description | DTN | Output Uncertainty | | |
			Sources of Uncertainty*	Uncertainty Distribution (if applicable)	Calculated Hydrogen Content
H_A	Hydrogen content in the drip shield	Output DTN: MO0408MWDHICDS.000	Uncertainties associated with R_{uc} and f_h	N/A	510 μg/g by using the 1-year corrosion rates

NOTE: * Bounding experimental values of R_{uc} were averaged (see above). The value of f_h is chosen as a conservative bound (Sections 5.6 and 6.1.6)

8.2 HYDROGEN-INDUCED CRACKING DUE TO GALVANIC COUPLING

With the assumptions described in Section 5.7, the mathematical model shows that in all cases of the parametric study, the hydrogen concentration does not exceed the estimated critical hydrogen concentration of 1,000 μg/g for Ti Grade 7 by a safety margin of about 100 percent (Section 6.3.3). The results of the parametric study are consistent with the qualitative assessment discussed in Section 6.3.2.

8.3 SUMMARY OF THE CONSERVATISMS EMBEDDED IN THE MODELING

In this report, several conservative approaches are adopted to ensure the model output is sufficiently conservative. These conservatisms are summarized below.

8.3.1 Conservatism in Assuming Constant Corrosion Rates

The assumption that the corrosion rates of titanium alloys are constant (and using the 1-year data for modeling) during the 10,000 years after closure is conservative in three aspects:

- The less conservative corrosion models assume that the rate decays with time as shown in *General Corrosion and Localized Corrosion of the Drip Shield* (BSC 2004 [DIRS 169845], Section 7.2).

- This estimate also implies that any hydrogen absorbed into the titanium remains within the remaining wall thickness and is not subsequently removed as the general corrosion process progresses with time. This is another conservative assumption, as any titanium hydride formed within the alloy will be unstable with respect to titanium oxide (Beck 1973 [DIRS 151089]) and should, therefore, be removed by the general corrosion process. This assumption is used in Sections 6.1.5, 6.1.6, and 6.2.3.

- *General Corrosion and Localized Corrosion of the Drip Shield* (BSC 2004 DIRS 169845], Section 7.2) shows the corrosion rates obtained from the 2.5-year (Ti Grade 7) and 5-year (Ti Grade 16) corrosion testing are much lower than that obtained after a 1-year immersion. Using the lower corrosion rates to predict H_A would lead to much lower value of H_A.

8.3.2 Conservatism in Using Fractional Efficiency of Hydrogen Absorption

The model predictions shown in Table 9 are based on a very conservative and constant upper bound value of 0.015 for f_h. However, published data for the absorption of hydrogen by titanium (f_h) indicate the absorption efficiency would be lower than this value (Section 5.6). Using this range of f_h for Ti Grade 7 under repository conditions is conservative because (1) they were measured on Ti Grade 2, which is an unalloyed titanium; and (2) they were obtained under constant applied current conditions with an applied current of 0.5 mA/cm^2 at 25°C in sodium sulfate solutions at pH = 4, a condition not achievable under the repository condition. Indeed the electrode potential achieved during these experiments was -1.14 V$_{(SCE)}$, about 500 mV more negative than the threshold value of -0.6 V$_{(SCE)}$ for hydrogen absorption. Moreover, the applied current density used was 5×10^5 nA/cm^2 (0.5 mA/cm^2), about three times higher than a value of

1.45 nA/cm^2 (1.45×10^{-6} mA/cm^2), a current density value converted from the general corrosion rate of 50 nm/yr (the 70th percentile value of general corrosion rates measured on weight-loss and crevice specimens of Ti Grade 16 at the LTCTF) (BSC 2004 [DIRS 169845], Section 6.5). Similar measurements on platinum- and nickel-coated Ti Grade 2 specimens gave a value of f_h only marginally higher under these conditions. Therefore, using a fractional efficiency of hydrogen absorption of 0.005 to 0.015 for Ti Grade 7 under repository conditions is sufficiently conservative.

8.3.3 Conservatism in Choosing Critical Hydrogen Concentration

The estimated value of H_C for Ti Grade 7 is conservative on a number of counts:

- The value of 400 µg/g is the lower limit of the measured range of 400 to 1,000 µg/g measured at ~25°C for Ti Grade 2 (Shoesmith et al. 1997 [DIRS 112203], pp. 7 to 11);

- The temperature of the drip shield will be well above ~25°C for the majority of the repository evaluation time and Clarke et al. (1995 [DIRS 151093]) have shown H_C for Ti Grades 2 and 12 rises from ~ 400 µg/g to ~1,000 µg/g at a temperature of 92°C to 100°C;

- The value of 400 µg/g was measured for Ti Grade 2, whereas the value for Ti Grade 16, a palladium-containing α-alloy with identical chemical composition to Ti Grade 7, is greater than 1,000 µg/g (Ikeda and Quinn 1998 [DIRS 144540], p.7).

8.3.4 Conservatism in Assuming Occurrence of Fast Fracture

The criterion for failure-adopted model is conservative (i.e., it is assumed that failure could occur instantly once the amount of hydrogen in the material (H_A) exceeds the critical value (H_C))(Section 5.3).

8.3.5 Conservatism in Evaluating Galvanic Effect

The approach to the galvanic effect on hydrogen-induced cracking adopted in this report is conservative based on the following assumptions:

- Corrosion of titanium will be driven by interaction with water to produce absorbable hydrogen (Assumption 5.4). Because conditions will be oxidizing, the reactions will be predominantly with dissolved oxygen, a process that does not produce hydrogen.

- Corrosion rates will be maintained constant over the lifetime of the drip shield (Assumption 5.5)

- Hydrogen release by conversion of the metal containing hydrogen to oxide as the corrosion progresses is negligible (Assumption 5.5)

- The value of the fractional efficiency of hydrogen absorption (f_h) obtained under extremely aggressive test conditions is used and assumed to be constant (Assumption 5.6).

These assumptions are conservative.

8.4 YUCCA MOUNTAIN REVIEW PLAN (YMRP) CRITERIA

According to the technical work plan (BSC 2004 [DIRS 169944], Table 3-1), the Yucca Mountain Review Plan (YMRP) Acceptance Criteria 2.2.1.1, System Description and Demonstration of Multiple Barriers, and 2.2.1.3.1, Degradation of Engineered Barriers must be met by this report.

Yucca Mountain Review Plan, Final Report (NRC 2003 [DIRS 163274]) contains acceptance criteria intended to establish the basis for the review of the material contained in the license application. As this report serves, in part, as the basis for the license application, it is important the information contained herein conform to those same acceptance criteria. This report addresses the degradation of a component of the engineered barriers, the drip shield. Based on the engineered barrier role of the drip shield, the processes involved with its degradation, and the potential impact of its degradation, the YMRP acceptance criteria that are applicable to this report are delineated below in italics. A discussion of how this report addresses appropriate criteria follows each acceptance criterion, coupled with an indication of where within the report the appropriate information can be found.

8.4.1 System Description & Demonstration of Multiple Barriers (YMRP 2.2.1.1)

The following acceptance criteria are based on meeting the requirements at 10 CFR 63.113(a) and 63.115(a)–(c).

Acceptance Criterion 1—Identification of Barriers Is Adequate

> *Barriers relied on to achieve compliance with 10 CFR 63.113(b), as demonstrated in the total system performance assessment, are adequately identified, and are clearly linked to their capability. The barriers identified include at least one from the engineered system and one from the natural system.*

The system this model report addresses is the engineering barrier system. The barrier that this report addresses is the drip shield. The identification of the barriers is described in Section 1.4.

Acceptance Criterion 2—Description of Barrier Capability to Isolate Waste Is Acceptable

> *The capability of the identified barriers to prevent or substantially reduce the rate of movement of water or radionuclides from the Yucca Mountain repository to the accessible environment, or prevent the release or substantially reduce the release rate of radionuclides from the waste is adequately identified and described:*

(1) The information on the time period over which each barrier performs its intended function, including any changes during the compliance period, is provided;

(2) The uncertainty associated with barrier capabilities is adequately described;

(3) The described capabilities are consistent with the results from the total system performance assessment; and

(4) The described capabilities are consistent with the definition of a barrier at 10 CFR 63.2.

The purpose of the drip shield is to divert any moisture that might seep from the drift walls, including condensed water vapor, around the waste packages to the drift floor for 10,000 years. The drip shield also reduces any damage to waste packages in the event of rockfalls, as the emplacement drifts degrade over time. This is described in Sections 1.4 and 6 as well as Section 7 as part of the conceptual model discussion for hydrogen-induced cracking of the drip shield.

Acceptance Criterion 3—Technical Basis for Barrier Capability Is Adequately Presented

The technical bases are consistent with the technical basis for the performance assessment. The technical basis for assertions of barrier capability is commensurate with the importance of each barrier's capability and the associated uncertainties.

The technical basis for the barrier capability is documented in Sections 6.1, 6.2, 6.3, and 6.4. Section 6.1 describes the technical basis for hydrogen-induced cracking model. Section 6.2 documents the technical basis for the hydrogen-induced cracking model when applied to drip shield. Section 6.3 documents the technical basis for the hydrogen-induced cracking model under galvanic coupling condition. Section 6.4 discusses the estimate of critical hydrogen concentration for Ti Grade 24.

8.4.2   Degradation of Engineered Barriers (YMRP 2.2.1.3.1)

The following acceptance criteria are based on meeting the requirements of 10 CFR 63.114(a)–(c) and (e)–(g), relating to the degradation of engineered barriers model abstraction. U.S. Nuclear Regulatory Commission staff should apply the following acceptance criteria, according to the level of importance established in the U.S. Department of Energy risk-informed license application.

Acceptance Criterion 1—System Description and Model Integration Are Adequate

(1) The total system performance assessment adequately incorporates important design features, physical phenomena, and couplings, and uses consistent and appropriate assumptions throughout the degradation of engineered barriers abstraction process;

(2) Assessment abstraction of the degradation of engineered barriers uses assumptions, technical bases, data, and models that are appropriate and consistent with other related U.S. Department of Energy abstractions.

(3) The descriptions of engineered barriers, design features, degradation processes, physical phenomena, and couplings that may affect the degradation of the engineered barriers are adequate.

(4) Boundary and initial conditions used in the total system performance assessment abstractions are propagated consistently throughout the abstraction approaches.

(5) Sufficient technical bases for the inclusion of features, events, and processes related to degradation of engineered barriers in the total system performance assessment abstractions are provided;

(6) Adequate technical bases are provided, for selecting the design criteria, that mitigate any potential impact of in-package criticality on repository performance, including considering all features, events, and processes that may increase the reactivity of the system inside the waste package.

(7) Guidance in NUREG–1297 and NUREG–1298, or other acceptable approaches, is followed.

The drip shield system this report addresses is described in Sections 1 and 6.1 as part of the conceptual model discussion for hydrogen-induced cracking of the drip shield. The system description and model integration are adequate.

The model abstraction outputs are supported by objective comparisons described in Sections 6 and 7. Sufficient data have been obtained, as documented in Sections 4.1, 5, 6, and 7 to develop and validate the model.

Uncertainties in the data used for the hydrogen-induced cracking model analysis were characterized and quantified, and propagated through the hydrogen-induced cracking model (Sections 6.2.4 and 6.3.4).

The physical phenomena, factors (including design features, environmental factors, and their coupling) are described in Sections 1.2 and 1.3 as part of the conceptual model discussion for hydrogen-induced cracking of the drip shield. The models developed in this report provide the basis for TSPA-LA to exclude the hydrogen-induced cracking of drip shield. Throughout this report, the analyses use assumptions, technical bases, input data and models that appropriately reflect the design of the drip shield and the humid air and groundwater media that may come in contact with the waste package. Assumptions used in this report are addressed in Section 5. The data, technical bases and models are addressed in Sections 4.1 and 6. This information is used in a manner that is consistent with other abstractions of processes associated with the degradation of the drip shield. Initial and boundary conditions are propagated consistently throughout the abstraction process as described in Sections 1.5, 6, and 8 of this report where the drip shield degradation models and ranges of application are discussed.

The features, events, and processes (FEPs) treated in this report are identified in Section 8.5. Sufficient technical bases for the exclusion of FEP 2.1.03.04.0B, *Hydride Cracking of Drip Shields*, are provided in Section 6 as part of the conceptual model discussion for drip shield degradation. The technical basis for the barrier capability is documented in Sections 6.2 and 6.3. Section 6.2 documents the technical basis for exclusion of hydrogen-induced cracking under general passive corrosion condition. Section 6.3 documents the technical basis for exclusion of hydrogen-induced cracking under the condition galvanic coupling to less noble metals (e.g. carbon steel and stainless steel).

DTN: MO0407SEPFEPLA.000 [DIRS 170760] also describes the FEP while *FEPs Screening of Processes and Issues in Drip Shield and Waste Package Degradation* (BSC 2004 [DIRS 169997]) provides a complete list of all FEPs related to waste package and drip shield degradation.

Those sections of the acceptance criterion relating to the selection of design criteria are not applicable to this report because design criteria are not selected in this report. Those sections of the acceptance criterion relating to the use of expert elicitation are not applicable to this report because expert elicitation was not used in this report.

Acceptance Criterion 2—Data Are Sufficient for Model Justification

> *(1) Parameters used to evaluate the degradation of engineered barriers in the license application are adequately justified (e.g., laboratory corrosion tests, site-specific data such as data from drift-scale tests, in-service experience in pertinent industrial applications, and test results not specifically performed for the Yucca Mountain site, etc.). The U.S. Department of Energy describes how the data were used, interpreted, and appropriately synthesized into the parameters;*

> *(2) Sufficient data have been collected on the characteristics of the engineered components, design features, and the natural system to establish initial and boundary conditions for abstraction of degradation of engineered barriers;*

> *(3) Data on the degradation of the engineered barriers (e.g., general and localized corrosion, microbially influenced corrosion, galvanic interactions, hydrogen embrittlement, and phase stability), used in the abstraction, are based on laboratory measurements, site-specific field measurements, industrial analog and/or natural analog research, and tests designed to replicate the range of conditions that may occur at the Yucca Mountain site. As appropriate, sensitivity or uncertainty analyses, used to support the U.S. Department of Energy total system performance assessment abstraction, are adequate to determine the possible need for additional data; and*

> *(4) Degradation models for the processes that may be significant to the performance of the engineered barriers are adequate.*

Section 4.1 documents that the input data and parameters used to evaluate the performance of the drip shield were obtained from controlled sources and were adequately justified for their intended use (Section 4.1). Section 4.1 shows that sufficient data have been collected to establish initial and boundary conditions for the models developed in this report. The data used was based

on laboratory measurements under testing conditions designed to replicate anticipated repository exposure conditions and from peer-reviewed literature data. Degradation models for the processes relevant to degradation of the drip shield were given appropriate consideration (Section 6) and were found to be adequate for their intended use (Section 7).

Acceptance Criterion 3—Data Uncertainty Is Characterized and Propagated Through the Model Abstraction

> *(1) Models use parameter values, assumed ranges, probability distributions, and/or bounding assumptions that are technically defensible, reasonably account for uncertainties and variabilities, and do not result in an under-representation of the risk estimate;*
>
> *(2) For those degradation processes that are significant to the performance of the engineered barriers, the U.S. Department of Energy provides appropriate parameters, based on techniques that may include laboratory experiments, field measurements, industrial analogs, and process-level modeling studies conducted under conditions relevant to the range of environmental conditions within the waste package emplacement drifts. The U.S. Department of Energy also demonstrates the capability to predict the degradation of the engineered barriers in laboratory and field tests;*
>
> *(3) For the selection of parameters used in conceptual and process-level models of engineered barrier degradation that can be expected under repository conditions, assumed range of values and probability distributions are not likely to underestimate the actual degradation and failure of engineered barriers as a result of corrosion;*
>
> *(4) The U.S. Department of Energy uses appropriate methods for nondestructive examination of fabricated engineered barriers to assess the type, size, and location of fabrication defects that may lead to premature failure as a result of rapidly initiated engineered barrier degradation. The U.S. Department of Energy specifies and justifies the allowable distribution of fabrication defects in the engineered barriers, and assesses the effects of defects that cannot be detected on the performance of the engineered barriers; and*
>
> *(5) Where sufficient data do not exist, the definition of parameter values and conceptual models, used by the U.S. Department of Energy, is based on appropriate use of other sources, such as expert elicitation conducted in accordance with NUREG–1563. If other approaches are used, the U.S. Department of Energy adequately justifies their use. Review Plan for Safety Analysis Report 2.2-25*

Each of the models developed in this report use parameter values, assumed ranges, probability distributions or bounding assumptions, or both, that are technically defensible, reasonably account for uncertainties and variabilities, and do not result in under-representation of the risk estimate. The various models developed in this report use data and parameters developed based on laboratory experiments (Section 4.1) or bounding assumptions, or both, that are technically defensible and reasonably account for uncertainties and variabilities. The effects of uncertainties

on the parameter ranges and uncertainty distributions in the models developed in this report are discussed in Sections 6.2.4 and 6.3.4.

Those sections of the acceptance criterion that relate to nondestructive examination of fabricated engineered barriers are not applicable to this report because no such analyses were made in this report. Those sections of the acceptance criterion that relate to the use of other sources, such as expert elicitation, are not applicable to this report because no other sources were used in the creation of this report.

Acceptance Criterion 4—Model Uncertainty Is Characterized and Propagated Through the Model Abstraction

> *(1) Alternative modeling approaches of features, events, and processes are considered and are consistent with available data and current scientific understanding, and the results and limitations are appropriately considered in the abstraction;*
>
> *(2) Consideration of conceptual model uncertainty is consistent with available site characterization data, laboratory experiments, field measurements, natural analog information and process-level modeling studies; and the treatment of conceptual model uncertainty does not result in an under-representation of the risk estimate; and*
>
> *(3) The U.S. Department of Energy uses alternative modeling approaches, consistent with available data and current scientific understanding, and evaluates the model results and limitations, using tests and analyses that are sensitive to the processes modeled.*

Alternative modeling approaches that are consistent with available data and current scientific understanding are considered and discussed throughout this report (Sections 6.1.6 and 6.3.6). Although these alternative models are not used in TSPA, they are used, where applicable, for model validation in Section 7.

Consideration of uncertainties of the models developed in this report is an integral part of the model development and validation. Conceptual model uncertainty is consistent with the information that has been developed through laboratory experiments (Section 4.1). The treatment of uncertainty is unlikely to result in under-representation of the risk estimates. The primary models for hydrogen-induced cracking are conservative relative to the alternative models. The conservatisms adopted in this report are summarized in Section 8.3. The effects of uncertainties on the parameter ranges and uncertainty distributions in the models developed in this report are discussed in Sections 6.2.4 and 6.3.4.

Acceptance Criterion 5—Model Abstraction Output Is Supported by Objective Comparisons

Models implemented in this total system performance assessment abstraction provide results consistent with output from detailed process-level models and/or empirical observations (laboratory and field testings and/or natural analogs);

(1) Numerical corrosion models used to calculate the lifetimes of the engineered barriers are adequate representations, considering the associated uncertainties in the expected long-term behaviors, the range of conditions (including residual stresses), and the variability in engineered barrier fabrication processes (including welding);

(2) Evidence is sufficient to show that models used to evaluate performance are not likely to underestimate the actual degradation and failure of engineered barriers, as a result of corrosion or other degradation processes;

(3) Mathematical models for the degradation of engineered barriers are based on the same environmental parameters, material factors, assumptions, and approximations shown to be appropriate for closely analogous engineering or industrial applications and experimental investigations;

(4) Accepted and well-documented procedures are used to construct and test the numerical models that simulate the engineered barrier chemical environment and degradation of engineered barriers; and Review Plan for Safety Analysis Report 2.2-26

(5) Sensitivity analyses or bounding analyses are provided to support the abstraction of degradation of engineered barriers that cover ranges consistent with the site data, field or laboratory experiments and tests, and industrial analogs.

The results of drip shield degradation models developed in this report are excluded from the TSPA-LA as specified in this report. As discussed in response to previous acceptance criteria, there is sufficient evidence that the models developed in this report will not underestimate the actual degradation and failure of the drip shield. The models developed in this report were constructed following the accepted and well-documented AP-SIII.10Q, *Models*.

8.5 EXCLUDED FEP(S)

This document is used to screen out the FEP 2.1.03.04.0B, *Hydride Cracking of Drip Shields* (DTN: MO0407SEPFEPLA.000 [DIRS 170760]). Based on the analysis (Section 6) and validation (Section 7) of this model report and the conservatisms adopted in the analysis (Section 8.3), it can be concluded that the hydrogen-induced cracking of Ti Grade 7 is not a possible scenario under the nuclear waste repository conditions for the 10,000 years of regulatory period. FEP 2.1.03.04.0B, *Hydride Cracking of Drip Shields* (DTN: MO0407SEPFEPLA.000 [DIRS 170760]) is excluded as shown in Table 10.

Table 10. Features, Events, and Processes Excluded (Screened Out) in This Model Report

FEP No.	FEP Name	Section Where Disposition is Described
2.1.03.04.0B	*Hydride Cracking of Drip Shields*	Entire

9.   INPUTS AND REFERENCES

9.1   DOCUMENTS CITED

103753   ASM International 1987. *Corrosion.* Volume 13 of *Metals Handbook.* 9th Edition. Metals Park, Ohio: ASM International. TIC: 209807.

100702   Baes, C.F., Jr. and Mesmer, R.E. 1986. *The Hydrolysis of Cations.* Malabar, Florida: Krieger Publishing Company. TIC: 223481.

151089   Beck, T.R. 1973. "Electrochemistry of Freshly-Generated Titanium Surfaces - I. Scraped-Rotating-Disk Experiments." *Electrochimica Acta, 18,* 807-814. New York, New York: Pergamon Press. TIC: 248519.

159792   Beck, T.R. 1982. "Initial Oxide Growth Rate on Newly Generated Surfaces." *Journal of the Electrochemical Society, 129,* (11), 2500-2501. New York, New York: Electrochemical Society. TIC: 253216.

159767   Been, J. and Grauman, J.S. 2000. "Titanium and Titanium Alloys." Chapter 47 of *Uhlig's Corrosion Handbook.* 2nd Edition. Revie, R.W., ed. New York, New York: John Wiley & Sons. TIC: 248360.

151090   Blackwood, D.J.; Peter, L.M.; and Williams, D.E. 1988. "Stability and Open Circuit Breakdown of the Passive Oxide Film on Titanium." *Electrochimica Acta, 33,* (8), 1143-1149. New York, New York: Pergamon Press. TIC: 248517.

157151   BSC (Bechtel SAIC Company) 2001. *Technical Update Impact Letter Report.* MIS-MGR-RL-000001 REV 00 ICN 02. Las Vegas, Nevada: Bechtel SAIC Company. ACC: MOL.20011211.0311.

164554   BSC 2003. *Safety Classification of SSCs and Barriers.* CAL-MGR-RL-000001 REV 00A. Las Vegas, Nevada: Bechtel SAIC Company. ACC: DOC.20030929.0014.

171024   BSC 2003. *Interlocking Drip Shield.* 000-MW0-TED0-00102-000-00A. Las Vegas, Nevada: Bechtel SAIC Company. ACC: ENG.20030205.0002.

168361   BSC 2004. *Q-List.* 000-30R-MGR0-00500-000-000 REV 00. Las Vegas, Nevada: Bechtel SAIC Company. ACC: ENG.20040721.0007.

169997   BSC 2004. *FEPs Screening of Processes and Issues in Drip Shield and Waste Package Degradation.* ANL-EBS-PA-000002 REV 03. Las Vegas, Nevada: Bechtel SAIC Company.

161237   BSC 2004. *Environment on the Surfaces of the Drip Shield and Waste Package Outer Barrier.* ANL-EBS-MD-000001 REV 01. Las Vegas, Nevada: Bechtel SAIC Company.

169565   BSC 2004. *Multiscale Thermohydrologic Model.* ANL-EBS-MD-000049 REV 02. Las Vegas, Nevada: Bechtel SAIC Company.

169944   BSC 2004. *Technical Work Plan for: Regulatory Integration Modeling and Analysis of the Waste Form and Waste Package.* TWP-WIS-MD-000009 REV 00. Las Vegas, Nevada: Bechtel SAIC Company. ACC: DOC.20040616.0006.

169860   BSC 2004. *Engineered Barrier System: Physical and Chemical Environment Model.* ANL-EBS-MD-000033 REV 03. Las Vegas, Nevada: Bechtel SAIC Company.

169845   BSC 2004. *General Corrosion and Localized Corrosion of the Drip Shield.* ANL-EBS-MD-000004 REV 02. Las Vegas, Nevada: Bechtel SAIC Company. MOL.20040728.0279.

169985   BSC 2004. *Stress Corrosion Cracking of the Drip Shield, the Waste Package Outer Barrier, and the Stainless Steel Structural Material.* ANL-EBS-MD-000005 REV 02. Las Vegas, Nevada: Bechtel SAIC Company.

166275   Canori, G.F. and Leitner, M.M. 2003. *Project Requirements Document.* TER-MGR-MD-000001 REV 02. Las Vegas, Nevada: Bechtel SAIC Company. ACC: DOC.20031222.0006.

151092   Clarke, C.F.; Hardie, D.; and Ikeda, B.M. 1994. "The Effect of Hydrogen Content on the Fracture of Pre-Cracked Titanium Specimens." *Corrosion Science, 36,* (3), 487-509. New York, New York: Pergamon Press. TIC: 248535.

151093   Clarke, C.F.; Hardie, D.; and Ikeda, B.M. 1995. *Hydrogen Induced Cracking of Grade-2 Titanium.* AECL-11284. Pinawa, Manitoba, Canada: Whiteshell Laboratories. TIC: 226150.

159758   Clarke, C.F.; Hardie, D.; and Ikeda, B.M. 1997. "Hydrogen-Induced Cracking of Commercial Purity Titanium." *Corrosion Science, 39,* (9), 1545-1559. New York, New York: Elsevier. TIC: 252835.

151096   Cotton, J.B. 1970. "Using Titanium in the Chemical Plant." *Chemical Engineering Progress, 66,* (10), 57-62. Philadelphia, Pennsylvania: American Institute of Chemical Engineers. TIC: 248561.

151097   Covington, L.C. 1979. "The Influence of Surface Condition and Environment on the Hydriding of Titanium." *Corrosion, 35,* (8), 378-382. Houston, Texas: National Association of Corrosion Engineers. TIC: 226671.

151098   Covington, L.C. and Schutz, R.W. 1981. "Effects of Iron on the Corrosion Resistance of Titanium." *Industrial Applications of Titanium and Zirconium, A Symposium held in New Orleans, Louisiana, 15-17 October, 1979.* Kleefisch, E.W., ed. *ASTM Special Technical Publication 728,* 163-180. Philadelphia, Pennsylvania: American Society for Testing and Materials. TIC: 248737.

102933   CRWMS M&O 1999. *Waste Package Materials Properties.* BBA000000-01717-0210-00017 REV 00. Las Vegas, Nevada: CRWMS M&O. ACC: MOL.19990407.0172.

154666   CRWMS M&O 2000. *Review of the Expected Behavior of Alpha Titanium Alloys Under Yucca Mountain Conditions.* TDR-EBS-MD-000015 REV 00. Las Vegas, Nevada: CRWMS M&O. ACC: MOL.20010108.0011.

171386   DOE (U.S. Department of Energy) 2004. *Quality Assurance Requirements and Description.* DOE/RW-0333P, Rev. 16. Washington, D.C.: U.S. Department of Energy, Office of Civilian Radioactive Waste Management. ACC: DOC.20040823.0004.

147480   Drever, J.I. 1997. "Evaporation and Saline Waters." Chapter 15 of *The Geochemistry of Natural Waters: Surface and Groundwater Environments.* 3rd Edition. Upper Saddle River, New Jersey: Prentice Hall. TIC: 246732.

159797   Fonseca, C. and Barbosa, M.A. 2001. "Corrosion Behaviour of Titanium in Biofluids Containing H_2O_2 Studied by Electrochemical Impedance Spectroscopy." *Corrosion Science, 43,* ([3]), 547-559. New York, New York: Elsevier. TIC: 253223.

159837   Foroulis, Z.A. 1980. "Factors Influencing Absorption of Hydrogen in Titanium from Aqueous Electrolytic Solutions." *Titanium '80, Science and Technology, Proceedings of the 4th International Conference on Titanium. 4,* 2705-2711. Warrendale, Pennsylvania: Metallurgical Society of AIME. TIC: 253253.

151105   Fukuzuka, T.; Shimogori, K.; and Satoh, H. 1980. "Role of Palladium in Hydrogen Absorption of Ti-Pd Alloy." *Titanium '80, Science and Technology: Proceedings of the Fourth International Conference on Titanium, Kyoto, Japan, May 19-20, 1980.* Pages 2695-2703. Warrendale, Pennsylvania: Metallurgical Society of AIME. TIC: 248723.

165241   Greene, C.A.; Henry, A.J.; Brossia, C.S.; and Ahn, T.M. 2001. "Evaluation of the Possible Susceptibility of Titanium Grade 7 to Hydrogen Embrittlement in a Geologic Repository Environment." *Scientific Basis for Nuclear Waste Management XXIV, Symposium held August 27-31, 2000, Sydney, Australia.* Hart, K.P. and Lumpkin, G.R., eds. *663,* 515-523. Warrendale, Pennsylvannia: Materials Research Society. TIC: 254939.

159757   Hardie, D. and Ouyang, S. 1999. "Effect of Hydrogen and Strain Rate Upon the Ductility of Mill-Annealed Ti6Al4V." *Corrosion Science, 41,* (1), 155-177. New York, New York: Elsevier. TIC: 253121.

100814   Harrar, J.E.; Carley, J.F.; Isherwood, W.F.; and Raber, E. 1990. *Report of the Committee to Review the Use of J-13 Well Water in Nevada Nuclear Waste Storage Investigations.* UCID-21867. Livermore, California: Lawrence Livermore National Laboratory. ACC: NNA.19910131.0274.

159787   Hodgkiess, T.; Maciver, A.; and Chong, P.Y. 1987. "Galvanic Studies Related to the Use in Desalination Plant of Corrosion-Resistant Materials." *Desalination, 66,* 147-170. New York, New York: Elsevier. TIC: 252840.

167022   Hua, F.; Mon, K.; Pasupathi, V.; Gordon, G.; and Shoesmith, D. 2004. "Corrosion of Ti Grade 7 and Other Ti Alloys in Nuclear Waste Repository Environments - A Review." *Corrosion/2004, 59th Annual Conference & Exposition, March 28-April 1, 2004, New Orleans.* Paper No. 04689. Houston, Texas: NACE International. TIC: 255943.

152481   Ikeda, B.M. and Quinn, M.J. 1998. *A Preliminary Examination of the Effects of Hydrogen on the Behaviour of Grade-16 Titanium at Room Temperature.* 06819-REP-01200-0078-ROO. Toronto, Ontario, Canada: Ontario Hydro. TIC: 248920.

144540   Ikeda, B.M. and Quinn, M.J. 1998. *Hydrogen Assisted Cracking of Grade-16 Titanium: A Preliminary Examination of Behaviour at Room Temperature.* 06819-REP-01200-0039 R00. Toronto, Ontario, Canada: Ontario Hydro. TIC: 247312.

159760   Ikeda, B.M.; Quinn, M.J.; Noël, J.J.; and Shoesmith, D.W. [2000]. "The Hydrogen-Induced Cracking and Hydrogen Absorption Behaviour of Grade-16 Titanium." *Environmentally Induced Cracking of Metals, Proceedings of the International Symposium, August 20—23, 2000, Ottawa, Ontario, Canada.* Elboujdaini, M.; Ghali, E. and Zheng, W.; eds. Pages 235-248. Montreal, Quebec, Canada: Canadian Institute of Mining, Metallurgy and Petroleum. TIC: 252836.

110236   Kim, Y.J. and Oriani, R.A. 1987. "Brine Radiolysis and its Effect on the Corrosion of Grade 12 Titanium (1)." *Corrosion, 43,* (2), 92-97. Houston, Texas: NACE. TIC: 246022.

110237   Kim, Y.J. and Oriani, R.A. 1987. "Corrosion Properties of the Oxide Film Formed on Grade 12 Titanium in Brine Under Gamma Radiation." *Corrosion, 43,* (2), 85-91. Houston, Texas: NACE International. TIC: 246049.

159803   Kitayama, S.; Shida, Y.; Ueda, M.; and Kudo, T. 1992. "Effect of Small PD Addition on the Corrosion Resistance of TI and TI Alloys in Severe Gas and Oil Environment." *Techniques for Corrosion Measurement, Papers Presented at the Corrosion/92 Symposium.* Paper No. 52. Houston, Texas: NACE International. TIC: 253165.

159788   Lee, J-I.; Chung, P.; and Tsai, C-H. 1986. "A Study of Hydriding of Titanium in Sea Water Under Cathodic Polarization." *Corrosion 86, The International Corrosion Forum Devoted Exclusively to The Protection and Performance of Materials, March 17-21, 1986, Houston, Texas.* Paper No. 259. Houston, Texas: National Association of Corrosion Engineers. TIC: 252878.

159791   Leitner, K.; Schultze, J.W.; and Stimming, U. 1986. "Photoelectrochemical Investigations of Passive Films on Titanium Electrodes." *Journal of the Electrochemical Society, 133,* (8), 1561-1568. New York, New York: Electrochemical Society. TIC: 253219.

151142   Lunde, L. and Nyborg, R. 1993. *Hydrogen Absorption of Titanium Alloys During Cathodic Polarization.* Paper No. 5. Houston, Texas: National Association of Corrosion Engineers. TIC: 248523.

154721   Macdonald, D.D. 1999. "Passivity–The Key to Our Metals-Based Civilization." *Pure and Applied Chemistry, 71,* (6), 951-978. Oxford, England: Blackwell Science. TIC: 249795.

111885   Mattsson, H. and Olefjord, I. 1990. "Analysis of Oxide Formed on Ti During Exposure in Bentonite Clay-I. The Oxide Growth." *Werkstoffe und Corrosion, 41,* (7), 383-390. Weinheim, Germany: VCH Verlagsgesellschaft mbH. TIC: 246290.

159793   McAleer, J.F. and Peter, L.M. 1982. "Instability of Anodic Oxide Films on Titanium." *Journal of the Electrochemical Society, 129,* (6), 1252-1260. New York, New York: Electrochemical Society. TIC: 253252.

160876   Mon, K. 2002. "Hydrogen Influence Cracking Inputs for TSPA-LA." Interoffice memorandum from K. Mon (BSC) to G. De (BSC), November 21, 2002, 1121025237, with attachments. ACC: MOL.20021126.0157.

111926   Murai T.; Ishikawa, M.; and Miura, C. 1977. "The Absorption of Hydrogen into Titanium Under Cathodic Polarization." *Corrosion Engineering, 26,* (4), 177-183. Tokyo, Japan: Japan Society of Corrosion Engineering. TIC: 246349.

159794   Nishimura, R. and Kudo, K. 1982. "Anodic Oxidation and Kinetics of Titanium in 1 M Chloride Solutions." *Corrosion Science, 22,* (7), 637-645. New York, New York: Pergamon Press. TIC: 253220.

111940   Noel, J.J.; Bailey, M.G.; Crosthwaite, J.P.; Ikeda, B.M.; Ryan, S.R.; and Shoesmith, D.W. 1996. *Hydrogen Absorption by Grade-2 Titanium.* AECL-11608. Pinawa, Manitoba, Canada: Atomic Energy of Canada Limited, Whiteshell Laboratories. TIC: 246232.

163274   NRC (U.S. Nuclear Regulatory Commission) 2003. *Yucca Mountain Review Plan, Final Report.* NUREG-1804, Rev. 2. Washington, D.C.: U.S. Nuclear Regulatory Commission, Office of Nuclear Material Safety and Safeguards. TIC: 254568.

115556   Okada, T. 1983. "Factors Influencing the Cathodic Charging Efficiency of Hydrogen by Modified Titanium Electrodes." *Electrochimica Acta, 28,* (8), 1113-1120. New York, New York: Pergamon Press. TIC: 246262.

159795   Pan, J.; Thierry, D.; and Leygraf, C. 1994. "Electrochemical and XPS Studies of Titanium for Biomaterial Applications with Respect to the Effect of Hydrogen Peroxide." *Journal of Biomedical Materials Research, 28,* 113-122. New York, New York: John Wiley & Sons. TIC: 253221.

151152   Phillips, I.I.; Poole, P.; and Shreir, L.L. 1974. "Hydride Formation During Cathodic Polarization of Ti–II. Effect of Temperature and pH of Solution on Hydride Growth." *Corrosion Science, 14,* 533-542. New York, New York: Pergamon Press. TIC: 248570.

151163   Schutz, R.W. 1988. "Titanium Alloy Crevice Corrosion: Influencing Factors and Methods of Prevention." *Proceedings of the Sixth World Conference on Titanium, Cannes, June 6-9, 1988.* Lacombe, P.; Tricot, R.; and Beranger, G., eds. *IV,* 1917-1922. Cedex, France: Societe Francaise de Metallurgie. TIC: 248782.

102790   Schutz, R.W. 1995. "Recent Titanium Alloy and Product Developments for Corrosive Industrial Service." *Corrosion 95, The NACE International Annual Conference and Corrosion Show, March 26-31, 1995, Orlando, Florida. Paper No. 244,* Pages 244/1-244/20. Houston, Texas: NACE International. TIC: 245067.

168772   Schutz, R.W. 2003. "2003 F.N. Speller Award Lecture: Platinum Group Metal Additions to Titanium: A Highly Effective Strategy for Enhancing Corrosion Resistance." *Corrosion, 59,* (12), 1043-1057. Houston, Texas: NACE International. TIC: 255969.

144302   Schutz, R.W. and Thomas, D.E. 1987. "Corrosion of Titanium and Titanium Alloys." In *Corrosion,* Volume 13, Pages 669-706 of *Metals Handbook.* 9th Edition. Metals Park, Ohio: ASM International. TIC: 209807.

151167   Schutz, R.W. and Xiao, M. 1993. "Optimized Lean-Pd Titanium Alloys for Aggressive Reducing Acid and Halide Service Environments." *Corrosion Control for Low-Cost Reliability, Proceedings, 12th International Corrosion Congress, [Houston, Texas, September 19-24, 1993]. 3A,* 1213-1225. Houston, Texas: NACE International. TIC: 248725.

159798   Schutz, R.W. and Xiao, M. 1994. "Development of Practical Guidelines for Titanium in Alkaline Peroxide Bleach Solutions." *[1994 International Pulp Bleaching Conference, June 13-16, 1994, Hyatt Regency Hotel, Vancouver, British Columbia]. [2],* 153-158. Montreal, Canada: Canadian Pulp and Paper Association. TIC: 253218.

159784   Shimogori, K.; Satoh, H.; and Kamikubo, F. 1985. "Investigation of Hydrogen Absorption-Embrittlement of Titanium Used in the Actual Equipment." *Titanium, Science and Technology, Proceedings of the Fifth International Conference on Titanium, Congress-Center, Munich, FRG, September 10-14, 1984.* Lütjering, G; Zwicker, U.; and Bunk, W.; eds. *2,* 1111-1118. Oberursel, Germany: Deutsche Gesellschaft für Metallkunde. TIC: 252879.

159778   Shimogori, K.; Satoh, H.; Tomari, H.; and Ooki, A. 1982. "Analysis of Passive Film on Titanium Formed in Dilute HCl Solutions at Elevated Temperatures." *Titanium and Titanium Alloys, Scientific and Technological Aspects, International Conference on Titanium, 3d, Moscow State University, 1976.* Williams, J.C. and Belov, A.F., eds. *2,* 881-890. New York, New York: Plenum Press. TIC: 252876.

151179   Shoesmith, D.W. and Ikeda, B.M. 1997. *The Resistance of Titanium to Pitting, Microbially Induced Corrosion and Corrosion in Unsaturated Conditions.* AECL-11709. Pinawa, Manitoba, Canada: Whiteshell Laboratories. TIC: 236226.

112203   Shoesmith, D.W.; Hardie, D.; Ikeda, B.M.; and Noel, J.J. 1997. *Hydrogen Absorption and the Lifetime Performance of Titanium Nuclear Waste Containers.* AECL-11770. Pinawa, Manitoba, Canada: Atomic Energy of Canada Limited. TIC: 236220.

117892   Shoesmith, D.W.; Ikeda, B.M.; Bailey, M.G.; Quinn, M.J.; and LeNeveu, D.M. 1995. *A Model for Predicting the Lifetimes of Grade-2 Titanium Nuclear Waste Containers.* AECL-10973. Pinawa, Manitoba,Canada: Atomic Energy of Canada Limited. TIC: 226419.

159759   Shoesmith, D.W.; Noël, J.J.; Hardie, D.; and Ikeda, B.M. 2000. "Hydrogen Absorption and the Lifetime Performance of Titanium Nuclear Waste Containers." *Corrosion Reviews, 18,* (4-5), 331-359. London, England: Freund Publishing House. TIC: 252989.

159774   Smailos, E. and Köster, R. 1987. "Corrosion Studies on Selected Packaging Materials for Disposal of High Level Wastes." *Materials Reliability in the Back End of the Nuclear Fuel Cycle, Proceedings of a Technical Committee Meeting, Vienna, 2-5 September 1986. IAEA TECHDOC-421,* 7-24. Vienna, Austria: International Atomic Energy Agency. TIC: 252877.

119592   Smailos, E.; Schwarzkopf, W.; and Koster, R. 1986. "Corrosion Behaviour of Container Materials for the Disposal of High-Level Wastes in Rock Salt Formations." *Nuclear Science and Technology.* EUR 10400. Luxembourg, Luxembourg: Commission of the European Communities. TIC: 248245.

159786   Tomari, H.; Masugata, T.; Shimogori, K.; Nishimura, T.; Wada, R.; Honda, A.; and Taniguchi, N. 1999. "Hydrogen Absorption of Titanium for Nuclear Waste Container in Reducing Condition." *Zairyo-to-Kankyo, 48,* 807-814. Tokyo, Japan: Japan Society of Corrosion Engineering. TIC: 252965.

128733   Weast, R.C., ed. 1978. *CRC Handbook of Chemistry and Physics.* 59th Edition. West Palm Beach, Florida: CRC Press. TIC: 246814.

151188   Westerman, R.E. 1990. "Hydrogen Absorption and Crevice Corrosion Behaviour of Titanium Grade-12 During Exposure to Irradiated Brine at 150ºC." *Corrosion of Nuclear Fuel Waste Containers, Proceedings of a Workshop, Winnipeg, Manitoba, 1988 February 9-10.* Shoesmith, D.W., ed. AECL-10121. Pages 67-84. Pinawa, Manitoba, Canada: Atomic Energy of Canada Limited. TIC: 227040.

159799   Wyllie, W.E., II.; Brown, B.E.; and Duquette, D.J. 1994. "The Corrosion of Titanium in Alkaline Peroxide Bleach Liquors." *Corrosion 94, The Annual Conference and Corrosion Show.* Paper No. 421. Houston, Texas: NACE International. TIC: 253214.

9.2   CODES, STANDARDS, REGULATIONS, AND PROCEDURES

156605   10 CFR 63. Energy: Disposal of High-Level Radioactive Wastes in a Geologic Repository at Yucca Mountain, Nevada. Readily available.

AP-2.14Q, Rev. 3, ICN 0. *Document Review.* Washington, D.C.: U.S. Department of Energy, Office of Civilian Radioactive Waste Management. ACC: DOC.20030827.0018.

AP-2.22Q, Rev. 1, ICN 1. *Classification Analyses and Maintenance of the Q-List.* Washington, D.C.: U.S. Department of Energy, Office of Civilian Radioactive Waste Management. ACC: DOC.20040714.0002.

AP-2.27Q, Rev. 1, ICN 4. *Planning for Science Activities.* Washington, D.C.: U.S. Department of Energy, Office of Civilian Radioactive Waste Management. ACC: DOC.20040610.0006.

AP-SIII.10Q, Rev. 2, ICN 6. *Models.* Washington, D.C.: U.S. Department of Energy, Office of Civilian Radioactive Waste Management. ACC: DOC.20040805.0005.

AP-SV.1Q, Rev. 1, ICN 1. *Control of the Electronic Management of Information.* Washington, D.C.: U.S. Department of Energy, Office of Civilian Radioactive Waste Management. ACC: DOC.20040308.0001

162726   ASTM B 265-02. 2002. *Standard Specification for Titanium and Titanium Alloy Strip, Sheet, and Plate.* West Conshohocken, Pennsylvania: American Society for Testing and Materials. TIC: 254000.

105725   ASTM C 1174-97. 1998. *Standard Practice for Prediction of the Long-Term Behavior of Materials, Including Waste Forms, Used in Engineered Barrier Systems (EBS) for Geological Disposal of High-Level Radioactive Waste.* West Conshohocken, Pennsylvania: American Society for Testing and Materials. TIC: 246015.

9.3   SOURCE DATA, LISTED BY DATA TRACKING NUMBER

171362   LL040803112251.117. Target Compositions of Aqueous Solutions Used for Corrosion Testing. Submittal date: 08/14/2004.

161755   LL030205912251.016. Titanium (Ti) Grade 16 Corrosion Rate Data in Simulated Diluted and Concentrated Well Water (SDW and SCW). Submittal date: 02/13/2003.

104994   LL990610605924.079. LTCTF Data for C-22, TIGR7, TIGR12 and TIGR16. Submittal date: 06/13/1999.

170760   MO0407SEPFEPLA.000. LA FEP List. Submittal date: 07/20/2004.

152926   MO0003RIB00073.000. Physical and Chemical Characteristics of TI Grades 7 and 16. Submittal date: 03/13/2000.

9.4   OUTPUT DATA, LISTED BY DATA TRACKING NUMBER

MO0408MWDHICDS.000. Hydrogen Induced Cracking of Drip Shield for LA. Submittal date: 08/23/2004.

INTENTIONALLY LEFT BLANK